THE ENVIRONMENTAL DEPENDENCE OF LOW-z LYα ABSORPTION

David M. French, Bart P. Wakker[1]

[1]*Department of Astronomy, University of Wisconsin, Madison, WI 53706, USA*

ABSTRACT

We present the results of a large-scale study of the Lyα-probed CGM of nearby galaxies. We have identified 1135 Lyα absorbers in the redshift range $0 \leq z \leq 0.033$ in the spectra of 264 background QSOs, and correlated their positions with the surrounding galaxy environment. This has produced a sample of 216 individual Lyα component-galaxy pairs, representing the largest-to-date dataset of its kind. By employing the likelihood-based matching scheme of French & Wakker (2017), we quantify the absorber-galaxy spacial correlation and identify 4 distinct absorber sub-samples based on their relative isolation from surrounding galaxies. We find that absorber equivalent width and Doppler-b parameter are enhanced with increasing proximity to galaxies. Confirming the findings of French & Wakker (2017), we find an overabundance of detections at high galaxy inclination ($\sim 4.5\sigma$). We also report the first significant detection of an azimuth dependence for Lyα absorption, with both an enhanced detection fraction and an overabundance of absorption near the major and minor axes (3.3σ). Taken together these results suggest a picture in which weak Lyα absorbers trace the filamentary Cosmic Web structure, with stronger absorbers found almost exclusively within $\sim 1.5R_{\rm vir}$ of a $0.1L^*$ or brighter galaxy. Within this region, galaxies clearly have an effect on the preferred orientation of absorption.

Keywords: galaxies:intergalactic medium, galaxies:evolution, galaxies:halos, quasars: absorption lines

1. INTRODUCTION

The relationship between high column-density H I absorption ($N(\text{H\,{\sc i}}) \gtrsim 10^{14}$ cm^{-2}) and galaxies has been well studied in the past several decades (e.g., Lanzetta et al. 1995; Bowen et al. 1998, 2002; Chen et al. 2003, 2005; Chen & Tinker 2008; Steidel et al. 2010; Prochaska et al. 2011). **What do these studies find?** Relatively few studies have probed the Lyα-forest - galaxy relationship below this column density however (e.g., Bowen et al. 2002; Wakker & Savage 2009; French & Wakker 2017). The most obvious reason for this is due to the technically demanding nature of detecting these weak absorption systems. The installation of the Cosmic Origins Spectrograph (COS) on the Hubble Space Telescope (*HST*) in 2009 however has finally opened a window to study this rich reservoir of intergalactic gas (see Green et al. 2012 for instrument details). Thanks to the high throughput and sensitivity available with COS, a large number of distant quasi-stellar objects (QSOs) have been observed with sufficiently high signal-to-noise for a large variety of science priorities.

...

The second major challenge for galaxy-absorber correlation studies is obtaining data on the galaxies. While the resolution of absorption line spectroscopy is redshift-independent (e.g., a $N(\text{H\,{\sc i}}) \gtrsim 10^{13}$ cm^{-2} Lyα absorber is just as readily detected at $z \sim 0$ as at $z \sim 1$), detecting and classifying galaxies is a photometric exercise whose difficulty rapidly increases with redshift. Thus, while we

wish to include all absorption systems in any particular sightline observation to maximize our sample size, we are instead limited by our ability to produce a matching galaxy sample. Different studies have gone about tackling this issue in different ways. ...

To make progress here we have completed the largest-to-date survey of low-$N(\text{H\,{\sc i}})$ Lyα absorbers in the local Universe and their relationship to nearby galaxies. This survey is made possible by taking advantage of the large archival sample of COS QSO sightlines, and the high completeness of existing galaxy data in the redshift range $cz \leq 10,000$ km s^{-1}. In Section 2 we present the datasets, sample selection, and galaxy-absorber matching methods. In Section 3 we present and discuss the results of the galaxy-absorber correlation, and in Section 4 we offer our conclusions and discuss areas of future work.

2. DATA ANALYSIS

In this section we discuss the selection and reduction of our sample of archival QSO spectra taken by the Cosmic Origins Spectrograph (COS) on *HST*. There currently exist over 700 COS spectra in the Barbara A. Mikulski Archive for Space Telescopes (MAST) with G130M exposures which cover the Lyα transition in our survey's redshift range ($cz \leq 10,000$ km s^{-1}). In order to choose the most useful spectra for our purposes, we first sort them by signal-to-noise (SN) and make a cut at approximately SN=10. A signal-to-noise of approximately 10 or higher measured near 1238Å allows us
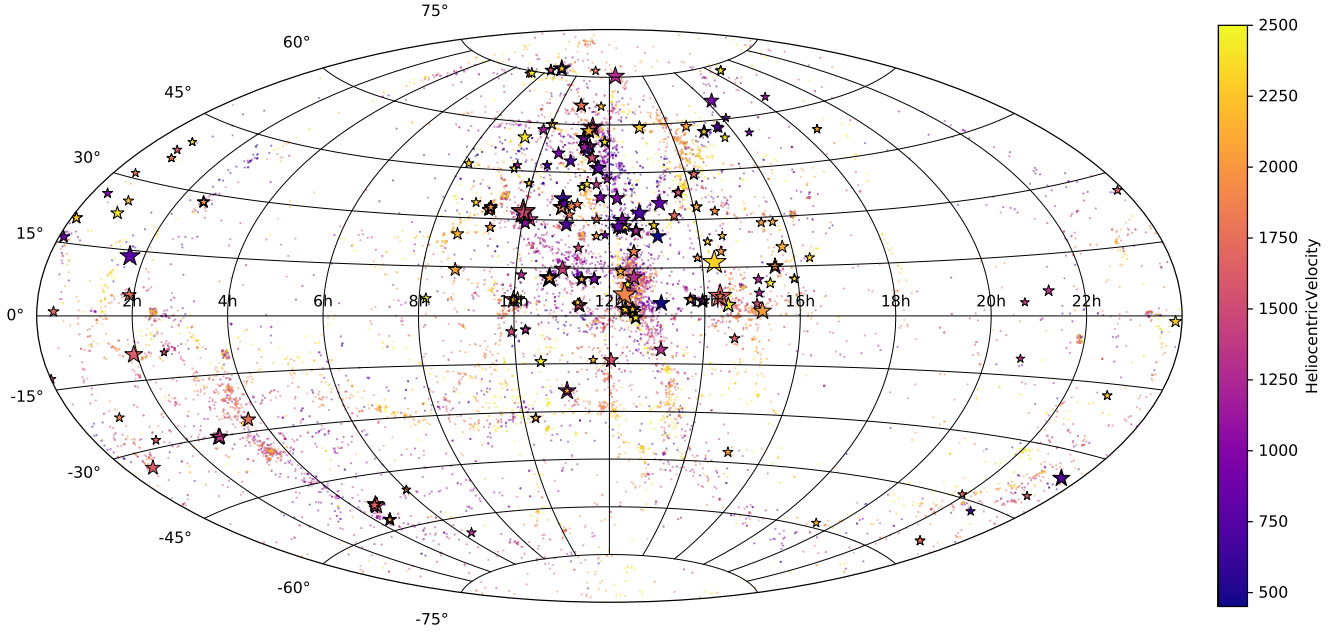
(a)
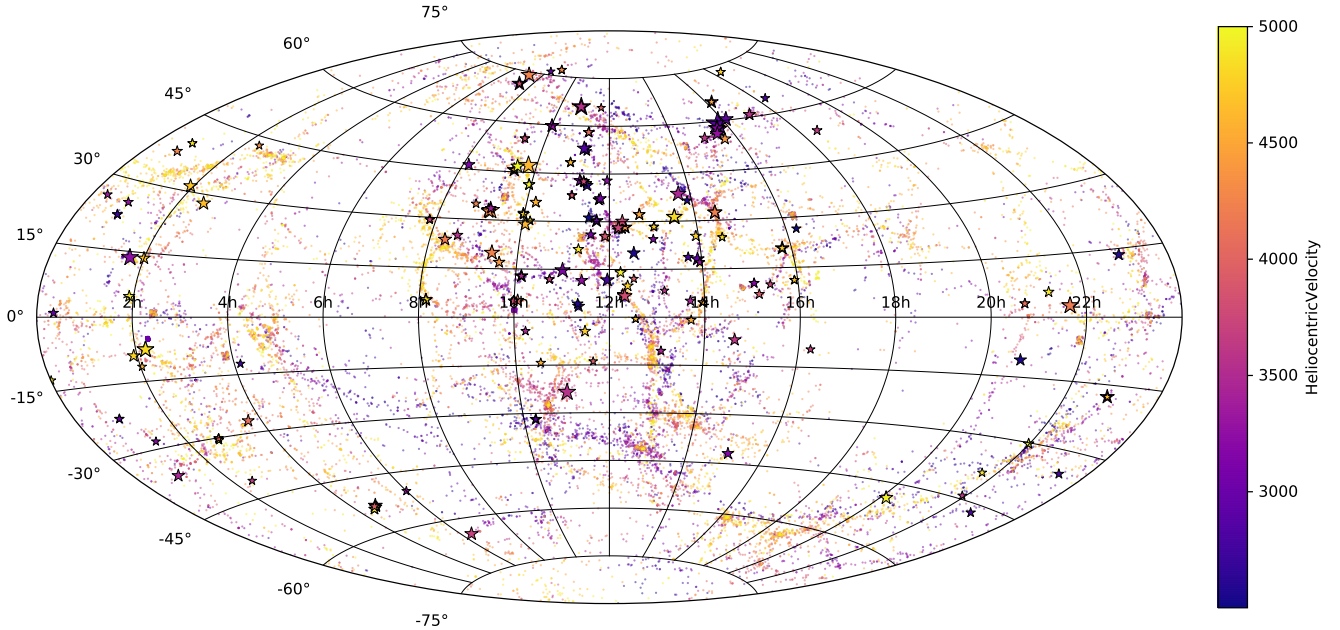
(b)

Figure 1. All sky maps of the locations of all absorbers and galaxies. Absorbers are plotted as stars and scaled in size based on their EW. Galaxies are plotted as dots. The colors of both galaxies and absorbers are mapped to their heliocentric velocities. (a) All galaxies and absorbers in the velocity range $450 \leq cz \leq 2500$ km s^{-1}. (b) All galaxies and absorbers in the velocity range $2500 < cz \leq 5000$ km s^{-1}.

(a)

(b)
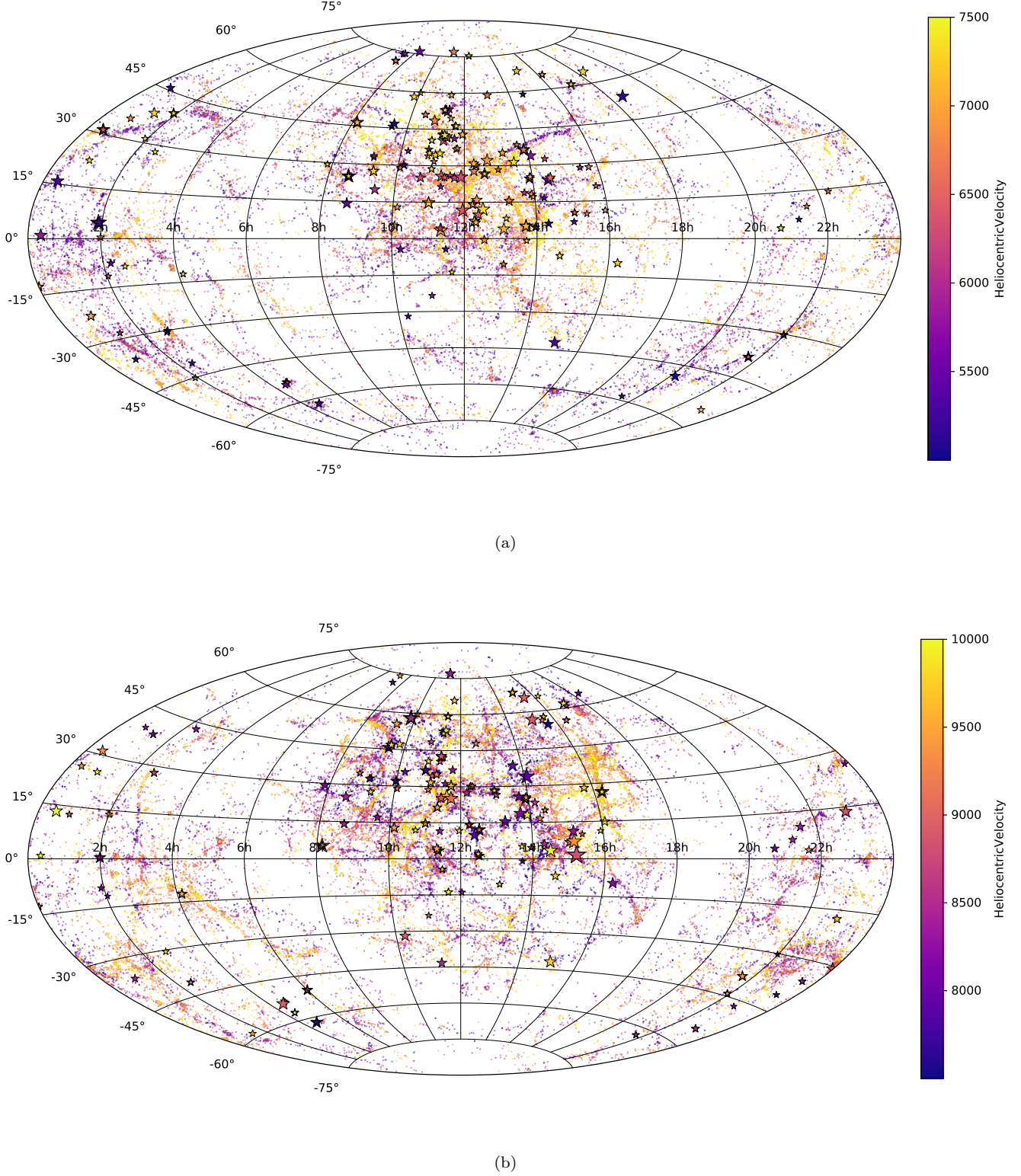
Figure 2. All sky maps of the locations of all absorbers and galaxies. Absorbers are plotted as stars and scaled in size based on their EW. Galaxies are plotted as dots. The colors of both galaxies and absorbers are mapped to their heliocentric velocities. (a) All galaxies and absorbers in the velocity range $5000 < cz \leq 7500 \ \mathrm{km \, s^{-1}}$. (b) All galaxies and absorbers in the velocity range $7500 < cz \leq 10,000 \ \mathrm{km \, s^{-1}}$.

to detect an absorption feature down to an equivalent width of $\sim 50\mathrm{m\AA}$ at 5σ. We then correlate the resulting

(SN $\gtrsim$ 10) sample with our galaxy catalog (see Chapter 2), and sort the spectra by proximity to a galaxy. While this introduces a slight bias against void or isolated absorption features, we are presently most interested in the absorber-galaxy relation and therefore choose this method to maximize the associated absorber-galaxy sample size. Additionally, because this sorting is done without knowledge of line locations, we will end up with significant sample of isolated absorbers simply based on their velocity, or z-direction, isolation from galaxies. Finally, from this galaxy-proximity sorted spectra list we choose 264 targets based on the relative ease of spectral feature identification. Because many of these archival sightlines were originally observed to study systems at $z > 0.03$ and not because of their proximity to any nearby galaxy, the resulting final sample is mostly randomly distributed across the sky.

Data reduction, continuum fitting and line measurement are then conducted in an identical fashion to French & Wakker (2017). In short, we determine the continuum around each line by fitting a 1st, 2nd or 3rd order polynomial to the line-free regions around each feature. All equivalent width measurements are integrated based on this fit, and we calculate the second moment of the apparent optical depth profiles to determine Doppler b-parameters. Table 2 summarizes the QSO targets included in this work.

In this sample of 264 QSOs we have detected 1135 Lyα absorbers. Figures 1 and 2 show all-sky maps of the positions of all absorbers split into 4 velocity bins ($v_{\mathrm{Ly}\alpha} = [0 - 2500]$, $(2500 - 5000)$, $(5000 - 7500)$, and $(7500 - 10,000]$ km s^{-1}). The distribution of galaxies in the same velocity ranges are include here also (galaxies are plotted as small circles, absorbers as stars; see Chapter 2). Comparing the galaxy to absorber positions and velocities within each velocity range by eye, we can clearly see that the Lyα absorbers broadly trace the locations of the galaxies. If the current Lambda Cold Dark Matter (ΛCDM) cosmology is to be believed, this should not be remarkably surprising. The baryons from which galaxies are built and those found within the IGM and traced by Lyα absorption should both follow the underlying potential produced by the Dark Matter, and should therefore be found in similar places. Beyond this big-picture result however, we want to know how the absorbers react to the presence of the galaxies on a more local scale.

2.1. Sub-sample selection

A major hurdle for galaxy-absorber correlation studies has always been matching any particular absorption line to a single nearby galaxy. The basic premise of matching relies on the assumption that, in at least some cases, one particular galaxy's potential, angular momentum, and radiation field dominates what an absorber "feels" (i.e., is the primary influencer for the EW, column density and Doppler b-parameter of an absorber).

With this assumption in place, the issue becomes that galaxies are generally not isolated. When faced with a distribution of galaxies of differing types, sizes, orientations and distances (impact parameters) and velocities ($\Delta v = v_{\mathrm{absorber}} - v_{\mathrm{galaxy}}$) from an absorption line, which, if any, are most likely to be "associated" with the line?

As first introduced in French & Wakker (2017), we employ a unique likelihood method for objectively matching absorbers with nearby galaxies in a consistent, analytical manner. We define likelihood, $\mathcal{L}$, as follows:

$$\mathcal{L} = A \times e^{-(\frac{\rho}{R_{\mathrm{eff}}})^2} \times e^{-(\frac{\Delta v}{v_{\mathrm{norm}}})^2}, \qquad (1)$$

where A is a normalization constant, ρ is the impact parameter between a galaxy and sightline, R_{eff} is one of two possible "effective - radii" we use for galaxies (virial radius and $D^{1.5}$, or diameter to the 1.5 power), Δv is the velocity separation between absorber and galaxy heliocentric, and v_{norm} is a velocity normalization (equal to one of 150, 200, or 250).

We calculate $\mathcal{L}$ for every absorber-galaxy combination, which then gives us a single number as a three-dimensional proxy for the physical separation between the two. Based on this $\mathcal{L}$ we then separate our sample into the following 5 distinct bins: $isolated$, $\mathcal{L} - isolated$, $\mathcal{L} - associated - isolated$, $\mathcal{L} - associated$, and $\mathcal{L} - two+$. The $isolated$ sample contains all the Lyα lines that are farther than 500 kpc and 400 km s^{-1} from any galaxy. The $\mathcal{L} - isolated$ sample contains those Lyα lines are far enough away from any galaxy so as to not meet our minimum-$\mathcal{L}$ criteria. The $\mathcal{L} - associated - isolated$ sample contains those Lyα lines which meet our $\mathcal{L}$ criteria to be associated with a single galaxy, and that galaxy is isolated by 500 kpc and 400 km s^{-1}. The $\mathcal{L} - associated$ sample contains those Lyα lines which meet our $\mathcal{L}$ criteria to be associated with a single galaxy, but that galaxy is not isolated. And finally, the $\mathcal{L} - two+$ sample contains those Lyα lines which meet our minimum-$\mathcal{L}$ criteria to be associated with $more$ than one galaxy.

Our standard criteria for a positive galaxy-absorber association are $\mathcal{L} \geq 0.01$ and $\mathcal{L}_1 \geq rigor \times \mathcal{L}_2$ with $rigor = 5$ (i.e., the $\mathcal{L}$-value for the most likely associated galaxy must be at least 5 times greater than that for the second most likely galaxy). However, we have also explored the results of adjusting the several possible $\mathcal{L}$ normalizations. We calculate $\mathcal{L}$ with R_{eff} equal to R_{vir} and $D^{1.5}$ and v_{norm} equal to 150, 200, and 250. For each of these combinations, we also calculate a variant with $A = 1$ and another with $A = 2$ if $R_{\mathrm{eff}} \geq \rho$, and $A = 1$ otherwise. Additionally, we investigate the effect of changing the minimum-$\mathcal{L}$ criteria to 0.005 and 0.001, and $rigor = 5$, 6, 7, and 8. Table 1 summarizes the resulting subsets for each of these combinations.

Overall, we find that none of these adjustments have a major effect on the resulting samples. To check, we performed Anderson-Darling statistical distribution analyses to check for differences between the EW distribu-

Table 1. Summary of $\mathcal{L}$ Variants

$\mathcal{L}$ Variant	$\mathcal{L} - isolated$	$\mathcal{L} - associated - isolated$	$\mathcal{L} - associated$	$\mathcal{L} - two+$
Total number of Lyα absorbers: 1135 571 are *isolated* regardless of normalization				
$\mathcal{L}_{min} = 0.01, rigor = 5$ (*Standard*)	267	56	146	58
$\mathcal{L}_{min} = 0.01, rigor = 5, A = 2 \ if \ \rho \leq R_{vir}$	267	56	160	55
$\mathcal{L}_{min} = 0.001, rigor = 5$	227	69	167	65
$\mathcal{L}_{min} = 0.001, rigor = 6$	227	69	162	68
$\mathcal{L}_{min} = 0.001, rigor = 7$	227	69	154	75
$\mathcal{L}_{min} = 0.001, rigor = 8$	227	69	145	78
$D^{1.5}, \mathcal{L}_{min} = 0.001, rigor = 5$	317	39	174	32
$\mathcal{L}_{min} = 0.001, rigor = 5, A = 2 \ if \ \rho \leq R_{vir}$	227	69	181	62
$\mathcal{L}_{min} = 0.005, v_{norm} = 150, rigor = 5$	265	58	148	63
$\mathcal{L}_{min} = 0.005, v_{norm} = 250, rigor = 5$	246	64	151	64

NOTE—A summary of the subset sizes resulting from varying the likelihood metric's normalization parameters. Different choices of normalization are simply shifting some of the non-*isolated* absorbers between different bins.

tions for each $\mathcal{L}$-variant and found no statistically significant difference between matching subsets (e.g., the EW distribution for the $\mathcal{L} - associated$ subset does not change significantly between these different $\mathcal{L}$ variants). For the remainder of this analysis we will concentrate on the $\mathcal{L}_{\min} = 0.01, v_{\mathrm{norm}} = 200, A = 2$ normalization subsets. This matches the normalization we adopted in French & Wakker (2017), and represents a middle ground option while also maximizing the size of the $\mathcal{L} - isolated - associated$, $\mathcal{L} - associated$, and $\mathcal{L} - two+$ subsets.

3. RESULTS & DISCUSSION

3.1. *Detection Fraction*

First we explore the Lyα detection fraction as a function of galaxy proximity. To calculate this, we start by correlating the position of every QSO with our galaxy sample. For every galaxy found within 1000 kpc in physical impact parameter of each sightline we then check if a Lyα line appears in that sightline and within 400 km s^{-1} of the galaxy's systemic velocity. This results in a detection fraction as a function of impact parameter. Additionally, we calculate the detection fraction as a function of likelihood, $\mathcal{L}$, in a similar manner. However, as we are calculating detection fraction without any a priori knowledge of the velocity of the absorption lines, the likelihood function we use is modified from Eq. 1 to simply $e^{-(\rho/R_{vir})^2}$, or only the impact parameter - virial radius portion of our usual likelihood function given by Eq. 1. Note that this adjusted likelihood function is identical to Eq. 1 when $\Delta v = 0$.

We have plotted the detection fraction as a function of both impact parameter and $\mathcal{L}$ in Figure 3. We also display the detection fraction for minimum Lyα EWs of 50, 100, 200, and 300 mÅ in purple, green, orange, and red (respectively). As expected, the detection fraction clearly increases with decreasing impact parameter
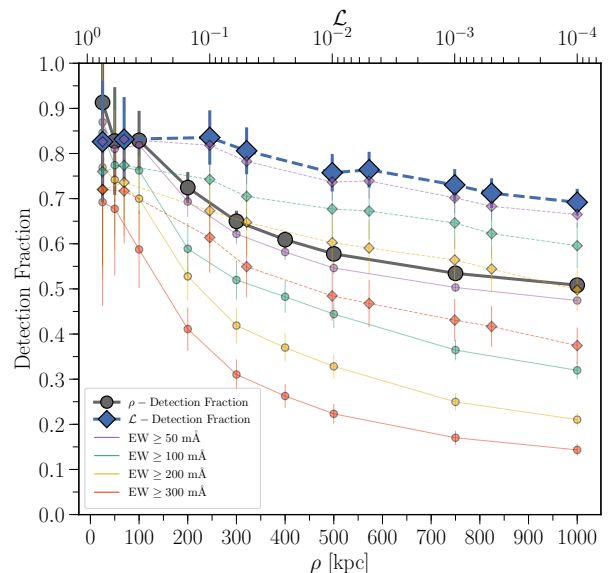
Figure 3. The detection fraction as a function of impact parameter (grey-circles) and $\mathcal{L}$ (blue-diamonds). Note that the impact parameter and $\mathcal{L}$ x-axis scales are quite different; the lowest $\mathcal{L}$ bin (0.0001) corresponds to $\sim 3R_{\mathrm{vir}}$, whereas the largest impact parameter bin (1000 kpc) is generally $\gg 3R_{\mathrm{vir}}$. Error bars show the 1σ Poisson errors.

and increasing $\mathcal{L}$. However, while the detection fraction as a function of impact parameter continues to rise all the way to the 25 kpc mark, it levels off at $\sim 1.5R_{\mathrm{vir}}$ ($\sim 0.1\mathcal{L}$) as a function of likelihood. **WHY? MORE**. While the detection fraction does not fall below $\sim 50\%$ when including all absorbers, it falls off more quickly for stronger absorbers (e.g., to below $\sim 20\%$ for EW$\geq$ 300mÅ absorbers). **MORE**

3.2. *Equivalent Width*

(a)

(b)
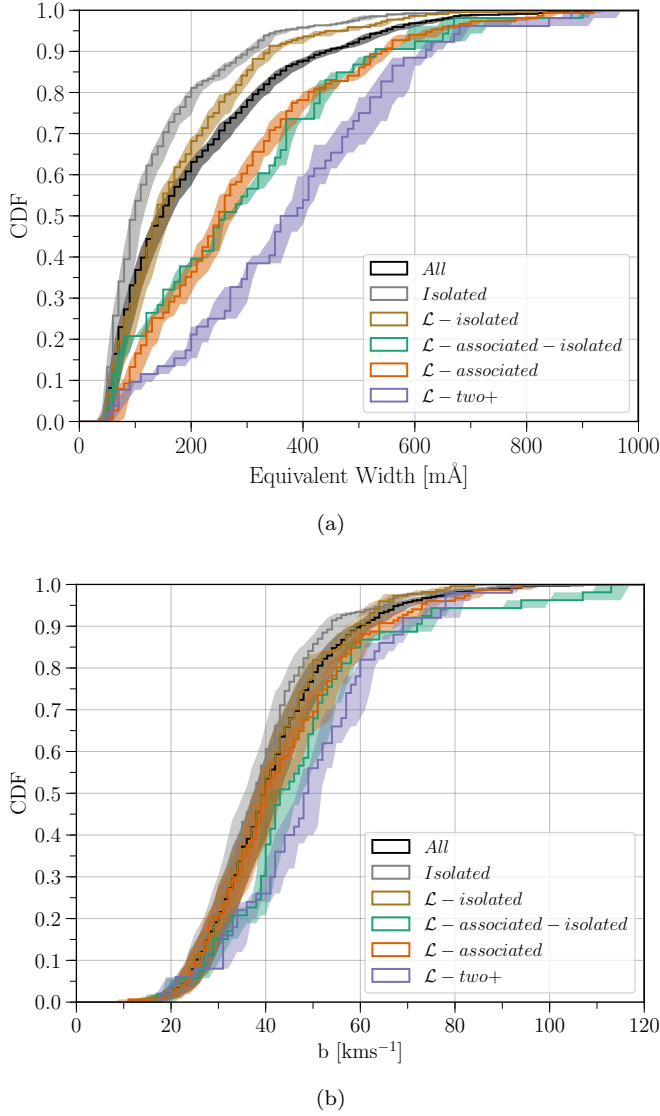
Figure 4. The equivalent width (a) and Doppler b-parameter (b) cumulative distribution functions for each subset of our Lyα absorber sample. From the top-left corner to the bottom-right the curves are the fully isolated absorbers (grey), the absorbers isolated enough from any galaxy to not be likelihood-matched (brown), the full distribution (black), the absorbers likelihood-matched to a single, non-isolated galaxy (orange), the absorbers matched to a single, isolated galaxy (green), and the absorbers likelihood-matched with two or more galaxies (purple). The shaded region around each curve gives the EW (b-parameter) measurement errors. Only EW ≥ 50 mÅ absorbers are included to mitigate any bias due to the detection limit of lower-SN targets.

Here we explore the effect of environment on the equivalent width of our Lyα absorber sample. Figure 4(a) shows the cumulative distribution function of equivalent widths for each of our 5 likelihood-separated subsets, along with that of the entire sample in black). We have only included EW ≥ 50 mÅ here to mitigate any bias due to the detection limit of lower-SN targets. We find that each subset occupies a distinct space aside from the $\mathcal{L} - associated - isolated$ and $\mathcal{L} - associated$ sets, which are essentially indistinguishable. The physical result of this is that the strength EW of Lyα absorption depends strongly on environment. Stronger absorption lines are preferentially found near to galaxies, and the strongest lines are found near multiple galaxy systems. The result of Anderson-Darling statistical distribution tests between each subset indicate that our *isolated* and $\mathcal{L} - isolated$ subsets are distinct from each of $\mathcal{L} - two+$, and $\mathcal{L} - associated - isolated$ and $\mathcal{L} - associated$ at a $> 95\%$ confidence level. Because $\mathcal{L} - associated - isolated$ and $\mathcal{L} - associated$ are found to be nearly indistinguishable via these test and by-eye, we will combine them for the remainder of this analysis.

This separation between EW distributions based on galaxy proximity is likely an effect of the distribution of the cosmic web; multiple galaxies should form from denser sections and intersections of intergalactic filaments, and these environments should thus also produce a stronger absorption profile.

This result on it's own does not however illuminate any deeper connection or relationship between the individual galaxies and absorbers. Let us now consider the dependence of EW on galaxy impact parameter, as illustrated in Figure 5(a). We have also plotted EW as a function of virial radius normalized impact parameter ($\rho/R_{\rm vir}$) in Figure 5(b). Firstly, we notice that weak (EW $\lesssim 400$ mÅ) absorbers are found at all impact parameters and $\rho/R_{\rm vir}$, which agrees with our findings above from Figure 4(a). Moreover, absorbers stronger than EW ~ 400 mÅ are preferentially found close to galaxies, and absorbers with EW ~ 800 mÅ are *only* found within 100 kpc and $1R_{\rm vir}$. Hence, weak EW $\lesssim 400$ mÅ absorbers are most likely Lyα-forest material, while the stronger absorbers are associated with the galaxies.

Secondly, we have included linear fits in both Figures 5(a) and 5(b) as shown by the dashed-black lines. In each case we find a strong negative slope, and by eye the virial radius normalized version appearing to be the stronger correlation. To test this we calculated the Pearson correlation coefficient r-value for each fit. For the purely impact parameter correlation we find a Pearson r-value $= -0.26$, with a p-value of $p = 1.2 \times 10^{-4}$, which indicates a weak but statistically significant negative correlation. For the virial radius normalized correlation we find $r = -0.35$ with $p = 1.2 \times 10^{-7}$, indicating a stronger and *more significant* negative correlation. If true, then the EW of Lyα absorption depends on the size of galaxy halos. Hence, either the physical or number density (or both) of absorbing cloudlets is greater closer to galaxies in a halo-scale dependent manner. The
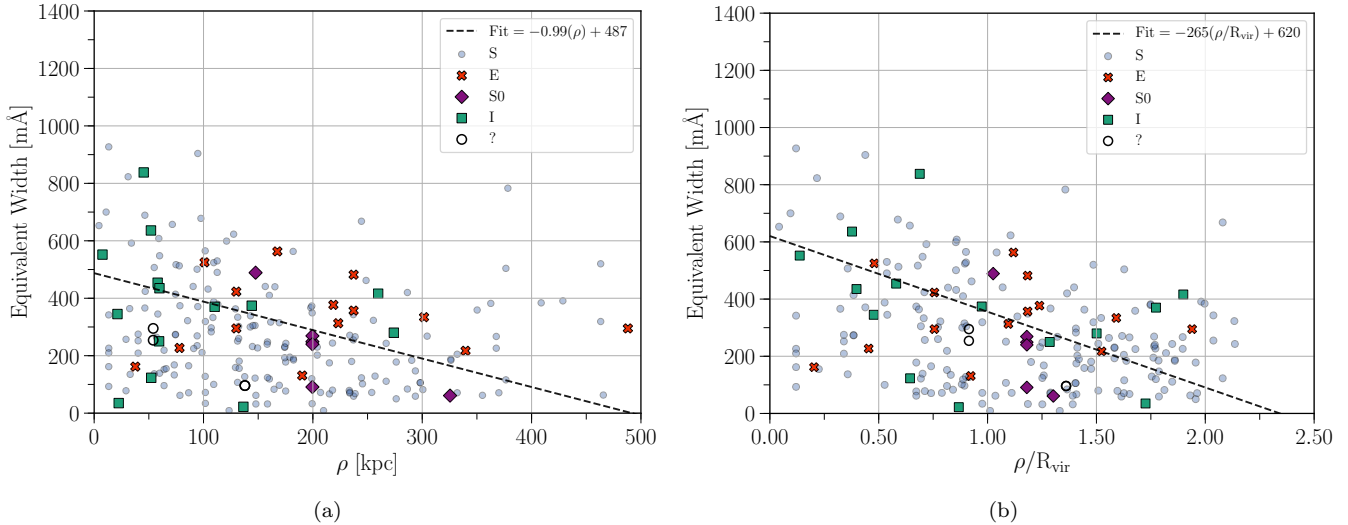
Figure 5. Left: The equivalent width (EW) of absorbers a function of impact parameter (ρ) to the associated galaxy. The best fit shown by the dashed-black line has the form: $EW = m(\rho) + b$, with $m = -0.99 \pm 0.25$ and $b = 487 \pm 49$. **Right:** The EW of absorbers a function of impact parameter to the associated galaxy normalized by the galaxy virial radius ($\rho/R_{\rm vir}$). The best fit shown by the dashed-black line has the form: $EW = m(\rho/R_{\rm vir}) + b$, with $m = -265 \pm 48$ and $b = 620 \pm 59$. **Both:** All $\mathcal{L} - associated - isolated$ and $\mathcal{L} - associated$ systems are included here. Blue-circles indicate spiral-type galaxies, green-squares indicate irregulars, red-crosses indicate ellipticals, purple-diamonds indicate S0's, and open black-circles indicate ambiguous morphological types.

increased density of this neutral material could signify both inflows or outflows from galaxies, with inflows expected to harbor a greater fraction of the cool, neutral H I most readily traced by Lyα. An analysis of metals associated with these neutral cloudlets could provide clues to which is the mechanism source at play here.

Thirdly, let us consider the effect of galaxy morphology on the associated absorption, which we have indicated in Figure 5 by the color and style of the plot points. In each figure blue-circles indicate spiral-type galaxies, green-squares indicate irregulars, red-crosses indicate ellipticals, purple-diamonds indicate S0's, and open black-circles indicate ambiguous or unknown types. Spiral galaxies are clearly the dominant type, and are found at all impact parameter and EW. **WHAT FRACTION OF ALL GALAXIES ARE SPIRAL VS E?**. Irregulars are the next most common, but are not spread around as evenly. All but two irregular-type systems are separated by less than 150 kpc in Figure 5(a), and few low-EW absorbers are found within $\sim 0.5R_{\rm vir}$ in Figure 5(b). In the first case, this can be explained by irregulars having a smaller average size ($\overline{R}_{\rm vir} = 101$ kpc for irregulars, compared to 145, 178, and 194 kpc for spirals, S0's, and ellipticals). When normalized by virial radius however, the lack of low-EW absorbers at low $\rho/R_{\rm vir}$ could be an indication of more gas-rich halos. This would make sense, since irregular galaxies are often tidally disturbed due to recent interactions which can result in extended, gas-rich halos.

Finally, we also see that elliptical and S0 galaxies are associated with mostly low-EW absorption, especially within 100 kpc and $\sim 0.5R_{\rm vir}$. **MORE**

3.3. *Doppler b-parameter*

Here we explore the effect of environment on the Doppler b-parameter of our Lyα absorber sample. In an analogous fashion as above, Figure 4(b) shows the cumulative distribution functions for the Doppler b-parameters of each subset of absorbers. Similar to the EW result, the Doppler b-parameters trend toward larger values based on their proximity to galaxies. The separation here however is far weaker. While the separation between, e.g., *isolated* and $\mathcal{L} - two+$ samples, remains statistically significant, we cannot claim any further significance between the other subsets.

Our b-parameters are derived via the second moment of the apparent optical depth profile, and therefore these b-parameter estimates become highly uncertain for EW $\gtrsim 350$ mÅ. For these stronger lines the profile becomes saturated, producing a degeneracy between EW and b. Unfortunately these are the very lines we expect to be most associated with near or multiple galaxy galaxy systems. This issue is illustrated by Figure 6, where we have show the b-parameters as a function of impact parameter and Δv for the full sample (Figures 6(a) and 6(c)) and for only those systems with EW ≤ 400mÅ (Figures 6(b) and 6(d)). While a strong correlation is implied between b and ρ without any cuts, this completely disappears once the stronger absorbers are re-

(a)

(b)

(c)

(d)

Figure 6. (a) The median inclination of galaxies is shown as a function of likelihood $\mathcal{L}$ for both detection (blue-diamonds) and non-detections (red-crosses) of associated absorbers. Detection and non-detection median inclinations are also shown for minimum EW ≥ 200 mÅ absorber equivalent widths by the thinner, semi-transparent lines. (b) The detection fraction plotted directly as a function of inclination for systems inside (blue-diamonds) and outside (red-crosses) $1.5\rho/R_{\mathrm{vir}}$.

moved. A similar albeit less extreme effect is seen for b as a function of Δv. A careful profile fitting analysis is the best way forward here, which we will reserve for a future work.

3.4. *Inclination*

Here we investigate the inclination dependence of Lyα absorber properties. In Figure 7 we display the distribution of all associated galaxies alongside the distribution of all galaxy inclinations in the survey volume (again, $\mathcal{L} - associated - isolated$ and $\mathcal{L} - associated$ subsets are combined here; see Chapter 2 for a full discussion of our galaxy dataset). As we first discovered in French & Wakker (2017), there is an overabundance of absorbers associated with high-inclination galaxies. To test the significance of this overabundance we used

the Anderson-Darling statistical distribution test, which yields a p-value of $AD_p = 7.2 \times 10^{-6}$. For a normal distribution this corresponds to $\sim 4.5\sigma$, indicating with a high confidence limit that these associated galaxies are *not* drawn from the same distribution as the all-sky galaxy population.

To further explore this phenomenon we have also calculated the detection fraction as a function of inclination and likelihood $\mathcal{L}$. Figure 8(a) shows the median inclination as a function of $\mathcal{L}$ for galaxies. For a galaxy at a given value of $\mathcal{L}$, the solid blue-diamond line gives the median inclination if we detect an absorber within $\Delta v \leq 400$ km s^{-1}, and the dashed blue-cross line gives the same for systems *without* a Lyα detection. The error bars shown are calculated by a 10,000 repetition bootstrap analysis with replacement (i.e., we randomly
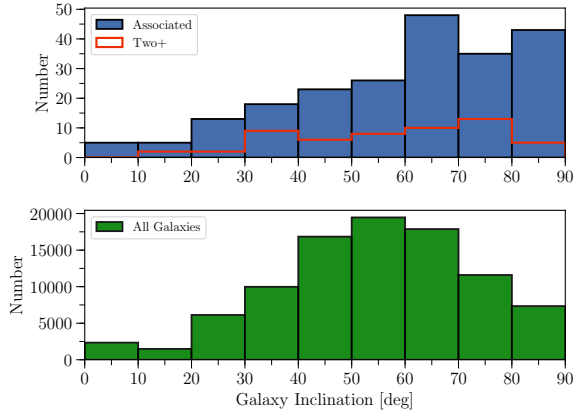
Figure 7. **Top:** The distribution of all associated galaxy inclinations is shown in blue. The overlaid red histogram shows the distribution of the highest $\mathcal{L}$-galaxy inclinations from the $\mathcal{L} - two+$ subset. **Bottom:** The distribution of all galaxies in the survey volume (i.e., $cz \leq 10,000 \text{ km s}^{-1}$).

resample the distribution of inclinations while allowing for duplicate entries, and then compute the standard deviation of the resulting sample distribution). Figure 8(a) shows that at very low $\mathcal{L}$ both detections and non-detections have the same median inclination, but the distributions then split at higher $\mathcal{L}$ where the sightline is closer to the galaxy halos. Thus, we are more likely to detect an absorber near a highly inclined galaxy.

This result is most easily explained by evoking a non-spherical H I galaxy halo. For example, if absorbers are distributed in a perfectly spherical manner around galaxies, then we would expect just as many non-detections as detections at any given galaxy inclination and impact parameter (or likelihood) from a sightline. We do not find this. Thus, the distribution of Lyα absorbers around galaxies must be non-spherical, with a flattened, disk-like Lyα halo fitting the bill nicely. Additionally, Figure 8(b) shows the detection fraction directly as a function of inclination, where we have separated our sample into near ($\rho/R_{\rm vir} \leq 1.5$) and far distributions. Here we can see that the detection fraction is more strongly dependent on inclination for the near systems, where we would expect a stronger effect due to a non-spherical halo.

3.5. *Azimuth*

Here we investigate the dependence of Lyα absorber properties on their orientation with respect to the major axis of nearby galaxies. Figure 9(a) shows the distribution of azimuth angles for systems from the combined $\mathcal{L} - associated$ and $\mathcal{L} - associated - isolated$ subsets in blue, along with the distribution for the $\mathcal{L} - two+$ subset in red. There appears to be a bimodal distribution here, with an excess of absorbers near low (major-axis) and high (minor-axis) azimuth angles. The same is not seen for the $\mathcal{L} - two+$ subset, suggesting the presence of other
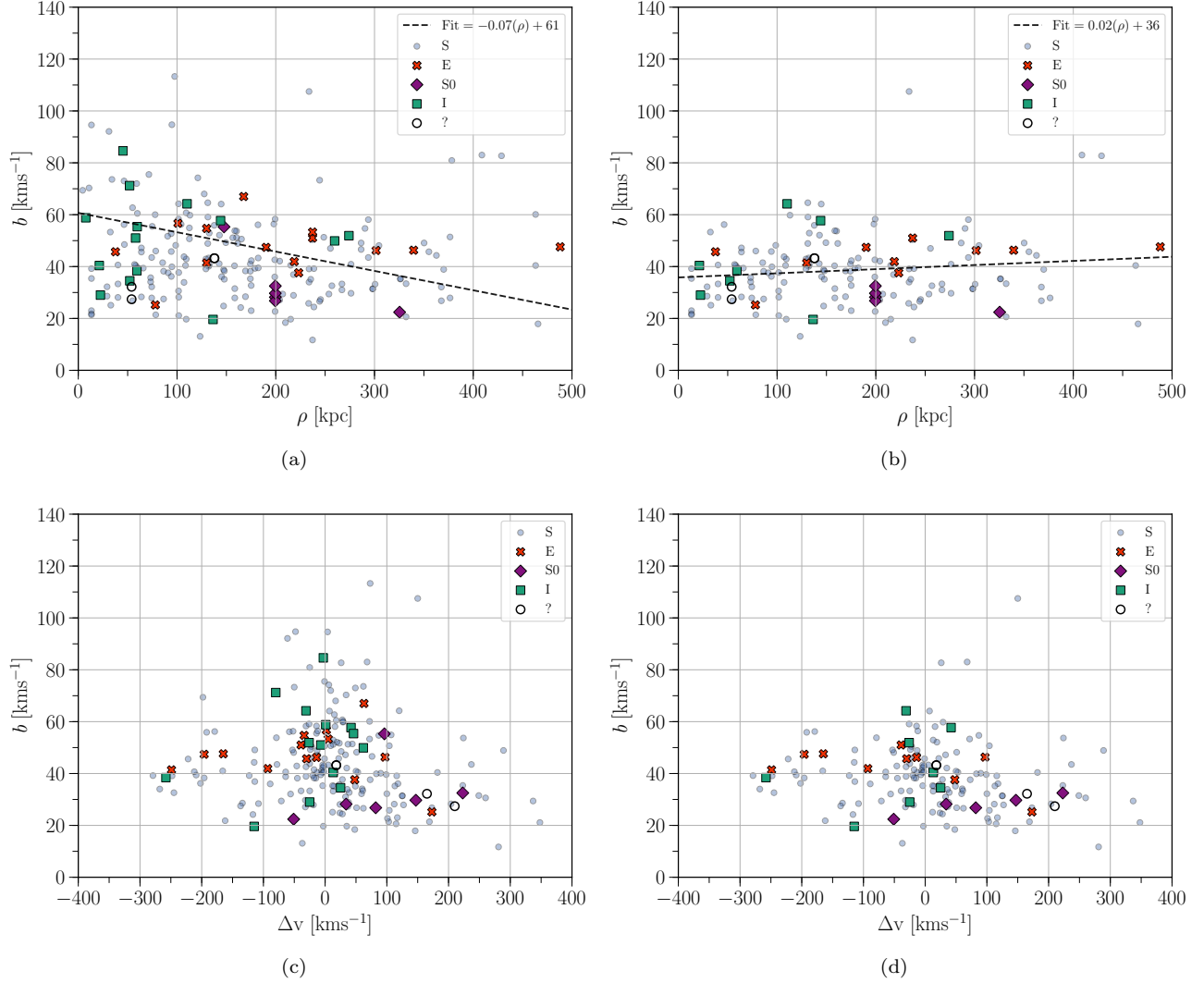

(a)

(b)
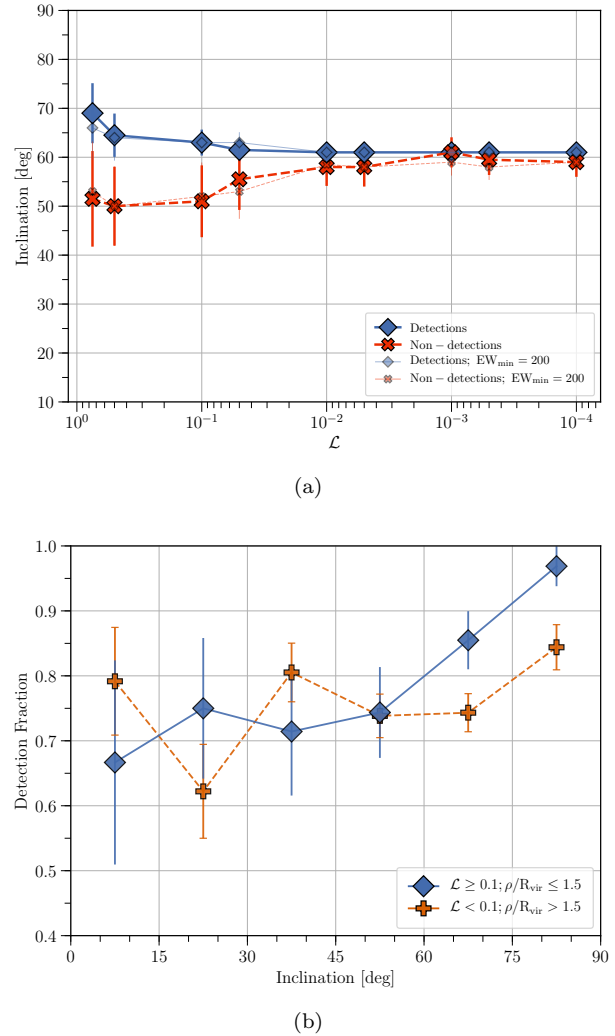
Figure 8. (a) The median inclination of galaxies is shown as a function of likelihood $\mathcal{L}$ for both detection (blue-diamonds) and non-detections (red-crosses) of associated absorbers. Detection and non-detection median inclinations are also shown for minimum EW ≥ 200 mÅ absorber equivalent widths by the thinner, semi-transparent lines. (b) The detection fraction plotted directly as a function of inclination for systems inside (blue-diamonds) and outside (red-crosses) $1.5\rho/R_{\rm vir}$.

nearby galaxies may be stirring up the Lyα absorbing material in these galaxies' halos.

Again, we can check the detection fraction as a function of azimuth. Figure 9(b) shows this, with the sample split into near ($\rho/R_{\rm vir} \leq 1.5$) and far distributions shown by blue-diamonds and red-crosses. This detection fraction further backs up the bimodal distribution suggested above, with an elevated detection fraction at both low (major-axis) and high (minor-axis) azimuth angles. The systems beyond $1.5\rho/R_{\rm vir}$ show a much weaker trend, as expected for systems beyond the direct influence of galaxy halos. This result also agrees

(a)

(b)
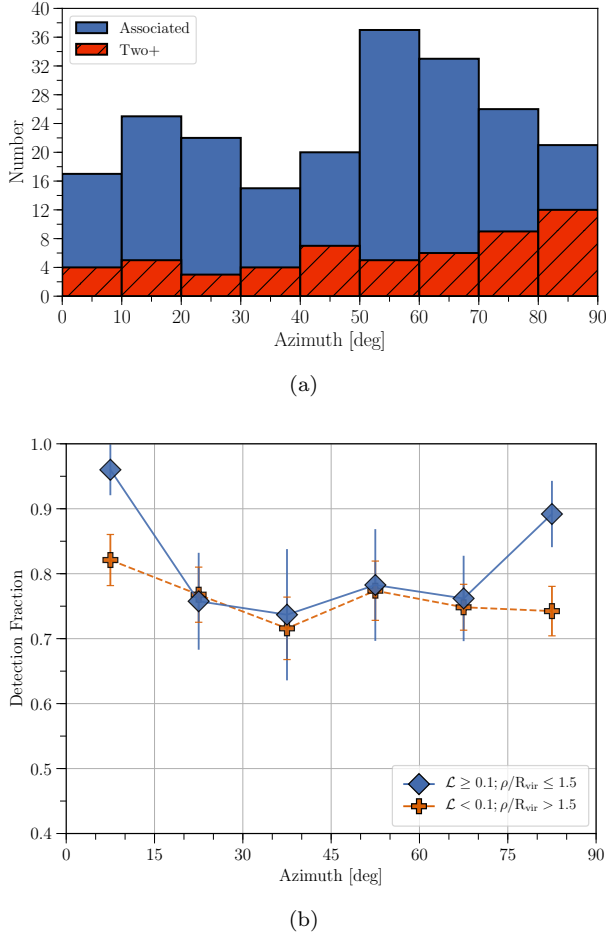
Figure 9. (a) The distribution of azimuth angles for the combined $\mathcal{L}-associated$ and $\mathcal{L}-associated-isolated$ subsets is shown in blue, with the $\mathcal{L}-two+$ subset shown in red. (b) The detection fraction plotted as a function of azimuth for systems inside (blue-diamonds) and outside (red-crosses) $1.5\rho/R_{\rm vir}$.

with the expectation that gas found near the major axis of a galaxy represents accreting material, while material around the minor axis represents outflows (e.g., Bordoloi et al. 2011; Bouché et al. 2012; Kacprzak et al. 2012; Bordoloi et al. 2014; Nielsen et al. 2015). While we cannot tell whether this material is actively inflowing or outflowing, simply the heightened presence of material in the expected regions provides tantalizing hints.

4. SUMMARY

Here we summarize the results of our study of the Lyα absorber-galaxy connection.

1. The equivalent width of Lyα absorbers depends strongly on environment. The most isolated absorbers are the weakest, with a smooth transition to the strongest absorbers residing very near to multiple galaxies. A similar but far weaker trend is seen for the absorber Doppler b-parameters.

2. Lyα absorber EW correlates most strongly with impact parameter when normalized by the associated galaxy virial radii. We find evidence for a lack of strong absorber within $\sim 0.5R_{\rm vir}$ of elliptical or S0 type galaxies, but we lack enough systems of these types to report strong limits on this observation.

3. Lyα absorbers with EW $\lesssim 100$mÅ are ubiquitous, making up nearly 50% of all Lyα systems in the nearby Universe, and do not correlate strongly with environment (70% of these weak absorbers are isolated).

4. We confirm the French & Wakker (2017) findings of an overabundance of absorbers located near highly inclined galaxies, and improve the significance of this finding to 4.5σ. We correspondingly find that the Lyα detection fraction increases with increasing galaxy inclination, and that this trend is strongest for systems separated by $1.5R_{\rm vir}$ or less.

5. We report the first detection of a Lyα azimuth angle dependence, finding the most absorbers associated with galaxy major and minor axes at a 3.3σ significance. We correspondingly find that the Lyα detection fraction is double peaked around the major and minor axes within $1.5R_{\rm vir}$, but mostly flat outside of this distance.

5. FUTURE WORK

We have established large, rich dataset with which to explore the relationship between circumgalactic material and the galaxies that reside in it. Much can still be learned by continuing to delving deeper into this data. The first future goal we have is to produce galaxy-Lyα two-point cross-correlation functions, as has been demonstrated by, e.g., Chen et al. (2005), among others. This will be our first goal as it does not involve any significant additions to the data already presented here.

Our next goal will be to produce Voigt profile fits for each absorber. While equivalent widths and second-moment derived b-parameters are an incredibly convenient and powerful tool to study

Metals

Facility: HST (COS)

REFERENCES

Bordoloi, R., Lilly, S. J., Kacprzak, G. G., & Churchill, C. W. 2014, ApJ, 784, 108

Bordoloi, R., Lilly, S. J., Knobel, C., et al. 2011, ApJ, 743, 10

Bouché, N., Hohensee, W., Vargas, R., et al. 2012, MNRAS, 426, 801

Bowen, D. V., Pettini, M., & Blades, J. C. 2002, ApJ, 580, 169

Bowen, D. V., Pettini, M., & Boyle, B. J. 1998, MNRAS, 297, 239

Chen, D. N., Jing, Y. P., & Yoshikaw, K. 2003, ApJ, 597, 35

Chen, H.-W., Prochaska, J. X., Weiner, B. J., Mulchaey, J. S., & Williger, G. M. 2005, ApJL, 629, L25

Chen, H.-W., & Tinker, J. L. 2008, ApJ, 687, 745

French, D. M., & Wakker, B. P. 2017, ApJ, 837, 138

Green, J. C., Froning, C. S., Osterman, S., et al. 2012, ApJ, 744, 60

Kacprzak, G. G., Churchill, C. W., & Nielsen, N. M. 2012, ApJL, 760, L7

Lanzetta, K. M., Bowen, D. V., Tytler, D., & Webb, J. K. 1995, ApJ, 442, 538

Nielsen, N. M., Churchill, C. W., Kacprzak, G. G., Murphy, M. T., & Evans, J. L. 2015, ApJ, 812, 83

Prochaska, J. X., Weiner, B., Chen, H.-W., Mulchaey, J., & Cooksey, K. 2011, ApJ, 740, 91

Steidel, C. C., Erb, D. K., Shapley, A. E., et al. 2010, ApJ, 717, 289

Wakker, B. P., & Savage, B. D. 2009, ApJS, 182, 378

APPENDIX

Here we provide the observation and measurement data for all targets included in this work.

Table 2. Summary of QSO Sample

Target	R.A.	Dec.	z	Program	$T_{\exp}$	S/N	$v_{\mathrm{Ly}\alpha}$	$EW_{\mathrm{Ly}\alpha}$	b
					(ks)	(1238 Å)	$(\mathrm{km\,s^{-1}})$	(mÅ)	$(\mathrm{km\,s^{-1}})$
(1)	(2)	(3)	(4)	(5)	(6)	(7)	(8)	(9)	(10)
1H0419-577	04 26 00.8	−57 12 01.0	0.10400	11686	20429	58.4	1075.0	249.0	28.2
1H0419-577	04 26 00.8	−57 12 01.0	0.10400	11686	20429	58.4	1123.0	269.0	26.8
1H0419-577	04 26 00.8	−57 12 01.0	0.10400	11686	20429	58.4	1188.0	240.0	29.7
1H0419-577	04 26 00.8	−57 12 01.0	0.10400	11686	20429	58.4	1264.0	91.0	32.5
1H0419-577	04 26 00.8	−57 12 01.0	0.10400	11686	20429	58.4	2020.0	9.0	17.5
1H0419-577	04 26 00.8	−57 12 01.0	0.10400	11686	20429	58.4	7801.0	122.0	43.9
1H0419-577	04 26 00.8	−57 12 01.0	0.10400	11686	20429	58.4	8819.0	39.0	30.4
1H0419-577	04 26 00.8	−57 12 01.0	0.10400	11686	20429	58.4	9962.0	34.0	23.3
1H0717+714	07 21 53.5	+71 20 36.0	0.23149	12025	6000	23.4	2873.0	349.0	58.3
1H0717+714	07 21 53.5	+71 20 36.0	0.23149	12025	6000	23.4	2988.0	33.0	22.7
1H0717+714	07 21 53.5	+71 20 36.0	0.23149	12025	6000	23.4	3840.0	39.0	38.2
1H0717+714	07 21 53.5	+71 20 36.0	0.23149	12025	6000	23.4	5283.0	51.0	49.9
1H0717+714	07 21 53.5	+71 20 36.0	0.23149	12025	6000	23.4	6271.0	167.0	44.4
1H0717+714	07 21 53.5	+71 20 36.0	0.23149	12025	6000	23.4	6595.0	64.0	38.6
1H0717+714	07 21 53.5	+71 20 36.0	0.23149	12025	6000	23.4	7799.0	52.0	27.9
1H1613-097	16 15 19.1	−09 36 13.0	0.06496	13448	4833	12.9	3678.0	39.0	17.5
1H1613-097	16 15 19.1	−09 36 13.0	0.06496	13448	4833	12.9	5259.0	55.0	19.6
1H1613-097	16 15 19.1	−09 36 13.0	0.06496	13448	4833	12.9	7326.0	212.0	42.9
1H1613-097	16 15 19.1	−09 36 13.0	0.06496	13448	4833	12.9	8204.0	339.0	40.5
2E1530+1511	15 33 14.3	+15 01 02.0	0.09000	14071	9348	9.1	1795.0	507.0	62.7
2E1530+1511	15 33 14.3	+15 01 02.0	0.09000	14071	9348	9.1	1953.0	137.0	26.8
2dFGRS_S393Z082	02 45 00.8	−30 07 23.0	0.33921	12988	17668	11.5	1236.0	563.0	60.9
2dFGRS_S393Z082	02 45 00.8	−30 07 23.0	0.33921	12988	17668	11.5	3011.0	48.0	19.2
2dFGRS_S393Z082	02 45 00.8	−30 07 23.0	0.33921	12988	17668	11.5	3759.0	58.0	40.2
2dFGRS_S393Z082	02 45 00.8	−30 07 23.0	0.33921	12988	17668	11.5	4042.0	36.0	17.9
3C232	09 58 20.9	+32 24 02.0	0.53060	P107	11000	11.4	1467.0	3822.0	386.5
3C232	09 58 20.9	+32 24 02.0	0.53060	P107	11000	11.4	1408.0	2092.0	212.8
3C232	09 58 20.9	+32 24 02.0	0.53060	P107	11000	11.4	1510.0	700.0	70.3
3C232	09 58 20.9	+32 24 02.0	0.53060	P107	11000	11.4	1641.0	1635.0	191.9
3C232	09 58 20.9	+32 24 02.0	0.53060	P107	11000	11.4	4528.0	128.0	76.8
3C249.1	11 04 13.8	+76 58 58.0	0.31150	4939	19157	9.1	1860.0	43.0	25.6
3C249.1	11 04 13.8	+76 58 58.0	0.31150	4939	19157	9.1	6674.0	249.0	53.9
3C249.1	11 04 13.8	+76 58 58.0	0.31150	4939	19157	9.1	7815.0	287.0	44.4
3C249.1	11 04 13.8	+76 58 58.0	0.31150	4939	19157	9.1	8383.0	294.0	39.4
3C263	11 39 57.0	+65 47 51.0	0.64600	11541	15360	35.7	2175.0	52.0	29.3
3C263	11 39 57.0	+65 47 51.0	0.64600	11541	15360	35.7	3910.0	12.0	17.1
3C263	11 39 57.0	+65 47 51.0	0.64600	11541	15360	35.7	8954.0	42.0	23.6
3C263	11 39 57.0	+65 47 51.0	0.64600	11541	15360	35.7	9651.0	13.0	14.8
3C263	11 39 57.0	+65 47 51.0	0.64600	11541	15360	35.7	9764.0	134.0	44.6
3C273.0	12 29 06.7	+02 03 09.0	0.15834	12038	4002	63.2	1013.0	382.0	44.3
3C273.0	12 29 06.7	+02 03 09.0	0.15834	12038	4002	63.2	1580.0	369.0	42.0
3C273.0	12 29 06.7	+02 03 09.0	0.15834	12038	4002	63.2	2156.0	42.0	57.9
3C273.0	12 29 06.7	+02 03 09.0	0.15834	12038	4002	63.2	2267.0	27.0	36.1
3C273.0	12 29 06.7	+02 03 09.0	0.15834	12038	4002	63.2	7857.0	42.0	30.6
3C273.0	12 29 06.7	+02 03 09.0	0.15834	12038	4002	63.2	8828.0	138.0	49.9

Table 2 continued

Table 2 *(continued)*

Target	R.A.	Dec.	z	Program	$T_{\exp}$	S/N	$v_{\mathrm{Ly}\alpha}$	$EW_{\mathrm{Ly}\alpha}$	b
					(ks)	(1238 Å)	$(\mathrm{km\,s^{-1}})$	(mÅ)	$(\mathrm{km\,s^{-1}})$
(1)	(2)	(3)	(4)	(5)	(6)	(7)	(8)	(9)	(10)
3C273.0	12 29 06.7	+02 03 09.0	0.15834	12038	4002	63.2	9835.0	39.0	30.0
3C323.1	15 47 43.6	+20 52 16.0	0.26430	13398	9841	24.2	2133.0	240.0	50.1
3C323.1	15 47 43.6	+20 52 16.0	0.26430	13398	9841	24.2	4222.0	290.0	46.1
3C323.1	15 47 43.6	+20 52 16.0	0.26430	13398	9841	24.2	4416.0	138.0	43.2
3C323.1	15 47 43.6	+20 52 16.0	0.26430	13398	9841	24.2	4749.0	55.0	35.9
3C323.1	15 47 43.6	+20 52 16.0	0.26430	13398	9841	24.2	6309.0	39.0	36.3
3C351.0	17 04 41.6	+60 44 29.0	0.37194	P108	142000	8.9	3462.0	147.0	49.0
3C351.0	17 04 41.6	+60 44 29.0	0.37194	P108	142000	8.9	3597.0	195.0	39.3
3C351.0	17 04 41.6	+60 44 29.0	0.37194	P108	142000	8.9	5078.0	81.0	33.7
3C351.0	17 04 41.6	+60 44 29.0	0.37194	P108	142000	8.9	5175.0	207.0	44.7
3C351.0	17 04 41.6	+60 44 29.0	0.37194	P108	142000	8.9	7172.0	60.0	27.6
3C351.0	17 04 41.6	+60 44 29.0	0.37194	P108	142000	8.9	8382.0	29.0	18.2
3C57	02 01 57.1	−11 32 34.0	0.66900	12038	10963	22.8	4581.0	35.0	20.9
3C57	02 01 57.1	−11 32 34.0	0.66900	12038	10963	22.8	5370.0	29.0	26.5
3C57	02 01 57.1	−11 32 34.0	0.66900	12038	10963	22.8	6685.0	32.0	20.2
3C57	02 01 57.1	−11 32 34.0	0.66900	12038	10963	22.8	8113.0	13.0	13.8
3C66A	02 22 39.6	+43 02 08.0	0.44400	12612	12600	25.9	4301.0	24.0	16.6
3C66A	02 22 39.6	+43 02 08.0	0.44400	12612	12600	25.9	8188.0	113.0	29.5
4C25.01	00 19 39.8	+26 02 52.0	0.28400	14268	3739	19.6	996.0	95.0	24.0
4C25.01	00 19 39.8	+26 02 52.0	0.28400	14268	3739	19.6	3351.0	55.0	39.0
4C25.01	00 19 39.8	+26 02 52.0	0.28400	14268	3739	19.6	9450.0	105.0	24.4
CSO1161	11 20 07.4	+42 35 51.0	0.22706	14772	4767	10	3144.0	164.0	39.3
CSO1161	11 20 07.4	+42 35 51.0	0.22706	14772	4767	10	3784.0	69.0	40.4
CSO1161	11 20 07.4	+42 35 51.0	0.22706	14772	4767	10	7322.0	253.0	48.0
CSO1161	11 20 07.4	+42 35 51.0	0.22706	14772	4767	10	7766.0	337.0	50.8
CSO1161	11 20 07.4	+42 35 51.0	0.22706	14772	4767	10	8827.0	187.0	55.0
CSO1161	11 20 07.4	+42 35 51.0	0.22706	14772	4767	10	8942.0	233.0	78.5
CSO1208	11 40 48.0	+46 22 05.0	0.11439	14729	7228	7.7	731.0	470.0	54.2
CSO1208	11 40 48.0	+46 22 05.0	0.11439	14729	7228	7.7	874.0	506.0	58.7
CSO1208	11 40 48.0	+46 22 05.0	0.11439	14729	7228	7.7	5339.0	129.0	25.5
CSO1208	11 40 48.0	+46 22 05.0	0.11439	14729	7228	7.7	6852.0	143.0	40.1
CSO1208	11 40 48.0	+46 22 05.0	0.11439	14729	7228	7.7	7281.0	83.0	23.8
CSO1208	11 40 48.0	+46 22 05.0	0.11439	14729	7228	7.7	7426.0	102.0	21.3
CSO1245	11 56 30.1	+42 52 54.0	1.01545	14772	4821	11	1178.0	74.0	23.7
CSO1245	11 56 30.1	+42 52 54.0	1.01545	14772	4821	11	3228.0	98.0	28.5
CSO1245	11 56 30.1	+42 52 54.0	1.01545	14772	4821	11	5590.0	33.0	17.9
CSO1245	11 56 30.1	+42 52 54.0	1.01545	14772	4821	11	7077.0	177.0	27.1
CSO1245	11 56 30.1	+42 52 54.0	1.01545	14772	4821	11	7139.0	204.0	24.9
CSO295	10 52 05.5	+36 40 40.0	0.60999	14772	2174	11.9	600.0	568.0	64.1
CSO295	10 52 05.5	+36 40 40.0	0.60999	14772	2174	11.9	662.0	585.0	77.5
CSO295	10 52 05.5	+36 40 40.0	0.60999	14772	2174	11.9	5658.0	117.0	38.0
CSO295	10 52 05.5	+36 40 40.0	0.60999	14772	2174	11.9	7640.0	352.0	68.3
CSO295	10 52 05.5	+36 40 40.0	0.60999	14772	2174	11.9	7774.0	150.0	31.4
CSO395	12 11 14.6	+36 57 39.0	0.17109	12248	3012	13.4	961.0	204.0	31.8
CSO395	12 11 14.6	+36 57 39.0	0.17109	12248	3012	13.4	1022.0	355.0	42.8
CSO395	12 11 14.6	+36 57 39.0	0.17109	12248	3012	13.4	961.0	204.0	31.8
CSO395	12 11 14.6	+36 57 39.0	0.17109	12248	3012	13.4	1022.0	355.0	42.8
CTS487	23 22 11.0	−34 47 57.0	0.42000	13448	8061	19.6	2750.0	80.0	44.4
ESO141-G55	19 21 14.3	−58 40 13.0	0.03600	12936	2178	37.1	2140.0	50.0	33.0
ESO141-G55	19 21 14.3	−58 40 13.0	0.03600	12936	2178	37.1	5283.0	26.0	35.4
ESO265-G23	11 20 47.9	−43 15 51.0	0.05600	12275	1983	14.7	8470.0	252.0	44.3
ESO350-IG38	00 36 52.9	−33 33 19.0	0.02060	13017	7596	17.8	1608.0	391.0	82.7

Table 2 continued

Table 2 *(continued)*

Target	R.A.	Dec.	z	Program	$T_{\exp}$	S/N	$v_{\mathrm{Ly}\alpha}$	$EW_{\mathrm{Ly}\alpha}$	b
					(ks)	(1238 Å)	$(\mathrm{km\,s}^{-1})$	(mÅ)	$(\mathrm{km\,s}^{-1})$
(1)	(2)	(3)	(4)	(5)	(6)	(7)	(8)	(9)	(10)
FAIRALL9	01 23 45.8	−58 48 21.0	0.04702	12604	4960	41.3	9515.0	73.0	34.0
FBQSJ0751+2919	07 51 12.3	+29 19 38.0	0.92240	11741	16531	27.5	3525.0	26.0	17.6
FBQSJ0751+2919	07 51 12.3	+29 19 38.0	0.92240	11741	16531	27.5	3560.0	41.0	23.8
FBQSJ0751+2919	07 51 12.3	+29 19 38.0	0.92240	11741	16531	27.5	3635.0	55.0	20.8
FBQSJ0751+2919	07 51 12.3	+29 19 38.0	0.92240	11741	16531	27.5	3677.0	44.0	23.9
FBQSJ0751+2919	07 51 12.3	+29 19 38.0	0.92240	11741	16531	27.5	6297.0	23.0	20.9
FBQSJ0751+2919	07 51 12.3	+29 19 38.0	0.92240	11741	16531	27.5	7380.0	22.0	24.8
FBQSJ0751+2919	07 51 12.3	+29 19 38.0	0.92240	11741	16531	27.5	8020.0	300.0	39.5
FBQSJ0908+3246	09 08 38.8	+32 46 20.0	0.25989	14240	7430	10	1915.0	202.0	27.1
FBQSJ0908+3246	09 08 38.8	+32 46 20.0	0.25989	14240	7430	10	1982.0	230.0	42.1
FBQSJ0908+3246	09 08 38.8	+32 46 20.0	0.25989	14240	7430	10	4287.0	367.0	56.4
FBQSJ0908+3246	09 08 38.8	+32 46 20.0	0.25989	14240	7430	10	7926.0	95.0	40.1
FBQSJ1134+2555	11 34 57.6	+25 55 28.0	0.70994	12248	4235	9.2	3070.0	106.0	32.3
FBQSJ1134+2555	11 34 57.6	+25 55 28.0	0.70994	12248	4235	9.2	6343.0	86.0	31.0
FBQSJ1134+2555	11 34 57.6	+25 55 28.0	0.70994	12248	4235	9.2	9552.0	636.0	71.2
FBQSJ1353+3620	13 53 26.0	+36 20 49.0	0.28504	13444	4777	13.9	2560.0	50.0	38.1
FBQSJ1353+3620	13 53 26.0	+36 20 49.0	0.28504	13444	4777	13.9	5464.0	86.0	43.2
FBQSJ1353+3620	13 53 26.0	+36 20 49.0	0.28504	13444	4777	13.9	6174.0	117.0	43.1
FBQSJ1353+3620	13 53 26.0	+36 20 49.0	0.28504	13444	4777	13.9	6587.0	395.0	67.3
FBQSJ1431+2442	14 31 25.8	+24 42 20.0	0.40691	12603	16501	17.5	2241.0	28.0	29.2
FBQSJ1431+2442	14 31 25.8	+24 42 20.0	0.40691	12603	16501	17.5	2804.0	29.0	18.3
FBQSJ1431+2442	14 31 25.8	+24 42 20.0	0.40691	12603	16501	17.5	4861.0	41.0	26.9
FBQSJ1431+2442	14 31 25.8	+24 42 20.0	0.40691	12603	16501	17.5	5662.0	94.0	50.5
FBQSJ1431+2442	14 31 25.8	+24 42 20.0	0.40691	12603	16501	17.5	6542.0	33.0	13.5
FBQSJ1431+2442	14 31 25.8	+24 42 20.0	0.40691	12603	16501	17.5	6623.0	285.0	47.0
FBS0150+396	01 53 06.7	+39 55 45.0	0.21190	14268	5022	9	5812.0	281.0	43.6
FBS0150+396	01 53 06.7	+39 55 45.0	0.21190	14268	5022	9	7270.0	74.0	49.0
FBS1526+659	15 27 28.5	+65 48 10.0	0.34500	12276	2032	10.8	7776.0	308.0	38.3
FBS1526+659	15 27 28.5	+65 48 10.0	0.34500	12276	2032	10.8	8975.0	466.0	50.8
H1101-232	11 03 37.7	−23 29 31.0	0.18600	12025	13341	16.4	1182.0	635.0	69.5
H1101-232	11 03 37.7	−23 29 31.0	0.18600	12025	13341	16.4	2117.0	46.0	34.6
H1101-232	11 03 37.7	−23 29 31.0	0.18600	12025	13341	16.4	3565.0	563.0	56.1
H1101-232	11 03 37.7	−23 29 31.0	0.18600	12025	13341	16.4	5835.0	38.0	29.4
H1101-232	11 03 37.7	−23 29 31.0	0.18600	12025	13341	16.4	8860.0	37.0	21.7
H1821+643	18 21 57.2	+64 20 36.0	0.29700	11484	12039	40.2	1100.0	33.0	26.1
H1821+643	18 21 57.2	+64 20 36.0	0.29700	11484	12039	40.2	2818.0	40.0	49.5
H1821+643	18 21 57.2	+64 20 36.0	0.29700	11484	12039	40.2	7313.0	338.0	42.6
H1821+643	18 21 57.2	+64 20 36.0	0.29700	11484	12039	40.2	7931.0	69.0	47.1
HE0056-3622	00 58 37.4	−36 06 05.0	0.16414	12604	4959	27.7	3462.0	227.0	49.2
HE0056-3622	00 58 37.4	−36 06 05.0	0.16414	12604	4959	27.7	5127.0	95.0	31.0
HE0056-3622	00 58 37.4	−36 06 05.0	0.16414	12604	4959	27.7	8455.0	120.0	38.2
HE0153-4520	01 55 13.2	−45 06 12.0	0.45100	11541	5228	29.8	6311.0	17.0	17.9
HE0153-4520	01 55 13.2	−45 06 12.0	0.45100	11541	5228	29.8	7101.0	31.0	28.2
HE0226-4110	02 28 15.2	−40 57 16.0	0.49500	11541	6775	27.7	3644.0	25.0	34.5
HE0226-4110	02 28 15.2	−40 57 16.0	0.49500	11541	6775	27.7	5233.0	72.0	33.1
HE0226-4110	02 28 15.2	−40 57 16.0	0.49500	11541	6775	27.7	7592.0	35.0	38.6
HE0226-4110	02 28 15.2	−40 57 16.0	0.49500	11541	6775	27.7	8027.0	102.0	43.4
HE0226-4110	02 28 15.2	−40 57 16.0	0.49500	11541	6775	27.7	9292.0	13.0	24.2
HE0241-3043	02 43 37.7	−30 30 48.0	0.66929	12988	6972	17.3	1219.0	77.0	23.0
HE0241-3043	02 43 37.7	−30 30 48.0	0.66929	12988	6972	17.3	1310.0	178.0	32.7
HE0241-3043	02 43 37.7	−30 30 48.0	0.66929	12988	6972	17.3	2299.0	65.0	45.4
HE0241-3043	02 43 37.7	−30 30 48.0	0.66929	12988	6972	17.3	2624.0	28.0	20.8

Table 2 continued

Table 2 *(continued)*

Target	R.A.	Dec.	z	Program	$T_{\rm exp}$	S/N	$v_{\rm Ly\alpha}$	$EW_{\rm Ly\alpha}$	b
					(ks)	(1238 Å)	$({\rm km\,s^{-1}})$	(mÅ)	$({\rm km\,s^{-1}})$
(1)	(2)	(3)	(4)	(5)	(6)	(7)	(8)	(9)	(10)
HE0241-3043	02 43 37.7	−30 30 48.0	0.66929	12988	6972	17.3	3096.0	34.0	33.3
HE0241-3043	02 43 37.7	−30 30 48.0	0.66929	12988	6972	17.3	4979.0	53.0	23.3
HE0241-3043	02 43 37.7	−30 30 48.0	0.66929	12988	6972	17.3	5681.0	29.0	13.9
HE0241-3043	02 43 37.7	−30 30 48.0	0.66929	12988	6972	17.3	7145.0	55.0	30.7
HE0241-3043	02 43 37.7	−30 30 48.0	0.66929	12988	6972	17.3	7487.0	57.0	41.1
HE0241-3043	02 43 37.7	−30 30 48.0	0.66929	12988	6972	17.3	9881.0	47.0	30.5
HE0340-2703	03 42 20.6	−26 53 59.0	0.28300	9378	4895	8.5	1345.0	268.0	48.1
HE0340-2703	03 42 20.6	−26 53 59.0	0.28300	9378	4895	8.5	1766.0	374.0	57.7
HE0340-2703	03 42 20.6	−26 53 59.0	0.28300	9378	4895	8.5	4083.0	194.0	36.6
HE0429-5343	04 30 40.0	−53 36 56.0	0.04001	12275	2067	15.1	1167.0	79.0	25.8
HE0429-5343	04 30 40.0	−53 36 56.0	0.04001	12275	2067	15.1	1358.0	136.0	57.8
HE0429-5343	04 30 40.0	−53 36 56.0	0.04001	12275	2067	15.1	3949.0	158.0	31.0
HE0429-5343	04 30 40.0	−53 36 56.0	0.04001	12275	2067	15.1	4951.0	134.0	34.1
HE0429-5343	04 30 40.0	−53 36 56.0	0.04001	12275	2067	15.1	5638.0	92.0	34.7
HE0429-5343	04 30 40.0	−53 36 56.0	0.04001	12275	2067	15.1	8953.0	555.0	61.1
HE0435-5304	04 36 50.8	−52 58 49.0	0.42616	11520	8372	13.3	1512.0	229.0	41.0
HE0435-5304	04 36 50.8	−52 58 49.0	0.42616	11520	8372	13.3	1633.0	231.0	38.2
HE0435-5304	04 36 50.8	−52 58 49.0	0.42616	11520	8372	13.3	1690.0	193.0	35.3
HE0435-5304	04 36 50.8	−52 58 49.0	0.42616	11520	8372	13.3	3936.0	88.0	42.3
HE0439-5254	04 40 12.0	−52 48 18.0	1.05300	11520	8402	26.7	613.0	154.0	61.3
HE0439-5254	04 40 12.0	−52 48 18.0	1.05300	11520	8402	26.7	1005.0	55.0	31.2
HE0439-5254	04 40 12.0	−52 48 18.0	1.05300	11520	8402	26.7	1148.0	72.0	42.5
HE0439-5254	04 40 12.0	−52 48 18.0	1.05300	11520	8402	26.7	1649.0	501.0	52.7
HE0439-5254	04 40 12.0	−52 48 18.0	1.05300	11520	8402	26.7	2780.0	48.0	25.4
HE0439-5254	04 40 12.0	−52 48 18.0	1.05300	11520	8402	26.7	3853.0	322.0	41.5
HE0439-5254	04 40 12.0	−52 48 18.0	1.05300	11520	8402	26.7	4656.0	64.0	29.8
HE0439-5254	04 40 12.0	−52 48 18.0	1.05300	11520	8402	26.7	5291.0	40.0	23.5
HE0439-5254	04 40 12.0	−52 48 18.0	1.05300	11520	8402	26.7	5879.0	38.0	28.9
HE0439-5254	04 40 12.0	−52 48 18.0	1.05300	11520	8402	26.7	6348.0	42.0	23.8
HE0439-5254	04 40 12.0	−52 48 18.0	1.05300	11520	8402	26.7	8063.0	33.0	18.4
HE1029-1401	10 31 54.4	−14 16 52.0	0.08600	MQ175	9598	30.2	2003.0	94.0	51.1
HE1029-1401	10 31 54.4	−14 16 52.0	0.08600	MQ175	9598	30.2	2457.0	178.0	46.1
HE1029-1401	10 31 54.4	−14 16 52.0	0.08600	MQ175	9598	30.2	4564.0	68.0	52.6
HE1136-1334	11 39 10.7	−13 50 43.0	0.55646	12275	7669	17.4	2211.0	34.0	36.4
HE1136-1334	11 39 10.7	−13 50 43.0	0.55646	12275	7669	17.4	3920.0	27.0	19.1
HE1136-1334	11 39 10.7	−13 50 43.0	0.55646	12275	7669	17.4	7381.0	32.0	39.6
HE1136-1334	11 39 10.7	−13 50 43.0	0.55646	12275	7669	17.4	8779.0	74.0	34.5
HE1136-1334	11 39 10.7	−13 50 43.0	0.55646	12275	7669	17.4	9723.0	57.0	34.2
HE1136-1334	11 39 10.7	−13 50 43.0	0.55646	12275	7669	17.4	9991.0	118.0	37.2
HE1159-1338	12 01 58.7	−13 55 00.0	0.50600	12275	7669	12.4	1524.0	378.0	46.5
HE1159-1338	12 01 58.7	−13 55 00.0	0.50600	12275	7669	12.4	8311.0	47.0	20.0
HE1217+0220	12 20 11.9	+02 03 42.0	0.24037	13852	2052	14.6	1789.0	250.0	38.4
HE1217+0220	12 20 11.9	+02 03 42.0	0.24037	13852	2052	14.6	2016.0	521.0	52.5
HE1217+0220	12 20 11.9	+02 03 42.0	0.24037	13852	2052	14.6	2235.0	548.0	60.5
HE1217+0220	12 20 11.9	+02 03 42.0	0.24037	13852	2052	14.6	2316.0	139.0	39.6
HE1228+0131	12 30 50.0	+01 15 23.0	0.11700	11686	11036	40.9	1176.0	9.0	18.4
HE1228+0131	12 30 50.0	+01 15 23.0	0.11700	11686	11036	40.9	1495.0	160.0	33.6
HE1228+0131	12 30 50.0	+01 15 23.0	0.11700	11686	11036	40.9	1571.0	23.0	17.9
HE1228+0131	12 30 50.0	+01 15 23.0	0.11700	11686	11036	40.9	1686.0	321.0	34.0
HE1228+0131	12 30 50.0	+01 15 23.0	0.11700	11686	11036	40.9	1721.0	303.0	33.0
HE1228+0131	12 30 50.0	+01 15 23.0	0.11700	11686	11036	40.9	1854.0	78.0	41.3
HE1228+0131	12 30 50.0	+01 15 23.0	0.11700	11686	11036	40.9	2311.0	343.0	39.3

Table 2 continued

Table 2 *(continued)*

Target	R.A.	Dec.	z	Program	$T_{\exp}$	S/N	$v_{\rm Ly\alpha}$	$EW_{\rm Ly\alpha}$	b
					(ks)	(1238 Å)	(km s^{-1})	(mÅ)	(km s^{-1})
(1)	(2)	(3)	(4)	(5)	(6)	(7)	(8)	(9)	(10)
HE1228+0131	12 30 50.0	+01 15 23.0	0.11700	11686	11036	40.9	7553.0	61.0	34.9
HE1228+0131	12 30 50.0	+01 15 23.0	0.11700	11686	11036	40.9	9240.0	248.0	53.8
HE1228+0131	12 30 50.0	+01 15 23.0	0.11700	11686	11036	40.9	9351.0	124.0	27.9
HE1228+0131	12 30 50.0	+01 15 23.0	0.11700	11686	11036	40.9	9568.0	32.0	31.5
HE1228+0131	12 30 50.0	+01 15 23.0	0.11700	11686	11036	40.9	9716.0	11.0	21.0
HE1340-0038	13 42 51.6	+00 53 45.0	0.32654	11598	4606	11.1	4547.0	78.0	41.6
HE1340-0038	13 42 51.6	+00 53 45.0	0.32654	11598	4606	11.1	7147.0	47.0	30.8
HE1340-0038	13 42 51.6	+00 53 45.0	0.32654	11598	4606	11.1	7781.0	32.0	23.3
HE2258-5524	23 01 52.0	−55 08 31.0	0.14100	13444	5185	17.9	1078.0	50.0	47.2
HE2259-5524	23 02 22.5	−55 08 27.0	0.85490	13444	10940	17.8	1729.0	88.0	59.0
HE2259-5524	23 02 22.5	−55 08 27.0	0.85490	13444	10940	17.8	7152.0	99.0	28.5
HE2259-5524	23 02 22.5	−55 08 27.0	0.85490	13444	10940	17.8	8035.0	51.0	48.4
HE2259-5524	23 02 22.5	−55 08 27.0	0.85490	13444	10940	17.8	8238.0	114.0	43.6
HE2259-5524	23 02 22.5	−55 08 27.0	0.85490	13444	10940	17.8	8384.0	31.0	14.4
HE2259-5524	23 02 22.5	−55 08 27.0	0.85490	13444	10940	17.8	8522.0	112.0	26.7
HE2332-3556	23 34 44.4	−35 39 47.0	0.11000	13444	7378	10.8	773.0	364.0	53.3
HE2332-3556	23 34 44.4	−35 39 47.0	0.11000	13444	7378	10.8	8391.0	64.0	24.8
HS0943+4725	09 46 21.2	+47 11 31.0	0.23022	12248	4436	4.4	4603.0	657.0	75.5
HS0943+4725	09 46 21.2	+47 11 31.0	0.23022	12248	4436	4.4	9847.0	181.0	35.9
HS1102+3441	11 05 39.8	+34 25 35.0	0.51000	11541	11381	17.4	1697.0	57.0	30.5
HS1102+3441	11 05 39.8	+34 25 35.0	0.51000	11541	11381	17.4	1927.0	191.0	46.0
HS1102+3441	11 05 39.8	+34 25 35.0	0.51000	11541	11381	17.4	7245.0	196.0	41.4
HS1102+3441	11 05 39.8	+34 25 35.0	0.51000	11541	11381	17.4	8944.0	75.0	34.7
HS1111+4309	11 13 57.4	+42 53 27.0	0.44204	14772	4797	12.9	3173.0	194.0	45.9
HS1111+4309	11 13 57.4	+42 53 27.0	0.44204	14772	4797	12.9	6429.0	70.0	28.6
HS1111+4309	11 13 57.4	+42 53 27.0	0.44204	14772	4797	12.9	6836.0	99.0	39.3
HS1111+4309	11 13 57.4	+42 53 27.0	0.44204	14772	4797	12.9	7351.0	40.0	24.0
HS1231+4814	12 33 35.1	+47 58 01.0	0.38223	11598	5929	12.9	9175.0	102.0	27.3
HS1302+2510	13 04 51.4	+24 54 46.0	0.60500	13382	5134	13.6	438.0	422.0	62.4
HS1543+5921	15 44 20.2	+59 12 27.0	0.80700	P108	8300	12.3	2889.0	8660.0	885.9
HS1831+5338	18 32 49.7	+53 40 22.0	0.04536	12275	8284	17.3	773.0	54.0	24.9
HS1831+5338	18 32 49.7	+53 40 22.0	0.04536	12275	8284	17.3	2122.0	35.0	32.5
HS1831+5338	18 32 49.7	+53 40 22.0	0.04536	12275	8284	17.3	3637.0	79.0	28.4
HS1831+5338	18 32 49.7	+53 40 22.0	0.04536	12275	8284	17.3	5145.0	520.0	76.9
IRAS_F09539-0439	09 56 30.2	−04 53 16.0	0.15700	12275	7696	17	1472.0	163.0	44.1
IRAS_F21325-6237	21 36 23.2	−62 24 00.0	0.05880	12936	4230	34.2	8329.0	71.0	33.8
IRAS_F21325-6237	21 36 23.2	−62 24 00.0	0.05880	12936	4230	34.2	8419.0	27.0	23.9
IRAS_Z06229-6434	06 23 07.7	−64 36 19.0	0.12889	11692	8728	28.2	1276.0	63.0	30.6
IRAS_Z06229-6434	06 23 07.7	−64 36 19.0	0.12889	11692	8728	28.2	3683.0	283.0	39.0
KAZ447	17 03 28.9	+61 41 09.0	0.07732	12276	5173	12.8	8296.0	333.0	46.2
KAZ447	17 03 28.9	+61 41 09.0	0.07732	12276	5173	12.8	9568.0	52.0	23.2
KAZ447	17 03 28.9	+61 41 09.0	0.07732	12276	5173	12.8	9994.0	176.0	44.0
LBQS1218+1611	12 21 02.5	+15 54 47.0	0.22945	11698	2263	6.7	6304.0	138.0	38.0
LBQS1218+1611	12 21 02.5	+15 54 47.0	0.22945	11698	2263	6.7	6788.0	66.0	31.2
LBQS1218+1611	12 21 02.5	+15 54 47.0	0.22945	11698	2263	6.7	6901.0	340.0	42.3
LBQS1220+1006	12 23 12.1	+09 50 19.0	0.27692	11698	2258	7	1531.0	59.0	11.7
LBQS1220+1006	12 23 12.1	+09 50 19.0	0.27692	11698	2258	7	1834.0	62.0	19.9
LBQS1220+1006	12 23 12.1	+09 50 19.0	0.27692	11698	2258	7	2458.0	86.0	28.3
LBQS1220+1006	12 23 12.1	+09 50 19.0	0.27692	11698	2258	7	4765.0	146.0	59.1
LBQS1220+1006	12 23 12.1	+09 50 19.0	0.27692	11698	2258	7	5505.0	170.0	45.2
LBQS1220+1006	12 23 12.1	+09 50 19.0	0.27692	11698	2258	7	6435.0	315.0	47.5
LBQS1220+1006	12 23 12.1	+09 50 19.0	0.27692	11698	2258	7	7865.0	443.0	50.1

Table 2 continued

Table 2 *(continued)*

Target	R.A.	Dec.	z	Program	$T_{\exp}$	S/N	$v_{\mathrm{Ly}\alpha}$	$EW_{\mathrm{Ly}\alpha}$	b
					(ks)	(1238 Å)	$(\mathrm{km\,s^{-1}})$	(mÅ)	$(\mathrm{km\,s^{-1}})$
(1)	(2)	(3)	(4)	(5)	(6)	(7)	(8)	(9)	(10)
LBQS1230-0015	12 33 04.1	+00 31 34.0	0.47095	11598	10323	13.8	1126.0	388.0	42.9
LBQS1230-0015	12 33 04.1	+00 31 34.0	0.47095	11598	10323	13.8	1163.0	100.0	19.7
LBQS1230-0015	12 33 04.1	+00 31 34.0	0.47095	11598	10323	13.8	2406.0	107.0	24.9
LBQS1230-0015	12 33 04.1	+00 31 34.0	0.47095	11598	10323	13.8	4308.0	28.0	24.7
LBQS1230-0015	12 33 04.1	+00 31 34.0	0.47095	11598	10323	13.8	4678.0	15.0	10.5
LBQS1230-0015	12 33 04.1	+00 31 34.0	0.47095	11598	10323	13.8	6828.0	186.0	37.9
MCG+10-16-111	11 18 57.9	+58 03 23.0	0.02710	12922	3714	22.5	947.0	205.0	62.0
MCG+10-16-111	11 18 57.9	+58 03 23.0	0.02710	12922	3714	22.5	1656.0	489.0	55.3
MCG+10-16-111	11 18 57.9	+58 03 23.0	0.02710	12922	3714	22.5	2021.0	162.0	45.7
MCG+10-16-111	11 18 57.9	+58 03 23.0	0.02710	12922	3714	22.5	2132.0	303.0	46.5
MCG+10-16-111	11 18 57.9	+58 03 23.0	0.02710	12922	3714	22.5	3111.0	128.0	70.1
MCG+10-16-111	11 18 57.9	+58 03 23.0	0.02710	12922	3714	22.5	3549.0	50.0	50.6
MCG+10-16-111	11 18 57.9	+58 03 23.0	0.02710	12922	3714	22.5	3794.0	72.0	49.0
MCG+10-16-111	11 18 57.9	+58 03 23.0	0.02710	12922	3714	22.5	4053.0	86.0	85.0
MRC2251-178	22 54 05.9	−17 34 55.0	0.06609	12029	4585	37.8	888.0	34.0	21.4
MRC2251-178	22 54 05.9	−17 34 55.0	0.06609	12029	4585	37.8	2265.0	76.0	39.4
MRC2251-178	22 54 05.9	−17 34 55.0	0.06609	12029	4585	37.8	3061.0	69.0	43.1
MRC2251-178	22 54 05.9	−17 34 55.0	0.06609	12029	4585	37.8	3205.0	335.0	52.9
MRC2251-178	22 54 05.9	−17 34 55.0	0.06609	12029	4585	37.8	4698.0	20.0	15.6
MRC2251-178	22 54 05.9	−17 34 55.0	0.06609	12029	4585	37.8	8429.0	40.0	35.8
MRC2251-178	22 54 05.9	−17 34 55.0	0.06609	12029	4585	37.8	9029.0	62.0	45.7
MRC2251-178	22 54 05.9	−17 34 55.0	0.06609	12029	4585	37.8	9735.0	188.0	40.8
MRK1014	01 59 50.2	+00 23 41.0	0.16308	12569	1828	19	7077.0	99.0	40.5
MRK1014	01 59 50.2	+00 23 41.0	0.16308	12569	1828	19	7560.0	409.0	45.8
MRK1014	01 59 50.2	+00 23 41.0	0.16308	12569	1828	19	8418.0	155.0	38.3
MRK106	09 19 55.3	+55 21 37.0	0.12337	12029	6538	23.5	2396.0	323.0	45.4
MRK106	09 19 55.3	+55 21 37.0	0.12337	12029	6538	23.5	3533.0	68.0	30.2
MRK106	09 19 55.3	+55 21 37.0	0.12337	12029	6538	23.5	3809.0	44.0	17.9
MRK106	09 19 55.3	+55 21 37.0	0.12337	12029	6538	23.5	8203.0	51.0	45.5
MRK106	09 19 55.3	+55 21 37.0	0.12337	12029	6538	23.5	8824.0	46.0	50.4
MRK106	09 19 55.3	+55 21 37.0	0.12337	12029	6538	23.5	9508.0	229.0	37.1
MRK1179	02 33 22.4	+27 56 13.0	0.03760	14268	5573	13	1023.0	178.0	33.8
MRK1179	02 33 22.4	+27 56 13.0	0.03760	14268	5573	13	1567.0	230.0	61.4
MRK1179	02 33 22.4	+27 56 13.0	0.03760	14268	5573	13	2007.0	58.0	20.0
MRK1179	02 33 22.4	+27 56 13.0	0.03760	14268	5573	13	2665.0	137.0	57.2
MRK1179	02 33 22.4	+27 56 13.0	0.03760	14268	5573	13	4656.0	313.0	37.6
MRK1179	02 33 22.4	+27 56 13.0	0.03760	14268	5573	13	7387.0	52.0	42.0
MRK1179	02 33 22.4	+27 56 13.0	0.03760	14268	5573	13	7945.0	91.0	52.6
MRK1179	02 33 22.4	+27 56 13.0	0.03760	14268	5573	13	8670.0	161.0	26.4
MRK1269	10 55 19.5	+40 27 16.0	0.12003	14772	4757	12.2	6492.0	104.0	41.4
MRK1269	10 55 19.5	+40 27 16.0	0.12003	14772	4757	12.2	7402.0	76.0	59.0
MRK1269	10 55 19.5	+40 27 16.0	0.12003	14772	4757	12.2	9939.0	90.0	31.4
MRK1298	11 29 16.7	−04 24 07.0	0.06000	12569	15595	24.3	4740.0	161.0	39.6
MRK1298	11 29 16.7	−04 24 07.0	0.06000	12569	15595	24.3	5271.0	61.0	53.6
MRK1298	11 29 16.7	−04 24 07.0	0.06000	12569	15595	24.3	8127.0	91.0	63.0
MRK1298	11 29 16.7	−04 24 07.0	0.06000	12569	15595	24.3	9820.0	25.0	18.7
MRK1392	15 05 56.6	+03 42 26.0	0.03613	13448	4846	39.5	1504.0	103.0	35.8
MRK1447	11 30 29.1	+49 34 58.0	0.09558	14772	9301	11.7	770.0	346.0	41.6
MRK1447	11 30 29.1	+49 34 58.0	0.09558	14772	9301	11.7	1524.0	250.0	47.2
MRK1447	11 30 29.1	+49 34 58.0	0.09558	14772	9301	11.7	6963.0	45.0	32.7
MRK1502	00 53 34.9	+12 41 36.0	0.06114	12569	9488	16.3	9058.0	13.0	12.7
MRK1502	00 53 34.9	+12 41 36.0	0.06114	12569	9488	16.3	9115.0	34.0	23.0

Table 2 continued

FRENCH & WAKKER

Table 2 *(continued)*

Target	R.A.	Dec.	z	Program	$T_{\exp}$	S/N	$v_{\mathrm{Ly}\alpha}$	$EW_{\mathrm{Ly}\alpha}$	b
					(ks)	(1238 Å)	(km s^{-1})	(mÅ)	(km s^{-1})
(1)	(2)	(3)	(4)	(5)	(6)	(7)	(8)	(9)	(10)
MRK1513	21 32 27.8	+10 08 19.0	0.06298	11524	5513	29.2	6658.0	45.0	41.6
MRK1513	21 32 27.8	+10 08 19.0	0.06298	11524	5513	29.2	8313.0	204.0	33.5
MRK205	12 21 44.1	+75 18 38.0	0.07085	4952	760	7.6	1278.0	653.0	69.4
MRK205	12 21 44.1	+75 18 38.0	0.07085	4952	760	7.6	7012.0	75.0	26.9
MRK205	12 21 44.1	+75 18 38.0	0.07085	4952	760	7.6	7393.0	57.0	17.6
MRK290	15 35 52.3	+57 54 09.0	0.02958	11524	3856	42.8	742.0	136.0	39.4
MRK290	15 35 52.3	+57 54 09.0	0.02958	11524	3856	42.8	3082.0	520.0	60.1
MRK290	15 35 52.3	+57 54 09.0	0.02958	11524	3856	42.8	3192.0	319.0	40.4
MRK304	22 17 12.2	+14 14 21.0	0.06576	12569	3950	25	6613.0	53.0	41.9
MRK335	00 06 19.5	+20 12 11.0	0.02578	11524	4192	64.7	1954.0	216.0	38.0
MRK335	00 06 19.5	+20 12 11.0	0.02578	11524	4192	64.7	2274.0	150.0	73.4
MRK380	07 19 50.8	+74 27 57.0	0.47500	12275	5491	20.2	2482.0	112.0	58.3
MRK380	07 19 50.8	+74 27 57.0	0.47500	12275	5491	20.2	5805.0	86.0	40.2
MRK421	11 04 27.3	+38 12 32.0	0.03002	11520	3684	49.7	3023.0	73.0	24.8
MRK421	11 04 27.3	+38 12 32.0	0.03002	11520	3684	49.7	3909.0	12.0	20.1
MRK486	15 36 38.3	+54 33 33.0	0.03893	12276	5001	12.1	2432.0	63.0	28.9
MRK486	15 36 38.3	+54 33 33.0	0.03893	12276	5001	12.1	4386.0	184.0	31.3
MRK486	15 36 38.3	+54 33 33.0	0.03893	12276	5001	12.1	7501.0	329.0	48.2
MRK509	20 44 09.7	−10 43 24.0	0.03440	12022	12754	92.3	1332.0	28.0	20.1
MRK509	20 44 09.7	−10 43 24.0	0.03440	12022	12754	92.3	2544.0	203.0	43.1
MRK771	12 32 03.7	+20 09 29.0	0.06301	12569	1868	16.5	1176.0	307.0	43.1
MRK771	12 32 03.7	+20 09 29.0	0.06301	12569	1868	16.5	1883.0	230.0	33.1
MRK771	12 32 03.7	+20 09 29.0	0.06301	12569	1868	16.5	2553.0	240.0	40.3
MRK817	14 36 22.1	+58 47 40.0	0.03146	11505	3426	48.8	2078.0	149.0	50.3
MRK817	14 36 22.1	+58 47 40.0	0.03146	11505	3426	48.8	5047.0	50.0	61.7
MRK841	15 04 01.2	+10 26 16.0	0.03642	13448	1740	26.4	3058.0	24.0	21.4
MRK841	15 04 01.2	+10 26 16.0	0.03642	13448	1740	26.4	3217.0	96.0	27.8
MRK841	15 04 01.2	+10 26 16.0	0.03642	13448	1740	26.4	5657.0	94.0	35.3
MRK841	15 04 01.2	+10 26 16.0	0.03642	13448	1740	26.4	6107.0	59.0	35.0
MRK841	15 04 01.2	+10 26 16.0	0.03642	13448	1740	26.4	6494.0	83.0	32.8
MRK841	15 04 01.2	+10 26 16.0	0.03642	13448	1740	26.4	6622.0	32.0	23.8
MRK876	16 13 57.2	+65 43 10.0	0.12900	D028	147800	59.7	939.0	379.0	59.8
MRK876	16 13 57.2	+65 43 10.0	0.12900	D028	147800	59.7	3478.0	280.0	51.9
MRK876	16 13 57.2	+65 43 10.0	0.12900	D028	147800	59.7	4508.0	16.0	22.4
MRK876	16 13 57.2	+65 43 10.0	0.12900	D028	147800	59.7	5036.0	10.0	14.0
MRK876	16 13 57.2	+65 43 10.0	0.12900	D028	147800	59.7	6037.0	96.0	35.4
MRK876	16 13 57.2	+65 43 10.0	0.12900	D028	147800	59.7	7005.0	28.0	41.6
MRK876	16 13 57.2	+65 43 10.0	0.12900	D028	147800	59.7	9895.0	13.0	19.2
MRK877	16 20 11.2	+17 24 28.0	0.11244	12569	1844	16	2312.0	72.0	38.6
MS0117.2-2837	01 19 35.7	−28 21 31.0	0.34700	RQ052	13199	24.7	1663.0	64.0	30.8
MS0117.2-2837	01 19 35.7	−28 21 31.0	0.34700	RQ052	13199	24.7	3212.0	35.0	15.5
MS0244.6-3020	02 46 49.9	−30 07 42.0	0.53000	12988	12230	10	1254.0	417.0	44.3
MS0244.6-3020	02 46 49.9	−30 07 42.0	0.53000	12988	12230	10	1378.0	455.0	48.8
MS0244.6-3020	02 46 49.9	−30 07 42.0	0.53000	12988	12230	10	5006.0	96.0	43.2
MS0244.6-3020	02 46 49.9	−30 07 42.0	0.53000	12988	12230	10	5006.0	96.0	43.2
MS1217.0+0700	12 19 30.9	+06 43 35.0	0.08058	13444	4639	16	1084.0	89.0	47.0
MS1217.0+0700	12 19 30.9	+06 43 35.0	0.08058	13444	4639	16	1720.0	36.0	24.0
MS1217.0+0700	12 19 30.9	+06 43 35.0	0.08058	13444	4639	16	3784.0	54.0	45.6
MS1217.0+0700	12 19 30.9	+06 43 35.0	0.08058	13444	4639	16	5701.0	76.0	27.9
MS1217.0+0700	12 19 30.9	+06 43 35.0	0.08058	13444	4639	16	7162.0	60.0	43.4
MS1228.6+1219	12 31 13.1	+12 03 07.0	0.11612	14071	10419	12.1	866.0	99.0	21.9
MS1228.6+1219	12 31 13.1	+12 03 07.0	0.11612	14071	10419	12.1	1046.0	176.0	34.5

Table 2 continued

Table 2 *(continued)*

Target	R.A.	Dec.	z	Program	$T_{\exp}$	S/N	$v_{\mathrm{Ly}\alpha}$	$EW_{\mathrm{Ly}\alpha}$	b
					(ks)	(1238 Å)	(km s^{-1})	(mÅ)	(km s^{-1})
(1)	(2)	(3)	(4)	(5)	(6)	(7)	(8)	(9)	(10)
MS1228.6+1219	12 31 13.1	+12 03 07.0	0.11612	14071	10419	12.1	1286.0	525.0	56.7
MS1228.6+1219	12 31 13.1	+12 03 07.0	0.11612	14071	10419	12.1	3956.0	37.0	21.5
MS1228.6+1219	12 31 13.1	+12 03 07.0	0.11612	14071	10419	12.1	7337.0	648.0	66.7
MS1228.6+1219	12 31 13.1	+12 03 07.0	0.11612	14071	10419	12.1	7811.0	513.0	60.0
MS1228.6+1219	12 31 13.1	+12 03 07.0	0.11612	14071	10419	12.1	9040.0	64.0	33.5
NAB1612+26	16 14 10.7	+26 32 50.0	0.39233	14277	25413	20	2507.0	52.0	29.9
NAB1612+26	16 14 10.7	+26 32 50.0	0.39233	14277	25413	20	9041.0	59.0	39.6
NAB1612+26	16 14 10.7	+26 32 50.0	0.39233	14277	25413	20	9391.0	676.0	71.5
NAB1612+26	16 14 10.7	+26 32 50.0	0.39233	14277	25413	20	9916.0	205.0	33.4
NAB1612+26	16 14 10.7	+26 32 50.0	0.39233	14277	25413	20	9970.0	71.0	20.6
NGC985	02 34 37.8	−08 47 17.0	0.04354	12953	7111	55.6	1473.0	9.0	13.1
NGC985	02 34 37.8	−08 47 17.0	0.04354	12953	7111	55.6	7439.0	49.0	49.1
PG0003+158	00 05 59.3	+16 09 49.0	0.45090	12038	10361	28.8	841.0	212.0	49.9
PG0026+129	00 29 13.8	+13 16 05.0	0.14200	12569	1868	15.6	9988.0	551.0	56.3
PG0052+251	00 54 52.2	+25 25 39.0	0.15500	14268	2497	29.3	2155.0	97.0	26.1
PG0052+251	00 54 52.2	+25 25 39.0	0.15500	14268	2497	29.3	3277.0	76.0	35.5
PG0052+251	00 54 52.2	+25 25 39.0	0.15500	14268	2497	29.3	9930.0	104.0	41.2
PG0804+761	08 10 58.5	+76 02 43.0	0.10200	11686	5510	43.7	1143.0	183.0	43.1
PG0804+761	08 10 58.5	+76 02 43.0	0.10200	11686	5510	43.7	1526.0	62.0	38.3
PG0804+761	08 10 58.5	+76 02 43.0	0.10200	11686	5510	43.7	1593.0	32.0	35.1
PG0804+761	08 10 58.5	+76 02 43.0	0.10200	11686	5510	43.7	2962.0	12.0	18.5
PG0804+761	08 10 58.5	+76 02 43.0	0.10200	11686	5510	43.7	5537.0	349.0	50.0
PG0832+251	08 35 35.9	+24 59 41.0	0.33100	12025	6134	16.2	2183.0	208.0	30.5
PG0832+251	08 35 35.9	+24 59 41.0	0.33100	12025	6134	16.2	3536.0	124.0	87.3
PG0832+251	08 35 35.9	+24 59 41.0	0.33100	12025	6134	16.2	5208.0	681.0	78.6
PG0832+251	08 35 35.9	+24 59 41.0	0.33100	12025	6134	16.2	5250.0	416.0	41.8
PG0832+251	08 35 35.9	+24 59 41.0	0.33100	12025	6134	16.2	5336.0	495.0	49.9
PG0832+251	08 35 35.9	+24 59 41.0	0.33100	12025	6134	16.2	5450.0	471.0	48.7
PG0832+251	08 35 35.9	+24 59 41.0	0.33100	12025	6134	16.2	6980.0	147.0	58.1
PG0832+251	08 35 35.9	+24 59 41.0	0.33100	12025	6134	16.2	7201.0	59.0	43.5
PG0832+251	08 35 35.9	+24 59 41.0	0.33100	12025	6134	16.2	7719.0	65.0	36.2
PG0832+251	08 35 35.9	+24 59 41.0	0.33100	12025	6134	16.2	7921.0	70.0	37.4
PG0832+251	08 35 35.9	+24 59 41.0	0.33100	12025	6134	16.2	8335.0	53.0	20.7
PG0832+251	08 35 35.9	+24 59 41.0	0.33100	12025	6134	16.2	8421.0	317.0	39.6
PG0838+770	08 44 45.3	+76 53 10.0	0.13100	11520	8865	25.8	721.0	552.0	58.8
PG0838+770	08 44 45.3	+76 53 10.0	0.13100	11520	8865	25.8	1341.0	44.0	33.0
PG0838+770	08 44 45.3	+76 53 10.0	0.13100	11520	8865	25.8	1522.0	60.0	25.1
PG0838+770	08 44 45.3	+76 53 10.0	0.13100	11520	8865	25.8	2203.0	70.0	46.8
PG0838+770	08 44 45.3	+76 53 10.0	0.13100	11520	8865	25.8	2911.0	59.0	36.8
PG0838+770	08 44 45.3	+76 53 10.0	0.13100	11520	8865	25.8	4326.0	36.0	31.0
PG0844+349	08 47 42.5	+34 45 05.0	0.06400	12569	1900	18.7	2310.0	67.0	54.4
PG0844+349	08 47 42.5	+34 45 05.0	0.06400	12569	1900	18.7	4243.0	57.0	47.8
PG0844+349	08 47 42.5	+34 45 05.0	0.06400	12569	1900	18.7	7652.0	65.0	28.3
PG0844+349	08 47 42.5	+34 45 05.0	0.06400	12569	1900	18.7	9009.0	30.0	28.9
PG0923+201	09 25 54.7	+19 54 04.0	0.19000	12569	1860	20.9	2512.0	245.0	49.2
PG0923+201	09 25 54.7	+19 54 04.0	0.19000	12569	1860	20.9	4244.0	387.0	64.2
PG0923+201	09 25 54.7	+19 54 04.0	0.19000	12569	1860	20.9	6018.0	289.0	75.2
PG0953+414	09 56 52.3	+41 15 23.0	0.23410	12038	4785	32.1	644.0	60.0	33.6
PG0953+414	09 56 52.3	+41 15 23.0	0.23410	12038	4785	32.1	2204.0	27.0	28.6
PG0953+414	09 56 52.3	+41 15 23.0	0.23410	12038	4785	32.1	4680.0	72.0	43.1
PG0953+414	09 56 52.3	+41 15 23.0	0.23410	12038	4785	32.1	4804.0	171.0	50.9
PG0953+414	09 56 52.3	+41 15 23.0	0.23410	12038	4785	32.1	4956.0	136.0	34.9

Table 2 continued

Table 2 *(continued)*

Target	R.A.	Dec.	z	Program	$T_{\exp}$	S/N	$v_{\mathrm{Ly}\alpha}$	$EW_{\mathrm{Ly}\alpha}$	b
					(ks)	(1238 Å)	(km s^{-1})	(mÅ)	(km s^{-1})
(1)	(2)	(3)	(4)	(5)	(6)	(7)	(8)	(9)	(10)
PG1001+054	10 04 20.1	+05 13 01.0	0.16100	13347	8225	21.8	640.0	40.0	21.4
PG1001+054	10 04 20.1	+05 13 01.0	0.16100	13347	8225	21.8	1306.0	76.0	44.8
PG1001+054	10 04 20.1	+05 13 01.0	0.16100	13347	8225	21.8	2425.0	350.0	44.7
PG1001+054	10 04 20.1	+05 13 01.0	0.16100	13347	8225	21.8	4092.0	217.0	46.3
PG1001+054	10 04 20.1	+05 13 01.0	0.16100	13347	8225	21.8	6840.0	205.0	53.6
PG1001+291	10 04 02.6	+28 55 36.0	0.32720	12038	6199	24.3	496.0	264.0	40.8
PG1001+291	10 04 02.6	+28 55 36.0	0.32720	12038	6199	24.3	1061.0	236.0	39.5
PG1001+291	10 04 02.6	+28 55 36.0	0.32720	12038	6199	24.3	4598.0	276.0	43.3
PG1001+291	10 04 02.6	+28 55 36.0	0.32720	12038	6199	24.3	6361.0	65.0	31.6
PG1001+291	10 04 02.6	+28 55 36.0	0.32720	12038	6199	24.3	6608.0	33.0	31.1
PG1001+291	10 04 02.6	+28 55 36.0	0.32720	12038	6199	24.3	8789.0	33.0	27.3
PG1001+291	10 04 02.6	+28 55 36.0	0.32720	12038	6199	24.3	9198.0	59.0	24.6
PG1004+130	10 07 26.2	+12 48 56.0	0.24000	12569	4107	12.9	1253.0	129.0	27.5
PG1004+130	10 07 26.2	+12 48 56.0	0.24000	12569	4107	12.9	2759.0	251.0	64.6
PG1004+130	10 07 26.2	+12 48 56.0	0.24000	12569	4107	12.9	3081.0	107.0	48.9
PG1004+130	10 07 26.2	+12 48 56.0	0.24000	12569	4107	12.9	3252.0	33.0	18.6
PG1004+130	10 07 26.2	+12 48 56.0	0.24000	12569	4107	12.9	3493.0	41.0	21.6
PG1004+130	10 07 26.2	+12 48 56.0	0.24000	12569	4107	12.9	6942.0	82.0	35.8
PG1004+130	10 07 26.2	+12 48 56.0	0.24000	12569	4107	12.9	9036.0	312.0	39.8
PG1004+130	10 07 26.2	+12 48 56.0	0.24000	12569	4107	12.9	9500.0	228.0	34.9
PG1011-040	10 14 20.7	−04 18 39.0	0.05800	PGOJS	32098	31.9	944.0	120.0	23.3
PG1011-040	10 14 20.7	−04 18 39.0	0.05800	PGOJS	32098	31.9	1301.0	62.0	40.3
PG1011-040	10 14 20.7	−04 18 39.0	0.05800	PGOJS	32098	31.9	3496.0	52.0	25.9
PG1011-040	10 14 20.7	−04 18 39.0	0.05800	PGOJS	32098	31.9	5471.0	134.0	33.0
PG1048+342	10 51 43.8	+33 59 26.0	0.16700	12024	7814	24.5	1593.0	313.0	38.8
PG1048+342	10 51 43.8	+33 59 26.0	0.16700	12024	7814	24.5	1724.0	593.0	59.4
PG1048+342	10 51 43.8	+33 59 26.0	0.16700	12024	7814	24.5	1822.0	207.0	28.3
PG1048+342	10 51 43.8	+33 59 26.0	0.16700	12024	7814	24.5	1908.0	304.0	62.4
PG1048+342	10 51 43.8	+33 59 26.0	0.16700	12024	7814	24.5	7229.0	49.0	28.3
PG1112+431	11 15 06.0	+42 49 50.0	0.30064	12275	7942	20.4	3158.0	88.0	46.1
PG1112+431	11 15 06.0	+42 49 50.0	0.30064	12275	7942	20.4	3443.0	67.0	23.5
PG1112+431	11 15 06.0	+42 49 50.0	0.30064	12275	7942	20.4	4381.0	75.0	42.9
PG1112+431	11 15 06.0	+42 49 50.0	0.30064	12275	7942	20.4	6402.0	126.0	44.6
PG1112+431	11 15 06.0	+42 49 50.0	0.30064	12275	7942	20.4	7018.0	95.0	38.4
PG1115+407	11 18 30.4	+40 25 55.0	0.15400	11519	5109	23.1	1987.0	65.0	29.7
PG1115+407	11 18 30.4	+40 25 55.0	0.15400	11519	5109	23.1	2491.0	22.0	17.3
PG1115+407	11 18 30.4	+40 25 55.0	0.15400	11519	5109	23.1	6414.0	422.0	47.6
PG1115+407	11 18 30.4	+40 25 55.0	0.15400	11519	5109	23.1	8843.0	89.0	35.3
PG1116+215	11 19 08.7	+21 19 18.0	0.17650	12038	4677	39.3	1480.0	107.0	49.7
PG1116+215	11 19 08.7	+21 19 18.0	0.17650	12038	4677	39.3	4885.0	126.0	51.6
PG1116+215	11 19 08.7	+21 19 18.0	0.17650	12038	4677	39.3	5806.0	39.0	29.4
PG1116+215	11 19 08.7	+21 19 18.0	0.17650	12038	4677	39.3	8482.0	212.0	37.8
PG1116+215	11 19 08.7	+21 19 18.0	0.17650	12038	4677	39.3	9657.0	108.0	37.0
PG1121+423	11 24 39.2	+42 01 45.0	0.22500	RQ005	8999	22.8	2580.0	61.0	24.6
PG1121+423	11 24 39.2	+42 01 45.0	0.22500	RQ005	8999	22.8	2976.0	56.0	25.8
PG1121+423	11 24 39.2	+42 01 45.0	0.22500	RQ005	8999	22.8	3138.0	39.0	21.4
PG1121+423	11 24 39.2	+42 01 45.0	0.22500	RQ005	8999	22.8	4336.0	98.0	35.1
PG1121+423	11 24 39.2	+42 01 45.0	0.22500	RQ005	8999	22.8	7126.0	159.0	39.1
PG1121+423	11 24 39.2	+42 01 45.0	0.22500	RQ005	8999	22.8	7328.0	363.0	42.9
PG1121+423	11 24 39.2	+42 01 45.0	0.22500	RQ005	8999	22.8	9284.0	69.0	22.6
PG1148+549	11 51 20.5	+54 37 33.0	0.96900	11741	17823	32.1	1988.0	192.0	30.0
PG1148+549	11 51 20.5	+54 37 33.0	0.96900	11741	17823	32.1	2426.0	65.0	25.8

Table 2 continued

Table 2 *(continued)*

Target	R.A.	Dec.	z	Program	$T_{\exp}$	S/N	$v_{\mathrm{Ly}\alpha}$	$EW_{\mathrm{Ly}\alpha}$	b
					(ks)	(1238 Å)	(km s^{-1})	(mÅ)	(km s^{-1})
(1)	(2)	(3)	(4)	(5)	(6)	(7)	(8)	(9)	(10)
PG1211+143	12 14 17.7	+14 03 13.0	0.08090	13947	2320	13.9	2124.0	127.0	55.9
PG1211+143	12 14 17.7	+14 03 13.0	0.08090	13947	2320	13.9	4943.0	153.0	37.0
PG1211+143	12 14 17.7	+14 03 13.0	0.08090	13947	2320	13.9	5022.0	228.0	43.2
PG1211+143	12 14 17.7	+14 03 13.0	0.08090	13947	2320	13.9	6617.0	96.0	30.5
PG1211+143	12 14 17.7	+14 03 13.0	0.08090	13947	2320	13.9	7000.0	128.0	32.6
PG1211+143	12 14 17.7	+14 03 13.0	0.08090	13947	2320	13.9	7745.0	155.0	67.1
PG1211+143	12 14 17.7	+14 03 13.0	0.08090	13947	2320	13.9	8392.0	16.0	18.8
PG1211+143	12 14 17.7	+14 03 13.0	0.08090	13947	2320	13.9	8814.0	9.0	8.7
PG1216+069	12 19 20.9	+06 38 38.0	0.33130	12025	5146	22.8	1906.0	2560.0	272.6
PG1216+069	12 19 20.9	+06 38 38.0	0.33130	12025	5146	22.8	2548.0	31.0	13.6
PG1216+069	12 19 20.9	+06 38 38.0	0.33130	12025	5146	22.8	2767.0	21.0	17.5
PG1216+069	12 19 20.9	+06 38 38.0	0.33130	12025	5146	22.8	3802.0	370.0	64.2
PG1216+069	12 19 20.9	+06 38 38.0	0.33130	12025	5146	22.8	5261.0	16.0	12.5
PG1216+069	12 19 20.9	+06 38 38.0	0.33130	12025	5146	22.8	5678.0	150.0	54.4
PG1216+069	12 19 20.9	+06 38 38.0	0.33130	12025	5146	22.8	7177.0	158.0	42.4
PG1218+304	12 21 21.9	+30 10 37.0	0.18200	14772	4688	14.5	6809.0	202.0	46.2
PG1218+304	12 21 21.9	+30 10 37.0	0.18200	14772	4688	14.5	6969.0	86.0	38.5
PG1218+304	12 21 21.9	+30 10 37.0	0.18200	14772	4688	14.5	9199.0	57.0	39.8
PG1259+593	13 01 12.9	+59 02 07.0	0.47780	11541	9200	26.6	646.0	133.0	35.7
PG1259+593	13 01 12.9	+59 02 07.0	0.47780	11541	9200	26.6	683.0	168.0	34.1
PG1259+593	13 01 12.9	+59 02 07.0	0.47780	11541	9200	26.6	2278.0	280.0	43.1
PG1259+593	13 01 12.9	+59 02 07.0	0.47780	11541	9200	26.6	6643.0	172.0	42.2
PG1302-102	13 05 33.0	−10 33 20.0	0.27840	8306	22119	26.4	1314.0	332.0	37.5
PG1302-102	13 05 33.0	−10 33 20.0	0.27840	8306	22119	26.4	3447.0	72.0	29.4
PG1302-102	13 05 33.0	−10 33 20.0	0.27840	8306	22119	26.4	5857.0	52.0	23.1
PG1302-102	13 05 33.0	−10 33 20.0	0.27840	8306	22119	26.4	6596.0	64.0	31.9
PG1302-102	13 05 33.0	−10 33 20.0	0.27840	8306	22119	26.4	7573.0	44.0	23.1
PG1302-102	13 05 33.0	−10 33 20.0	0.27840	8306	22119	26.4	7744.0	27.0	29.8
PG1302-102	13 05 33.0	−10 33 20.0	0.27840	8306	22119	26.4	9805.0	21.0	16.1
PG1302-102	13 05 33.0	−10 33 20.0	0.27840	8306	22119	26.4	9856.0	35.0	21.5
PG1307+085	13 09 47.0	+08 19 47.0	0.15500	12569	1836	20.6	3575.0	30.0	17.3
PG1307+085	13 09 47.0	+08 19 47.0	0.15500	12569	1836	20.6	7281.0	64.0	27.7
PG1309+355	13 12 17.7	+35 15 20.0	0.18400	12569	1896	14.9	829.0	503.0	54.2
PG1309+355	13 12 17.7	+35 15 20.0	0.18400	12569	1896	14.9	6931.0	53.0	30.7
PG1309+355	13 12 17.7	+35 15 20.0	0.18400	12569	1896	14.9	7039.0	162.0	48.1
PG1341+258	13 43 56.8	+25 38 48.0	0.08700	13314	8415	29.1	7980.0	295.0	47.6
PG1352+183	13 54 35.7	+18 05 17.0	0.15200	13448	4856	26	842.0	22.0	19.6
PG1352+183	13 54 35.7	+18 05 17.0	0.15200	13448	4856	26	2036.0	47.0	35.4
PG1352+183	13 54 35.7	+18 05 17.0	0.15200	13448	4856	26	2872.0	52.0	24.1
PG1352+183	13 54 35.7	+18 05 17.0	0.15200	13448	4856	26	2946.0	288.0	38.3
PG1352+183	13 54 35.7	+18 05 17.0	0.15200	13448	4856	26	5276.0	44.0	33.3
PG1352+183	13 54 35.7	+18 05 17.0	0.15200	13448	4856	26	6967.0	161.0	67.0
PG1352+183	13 54 35.7	+18 05 17.0	0.15200	13448	4856	26	8156.0	20.0	13.2
PG1352+183	13 54 35.7	+18 05 17.0	0.15200	13448	4856	26	9964.0	336.0	48.5
PG1352+183	13 54 35.7	+18 05 17.0	0.15200	13448	4856	26	10083.0	39.0	24.2
PG1411+442	14 13 48.3	+44 00 14.0	0.08960	12569	16799	41.9	1522.0	196.0	104.3
PG1411+442	14 13 48.3	+44 00 14.0	0.08960	12569	16799	41.9	1747.0	127.0	68.5
PG1424+240	14 27 00.4	+23 48 00.0	0.61709	12612	3750	19.9	5218.0	181.0	65.8
PG1424+240	14 27 00.4	+23 48 00.0	0.61709	12612	3750	19.9	5608.0	484.0	59.2
PG1435-067	14 38 16.2	−06 58 21.0	0.12600	12569	1864	16.3	1650.0	113.0	52.6
PG1435-067	14 38 16.2	−06 58 21.0	0.12600	12569	1864	16.3	3615.0	217.0	47.2
PG1435-067	14 38 16.2	−06 58 21.0	0.12600	12569	1864	16.3	7346.0	90.0	44.5

Table 2 continued

FRENCH & WAKKER

Table 2 *(continued)*

Target	R.A.	Dec.	z	Program	$T_{\rm exp}$	S/N	$v_{\rm Ly\alpha}$	$EW_{\rm Ly\alpha}$	b
					(ks)	(1238 Å)	(km s^{-1})	(mÅ)	(km s^{-1})
(1)	(2)	(3)	(4)	(5)	(6)	(7)	(8)	(9)	(10)
PG1435-067	14 38 16.2	−06 58 21.0	0.12600	12569	1864	16.3	7460.0	98.0	31.8
PG1435-067	14 38 16.2	−06 58 21.0	0.12600	12569	1864	16.3	9710.0	208.0	45.7
PG1522+101	15 24 24.5	+09 58 30.0	1.32801	11741	16401	21.8	2438.0	138.0	35.3
PG1522+101	15 24 24.5	+09 58 30.0	1.32801	11741	16401	21.8	3726.0	44.0	32.6
PG1522+101	15 24 24.5	+09 58 30.0	1.32801	11741	16401	21.8	6741.0	49.0	25.4
PG1522+101	15 24 24.5	+09 58 30.0	1.32801	11741	16401	21.8	8929.0	20.0	16.6
PG1553+113	15 55 43.2	+11 11 25.0	0.46699	BLIHM	31197	33	2128.0	95.0	32.5
PG1553+113	15 55 43.2	+11 11 25.0	0.46699	BLIHM	31197	33	2371.0	17.0	14.4
PG1553+113	15 55 43.2	+11 11 25.0	0.46699	BLIHM	31197	33	2537.0	48.0	28.9
PG1553+113	15 55 43.2	+11 11 25.0	0.46699	BLIHM	31197	33	3001.0	48.0	31.8
PG1553+113	15 55 43.2	+11 11 25.0	0.46699	BLIHM	31197	33	4695.0	28.0	38.1
PG1553+113	15 55 43.2	+11 11 25.0	0.46699	BLIHM	31197	33	5193.0	35.0	35.3
PG1553+113	15 55 43.2	+11 11 25.0	0.46699	BLIHM	31197	33	7128.0	48.0	20.6
PG1553+113	15 55 43.2	+11 11 25.0	0.46699	BLIHM	31197	33	9741.0	29.0	31.6
PG1626+554	16 27 56.2	+55 22 32.0	0.13300	12029	3318	25.9	985.0	23.0	30.2
PG1626+554	16 27 56.2	+55 22 32.0	0.13300	12029	3318	25.9	8251.0	76.0	34.6
PG1626+554	16 27 56.2	+55 22 32.0	0.13300	12029	3318	25.9	9193.0	35.0	31.8
PG2112+059	21 14 52.6	+06 07 42.0	0.46600	13840	7891	15	1310.0	156.0	26.5
PG2112+059	21 14 52.6	+06 07 42.0	0.46600	13840	7891	15	4919.0	124.0	55.1
PG2112+059	21 14 52.6	+06 07 42.0	0.46600	13840	7891	15	5240.0	34.0	23.2
PG2112+059	21 14 52.6	+06 07 42.0	0.46600	13840	7891	15	8440.0	120.0	56.7
PG2349-014	23 51 56.1	−01 09 13.0	0.17400	12569	1844	23.1	2281.0	196.0	38.3
PHL1226	01 54 28.0	+04 48 18.0	0.40400	12536	14542	14	1721.0	323.0	47.0
PHL1226	01 54 28.0	+04 48 18.0	0.40400	12536	14542	14	4920.0	162.0	39.2
PHL1226	01 54 28.0	+04 48 18.0	0.40400	12536	14542	14	5037.0	93.0	21.8
PHL1226	01 54 28.0	+04 48 18.0	0.40400	12536	14542	14	5203.0	927.0	94.6
PHL1226	01 54 28.0	+04 48 18.0	0.40400	12536	14542	14	5316.0	226.0	23.0
PHL1226	01 54 28.0	+04 48 18.0	0.40400	12536	14542	14	5368.0	210.0	21.4
PHL1226	01 54 28.0	+04 48 18.0	0.40400	12536	14542	14	5422.0	342.0	35.4
PHL2525	00 00 24.4	−12 45 48.0	0.20000	12604	2146	22.9	1433.0	64.0	35.4
PHL2525	00 00 24.4	−12 45 48.0	0.20000	12604	2146	22.9	4896.0	45.0	24.5
PHL2525	00 00 24.4	−12 45 48.0	0.20000	12604	2146	22.9	6889.0	257.0	43.2
PHL2525	00 00 24.4	−12 45 48.0	0.20000	12604	2146	22.9	7123.0	117.0	34.4
PHL2525	00 00 24.4	−12 45 48.0	0.20000	12604	2146	22.9	8461.0	65.0	33.8
PHL2525	00 00 24.4	−12 45 48.0	0.20000	12604	2146	22.9	8818.0	38.0	41.7
PHL2525	00 00 24.4	−12 45 48.0	0.20000	12604	2146	22.9	9009.0	57.0	36.7
PKS0405-12	04 07 48.4	−12 11 37.0	0.57259	11508	24147	64	2752.0	33.0	27.0
PKS0405-12	04 07 48.4	−12 11 37.0	0.57259	11508	24147	64	5026.0	35.0	28.7
PKS0405-12	04 07 48.4	−12 11 37.0	0.57259	11508	24147	64	6933.0	6.0	18.7
PKS0405-12	04 07 48.4	−12 11 37.0	0.57259	11508	24147	64	7401.0	33.0	31.6
PKS0405-12	04 07 48.4	−12 11 37.0	0.57259	11508	24147	64	8980.0	315.0	38.8
PKS0405-12	04 07 48.4	−12 11 37.0	0.57259	11508	24147	64	9567.0	132.0	66.6
PKS0558-504	05 59 47.4	−50 26 51.0	0.13700	11692	1075	19.8	1134.0	29.0	16.3
PKS0558-504	05 59 47.4	−50 26 51.0	0.13700	11692	1075	19.8	1820.0	27.0	25.6
PKS0558-504	05 59 47.4	−50 26 51.0	0.13700	11692	1075	19.8	3289.0	42.0	41.5
PKS0558-504	05 59 47.4	−50 26 51.0	0.13700	11692	1075	19.8	7644.0	140.0	54.7
PKS0558-504	05 59 47.4	−50 26 51.0	0.13700	11692	1075	19.8	8247.0	324.0	43.1
PKS0558-504	05 59 47.4	−50 26 51.0	0.13700	11692	1075	19.8	8402.0	85.0	47.2
PKS0558-504	05 59 47.4	−50 26 51.0	0.13700	11692	1075	19.8	8574.0	106.0	27.7
PKS2005-489	20 09 25.4	−48 49 54.0	0.07100	11520	2461	22.9	4967.0	293.0	48.5
PKS2005-489	20 09 25.4	−48 49 54.0	0.07100	11520	2461	22.9	5070.0	316.0	35.5
PKS2155-304	21 58 52.1	−30 13 32.0	0.11600	5889	6682	46.1	2644.0	51.0	62.6

Table 2 continued

Table 2 *(continued)*

Target	R.A.	Dec.	z	Program	T_{exp}	S/N	$v_{\text{Ly}\alpha}$	$EW_{\text{Ly}\alpha}$	b
					(ks)	(1238 Å)	(km s^{-1})	(mÅ)	(km s^{-1})
(1)	(2)	(3)	(4)	(5)	(6)	(7)	(8)	(9)	(10)
PKS2155-304	21 58 52.1	−30 13 32.0	0.11600	5889	6682	46.1	4996.0	116.0	31.0
PKS2155-304	21 58 52.1	−30 13 32.0	0.11600	5889	6682	46.1	5113.0	155.0	33.3
PKS2155-304	21 58 52.1	−30 13 32.0	0.11600	5889	6682	46.1	5171.0	61.0	25.7
PKS2155-304	21 58 52.1	−30 13 32.0	0.11600	5889	6682	46.1	5683.0	67.0	44.5
PKS2155-304	21 58 52.1	−30 13 32.0	0.11600	5889	6682	46.1	7745.0	21.0	22.8
QSO1500-4140	15 03 33.9	−41 52 24.0	0.33500	8244	6000	10	2023.0	95.0	28.2
QSO1500-4140	15 03 33.9	−41 52 24.0	0.33500	8244	6000	10	3138.0	177.0	27.1
QSO1500-4140	15 03 33.9	−41 52 24.0	0.33500	8244	6000	10	5286.0	398.0	54.5
QSO1500-4140	15 03 33.9	−41 52 24.0	0.33500	8244	6000	10	8503.0	156.0	34.0
QSO1500-4140	15 03 33.9	−41 52 24.0	0.33500	8244	6000	10	8972.0	64.0	37.3
QSO1500-4140	15 03 33.9	−41 52 24.0	0.33500	8244	6000	10	9621.0	294.0	45.4
QSO1500-4140	15 03 33.9	−41 52 24.0	0.33500	8244	6000	10	9757.0	503.0	66.6
RBS1024	11 44 30.0	+36 53 09.0	0.03806	14772	4712	18.3	3041.0	169.0	44.1
RBS1024	11 44 30.0	+36 53 09.0	0.03806	14772	4712	18.3	3541.0	65.0	35.4
RBS1024	11 44 30.0	+36 53 09.0	0.03806	14772	4712	18.3	7042.0	107.0	35.7
RBS1024	11 44 30.0	+36 53 09.0	0.03806	14772	4712	18.3	8310.0	150.0	34.1
RBS1090	12 17 21.3	+30 56 31.0	0.30040	14772	4633	5.1	7123.0	251.0	33.7
RBS1307	13 42 31.2	+38 29 05.0	0.17190	12248	3034	15.1	1146.0	152.0	45.6
RBS1307	13 42 31.2	+38 29 05.0	0.17190	12248	3034	15.1	1401.0	219.0	47.2
RBS1307	13 42 31.2	+38 29 05.0	0.17190	12248	3034	15.1	1572.0	96.0	28.3
RBS1307	13 42 31.2	+38 29 05.0	0.17190	12248	3034	15.1	3465.0	435.0	55.4
RBS1307	13 42 31.2	+38 29 05.0	0.17190	12248	3034	15.1	5664.0	47.0	26.2
RBS1307	13 42 31.2	+38 29 05.0	0.17190	12248	3034	15.1	6641.0	52.0	34.8
RBS1307	13 42 31.2	+38 29 05.0	0.17190	12248	3034	15.1	8043.0	327.0	51.8
RBS1454	15 02 04.1	+06 45 16.0	0.28600	12603	2239	14.9	5303.0	69.0	49.3
RBS1454	15 02 04.1	+06 45 16.0	0.28600	12603	2239	14.9	7656.0	54.0	26.0
RBS1454	15 02 04.1	+06 45 16.0	0.28600	12603	2239	14.9	8925.0	256.0	42.8
RBS1503	15 29 07.5	+56 16 06.0	0.09900	12276	1964	14.3	3274.0	319.0	63.2
RBS1503	15 29 07.5	+56 16 06.0	0.09900	12276	1964	14.3	9115.0	44.0	19.7
RBS1768	21 38 49.9	−38 28 40.0	0.18299	12936	6962	24.8	4869.0	39.0	29.7
RBS1768	21 38 49.9	−38 28 40.0	0.18299	12936	6962	24.8	5755.0	378.0	45.8
RBS1768	21 38 49.9	−38 28 40.0	0.18299	12936	6962	24.8	5863.0	102.0	32.0
RBS1768	21 38 49.9	−38 28 40.0	0.18299	12936	6962	24.8	6531.0	15.0	14.7
RBS1768	21 38 49.9	−38 28 40.0	0.18299	12936	6962	24.8	9308.0	63.0	17.9
RBS1768	21 38 49.9	−38 28 40.0	0.18299	12936	6962	24.8	9360.0	306.0	31.8
RBS1768	21 38 49.9	−38 28 40.0	0.18299	12936	6962	24.8	9434.0	161.0	25.2
RBS1795	21 54 51.1	−44 14 06.0	0.34400	11541	8173	30.3	1795.0	35.0	47.7
RBS1795	21 54 51.1	−44 14 06.0	0.34400	11541	8173	30.3	3588.0	42.0	41.6
RBS1795	21 54 51.1	−44 14 06.0	0.34400	11541	8173	30.3	8103.0	52.0	25.1
RBS1795	21 54 51.1	−44 14 06.0	0.34400	11541	8173	30.3	9038.0	102.0	35.5
RBS1795	21 54 51.1	−44 14 06.0	0.34400	11541	8173	30.3	9517.0	18.0	13.7
RBS1892	22 45 18.0	−46 51 59.0	0.20100	12604	2228	28.1	673.0	44.0	25.4
RBS1892	22 45 18.0	−46 51 59.0	0.20100	12604	2228	28.1	2821.0	63.0	40.9
RBS1892	22 45 18.0	−46 51 59.0	0.20100	12604	2228	28.1	8067.0	23.0	25.2
RBS2000	23 24 44.7	−40 40 49.0	0.17359	13448	5046	18.8	1598.0	35.0	29.0
RBS2000	23 24 44.7	−40 40 49.0	0.17359	13448	5046	18.8	7681.0	45.0	21.9
RBS2023	23 34 52.4	−35 38 42.0	0.09800	13444	10049	15	763.0	592.0	73.6
RBS2023	23 34 52.4	−35 38 42.0	0.09800	13444	10049	15	8391.0	85.0	31.1
RBS2055	23 51 52.8	+26 19 32.0	0.03800	14268	7029	27.8	1635.0	76.0	45.3
RBS2055	23 51 52.8	+26 19 32.0	0.03800	14268	7029	27.8	8051.0	32.0	27.4
RBS2070	23 59 07.8	−30 37 39.0	0.16539	12864	17033	17.3	8922.0	357.0	51.0
RBS2070	23 59 07.8	−30 37 39.0	0.16539	12864	17033	17.3	8966.0	482.0	53.3

Table 2 continued

Table 2 *(continued)*

Target	R.A.	Dec.	z	Program	$T_{\exp}$	S/N	$v_{\mathrm{Ly}\alpha}$	$EW_{\mathrm{Ly}\alpha}$	b
					(ks)	(1238 Å)	$(\mathrm{km\,s^{-1}})$	(mÅ)	$(\mathrm{km\,s^{-1}})$
(1)	(2)	(3)	(4)	(5)	(6)	(7)	(8)	(9)	(10)
RBS563	04 38 29.2	−61 48 00.0	0.06900	11692	4628	13.7	5111.0	117.0	36.8
RBS563	04 38 29.2	−61 48 00.0	0.06900	11692	4628	13.7	5178.0	168.0	56.7
RBS563	04 38 29.2	−61 48 00.0	0.06900	11692	4628	13.7	7529.0	471.0	51.4
RBS563	04 38 29.2	−61 48 00.0	0.06900	11692	4628	13.7	7659.0	80.0	30.2
RBS567	04 39 38.7	−53 11 31.0	0.24300	11520	8176	20.9	613.0	87.0	39.4
RBS567	04 39 38.7	−53 11 31.0	0.24300	11520	8176	20.9	1664.0	517.0	55.5
RBS567	04 39 38.7	−53 11 31.0	0.24300	11520	8176	20.9	3947.0	93.0	32.7
RBS567	04 39 38.7	−53 11 31.0	0.24300	11520	8176	20.9	4332.0	50.0	33.2
RBS567	04 39 38.7	−53 11 31.0	0.24300	11520	8176	20.9	5259.0	134.0	40.0
RBS567	04 39 38.7	−53 11 31.0	0.24300	11520	8176	20.9	6370.0	35.0	17.9
RBS567	04 39 38.7	−53 11 31.0	0.24300	11520	8176	20.9	8033.0	13.0	8.1
RBS567	04 39 38.7	−53 11 31.0	0.24300	11520	8176	20.9	9119.0	32.0	27.8
RBS877	10 31 18.5	+50 53 36.0	0.36040	12025	14651	21.3	725.0	78.0	28.6
RBS877	10 31 18.5	+50 53 36.0	0.36040	12025	14651	21.3	959.0	257.0	32.2
RBS877	10 31 18.5	+50 53 36.0	0.36040	12025	14651	21.3	6550.0	79.0	34.4
RBS877	10 31 18.5	+50 53 36.0	0.36040	12025	14651	21.3	6758.0	82.0	52.8
RBS918	10 54 44.7	+48 31 39.0	0.28634	14772	2264	17.2	694.0	255.0	34.7
RBS918	10 54 44.7	+48 31 39.0	0.28634	14772	2264	17.2	3046.0	109.0	35.3
RBS918	10 54 44.7	+48 31 39.0	0.28634	14772	2264	17.2	4641.0	49.0	28.6
RBS918	10 54 44.7	+48 31 39.0	0.28634	14772	2264	17.2	6624.0	255.0	50.4
RBS918	10 54 44.7	+48 31 39.0	0.28634	14772	2264	17.2	6750.0	343.0	50.7
RBS918	10 54 44.7	+48 31 39.0	0.28634	14772	2264	17.2	8742.0	71.0	29.1
RBS970	11 20 48.1	+42 12 13.0	0.50035	14772	4807	16.7	3144.0	64.0	39.9
RBS970	11 20 48.1	+42 12 13.0	0.50035	14772	4807	16.7	6400.0	243.0	42.3
RBS970	11 20 48.1	+42 12 13.0	0.50035	14772	4807	16.7	7117.0	104.0	35.3
RBS970	11 20 48.1	+42 12 13.0	0.50035	14772	4807	16.7	7277.0	57.0	24.3
RBS970	11 20 48.1	+42 12 13.0	0.50035	14772	4807	16.7	9968.0	207.0	47.3
RBS982	11 25 40.7	+41 22 31.0	0.19721	14772	4789	16.3	2385.0	77.0	50.0
RBS982	11 25 40.7	+41 22 31.0	0.19721	14772	4789	16.3	2624.0	204.0	44.7
RBS982	11 25 40.7	+41 22 31.0	0.19721	14772	4789	16.3	6494.0	146.0	52.8
RXS_J0118.8+3836	01 18 49.4	+38 36 20.0	0.21600	14268	9191	16.7	6746.0	26.0	18.2
RXS_J0118.8+3836	01 18 49.4	+38 36 20.0	0.21600	14268	9191	16.7	7290.0	342.0	57.7
RXS_J0118.8+3836	01 18 49.4	+38 36 20.0	0.21600	14268	9191	16.7	7852.0	142.0	63.3
RXS_J0155.6+3115	01 55 36.0	+31 15 17.0	0.13500	14268	11948	15	4696.0	300.0	44.0
RXS_J0155.6+3115	01 55 36.0	+31 15 17.0	0.13500	14268	11948	15	7297.0	66.0	39.1
RX_J0023.5+1547	00 23 30.6	+15 47 44.0	0.41188	14071	7431	6.8	5279.0	529.0	60.2
RX_J0028.1+3103	00 28 10.7	+31 03 48.0	0.50000	14268	3714	16.3	1790.0	35.0	13.6
RX_J0028.1+3103	00 28 10.7	+31 03 48.0	0.50000	14268	3714	16.3	6063.0	399.0	44.4
RX_J0028.1+3103	00 28 10.7	+31 03 48.0	0.50000	14268	3714	16.3	6228.0	430.0	45.1
RX_J0028.1+3103	00 28 10.7	+31 03 48.0	0.50000	14268	3714	16.3	6342.0	504.0	51.4
RX_J0028.1+3103	00 28 10.7	+31 03 48.0	0.50000	14268	3714	16.3	6425.0	116.0	27.9
RX_J0028.1+3103	00 28 10.7	+31 03 48.0	0.50000	14268	3714	16.3	9332.0	359.0	49.1
RX_J0043.6+3725	00 43 42.6	+37 25 19.0	0.07990	14268	5532	20.3	1607.0	53.0	40.0
RX_J0043.6+3725	00 43 42.6	+37 25 19.0	0.07990	14268	5532	20.3	4269.0	103.0	42.0
RX_J0048.3+3941	00 48 19.0	+39 41 11.0	0.13400	11632	13484	27.2	1836.0	24.0	26.9
RX_J0048.3+3941	00 48 19.0	+39 41 11.0	0.13400	11632	13484	27.2	2401.0	17.0	20.6
RX_J0048.3+3941	00 48 19.0	+39 41 11.0	0.13400	11632	13484	27.2	3960.0	35.0	36.0
RX_J0048.3+3941	00 48 19.0	+39 41 11.0	0.13400	11632	13484	27.2	4886.0	46.0	31.9
RX_J0048.3+3941	00 48 19.0	+39 41 11.0	0.13400	11632	13484	27.2	8340.0	21.0	28.8
RX_J0050.8+3536	00 50 50.7	+35 36 43.0	0.05800	14268	3679	21	1713.0	13.0	10.2
RX_J0050.8+3536	00 50 50.7	+35 36 43.0	0.05800	14268	3679	21	1890.0	41.0	18.3
RX_J0050.8+3536	00 50 50.7	+35 36 43.0	0.05800	14268	3679	21	6849.0	117.0	26.9

Table 2 continued

Table 2 *(continued)*

Target	R.A.	Dec.	z	Program	T_{exp}	S/N	$v_{\mathrm{Ly}\alpha}$	$EW_{\mathrm{Ly}\alpha}$	b
					(ks)	(1238 Å)	$(\mathrm{km\,s^{-1}})$	(mÅ)	$(\mathrm{km\,s^{-1}})$
(1)	(2)	(3)	(4)	(5)	(6)	(7)	(8)	(9)	(10)
RX_J0053.7+2232	00 53 46.2	+22 32 22.0	0.14800	14268	3749	13.2	1692.0	109.0	48.3
RX_J0053.7+2232	00 53 46.2	+22 32 22.0	0.14800	14268	3749	13.2	2426.0	267.0	42.9
RX_J0053.7+2232	00 53 46.2	+22 32 22.0	0.14800	14268	3749	13.2	2587.0	57.0	38.6
RX_J0053.7+2232	00 53 46.2	+22 32 22.0	0.14800	14268	3749	13.2	2731.0	91.0	36.9
RX_J0053.7+2232	00 53 46.2	+22 32 22.0	0.14800	14268	3749	13.2	7446.0	78.0	29.7
RX_J0714.5+7408	07 14 36.2	+74 08 11.0	0.37100	12275	8333	17.6	1339.0	20.0	18.9
RX_J0714.5+7408	07 14 36.2	+74 08 11.0	0.37100	12275	8333	17.6	2650.0	94.0	40.0
RX_J0714.5+7408	07 14 36.2	+74 08 11.0	0.37100	12275	8333	17.6	4074.0	84.0	49.1
RX_J0714.5+7408	07 14 36.2	+74 08 11.0	0.37100	12275	8333	17.6	4264.0	420.0	46.6
RX_J0714.5+7408	07 14 36.2	+74 08 11.0	0.37100	12275	8333	17.6	5317.0	55.0	54.2
RX_J0714.5+7408	07 14 36.2	+74 08 11.0	0.37100	12275	8333	17.6	9558.0	25.0	26.8
RX_J0925.9+4535	09 25 54.5	+45 35 44.0	0.32989	12248	4436	14.6	1817.0	25.0	19.5
RX_J0925.9+4535	09 25 54.5	+45 35 44.0	0.32989	12248	4436	14.6	2484.0	32.0	17.6
RX_J0925.9+4535	09 25 54.5	+45 35 44.0	0.32989	12248	4436	14.6	2767.0	84.0	54.4
RX_J0925.9+4535	09 25 54.5	+45 35 44.0	0.32989	12248	4436	14.6	4284.0	319.0	37.7
RX_J0925.9+4535	09 25 54.5	+45 35 44.0	0.32989	12248	4436	14.6	4368.0	72.0	28.2
RX_J0925.9+4535	09 25 54.5	+45 35 44.0	0.32989	12248	4436	14.6	4604.0	34.0	21.1
RX_J0925.9+4535	09 25 54.5	+45 35 44.0	0.32989	12248	4436	14.6	5109.0	105.0	29.9
RX_J0925.9+4535	09 25 54.5	+45 35 44.0	0.32989	12248	4436	14.6	7826.0	487.0	55.8
RX_J0925.9+4535	09 25 54.5	+45 35 44.0	0.32989	12248	4436	14.6	8072.0	116.0	58.2
RX_J1017.5+4702	10 17 30.9	+47 02 25.0	0.33544	13314	8655	12.5	629.0	71.0	38.9
RX_J1054.2+3511	10 54 16.1	+35 11 24.0	0.20466	14772	2132	13.3	703.0	184.0	54.7
RX_J1054.2+3511	10 54 16.1	+35 11 24.0	0.20466	14772	2132	13.3	7329.0	95.0	43.0
RX_J1100.8+2839	11 00 52.4	+28 38 01.0	0.24298	13749	4659	11.3	615.0	360.0	42.4
RX_J1100.8+2839	11 00 52.4	+28 38 01.0	0.24298	13749	4659	11.3	695.0	406.0	44.8
RX_J1100.8+2839	11 00 52.4	+28 38 01.0	0.24298	13749	4659	11.3	5782.0	80.0	27.1
RX_J1100.8+2839	11 00 52.4	+28 38 01.0	0.24298	13749	4659	11.3	7272.0	60.0	32.0
RX_J1100.8+2839	11 00 52.4	+28 38 01.0	0.24298	13749	4659	11.3	7350.0	93.0	25.9
RX_J1100.8+2839	11 00 52.4	+28 38 01.0	0.24298	13749	4659	11.3	9219.0	68.0	33.9
RX_J1117.6+5301	11 17 40.5	+53 01 50.0	0.15871	14240	4943	11.5	685.0	342.0	50.6
RX_J1117.6+5301	11 17 40.5	+53 01 50.0	0.15871	14240	4943	11.5	1131.0	374.0	46.0
RX_J1117.6+5301	11 17 40.5	+53 01 50.0	0.15871	14240	4943	11.5	1259.0	62.0	21.4
RX_J1117.6+5301	11 17 40.5	+53 01 50.0	0.15871	14240	4943	11.5	2374.0	190.0	37.0
RX_J1117.6+5301	11 17 40.5	+53 01 50.0	0.15871	14240	4943	11.5	2874.0	120.0	50.2
RX_J1117.6+5301	11 17 40.5	+53 01 50.0	0.15871	14240	4943	11.5	5798.0	220.0	43.4
RX_J1117.6+5301	11 17 40.5	+53 01 50.0	0.15871	14240	4943	11.5	7957.0	91.0	37.1
RX_J1121.2+0326	11 21 14.2	+03 25 46.0	0.15200	12248	2695	4.2	1471.0	227.0	25.2
RX_J1121.2+0326	11 21 14.2	+03 25 46.0	0.15200	12248	2695	4.2	2605.0	190.0	43.3
RX_J1121.2+0326	11 21 14.2	+03 25 46.0	0.15200	12248	2695	4.2	6384.0	182.0	39.4
RX_J1121.2+0326	11 21 14.2	+03 25 46.0	0.15200	12248	2695	4.2	6975.0	678.0	113.3
RX_J1125.0+2513	11 25 03.6	+25 13 02.0	0.27150	14772	2134	10.7	6435.0	139.0	33.6
RX_J1125.0+2513	11 25 03.6	+25 13 02.0	0.27150	14772	2134	10.7	8849.0	298.0	39.0
RX_J1140.1+4115	11 40 03.4	+41 15 04.0	0.07132	14772	4790	11.1	1360.0	128.0	35.5
RX_J1140.1+4115	11 40 03.4	+41 15 04.0	0.07132	14772	4790	11.1	5718.0	147.0	47.1
RX_J1142.5+2503	11 42 31.7	+25 03 36.0	0.18417	14772	4687	15.3	855.0	13.0	10.7
RX_J1142.5+2503	11 42 31.7	+25 03 36.0	0.18417	14772	4687	15.3	2126.0	60.0	34.9
RX_J1142.5+2503	11 42 31.7	+25 03 36.0	0.18417	14772	4687	15.3	6133.0	257.0	47.2
RX_J1142.5+2503	11 42 31.7	+25 03 36.0	0.18417	14772	4687	15.3	9067.0	654.0	67.2
RX_J1142.7+4625	11 42 41.3	+46 24 37.0	0.11522	14772	4733	10	818.0	375.0	47.9
RX_J1142.7+4625	11 42 41.3	+46 24 37.0	0.11522	14772	4733	10	7420.0	62.0	27.1
RX_J1154.1+2521	11 54 08.0	+25 21 44.0	0.33664	14772	4631	11.2	886.0	42.0	21.1
RX_J1154.1+2521	11 54 08.0	+25 21 44.0	0.33664	14772	4631	11.2	3611.0	77.0	37.5

Table 2 continued

FRENCH & WAKKER

Table 2 *(continued)*

Target	R.A.	Dec.	z	Program	$T_{\rm exp}$	S/N	$v_{\rm Ly\alpha}$	$EW_{\rm Ly\alpha}$	b
					(ks)	(1238 Å)	(km s^{-1})	(mÅ)	(km s^{-1})
(1)	(2)	(3)	(4)	(5)	(6)	(7)	(8)	(9)	(10)
RX_J1154.1+2521	11 54 08.0	+25 21 44.0	0.33664	14772	4631	11.2	3866.0	149.0	38.0
RX_J1154.1+2521	11 54 08.0	+25 21 44.0	0.33664	14772	4631	11.2	6299.0	584.0	62.0
RX_J1210.7+2725	12 10 45.6	+27 25 36.0	0.23039	14772	4607	14.1	880.0	148.0	31.7
RX_J1210.7+2725	12 10 45.6	+27 25 36.0	0.23039	14772	4607	14.1	4022.0	52.0	24.6
RX_J1210.7+2725	12 10 45.6	+27 25 36.0	0.23039	14772	4607	14.1	8512.0	156.0	37.8
RX_J1212.2+2803	12 12 17.2	+28 03 50.0	0.16758	14772	4655	13.2	788.0	433.0	47.8
RX_J1212.2+2803	12 12 17.2	+28 03 50.0	0.16758	14772	4655	13.2	2680.0	194.0	46.0
RX_J1212.2+2803	12 12 17.2	+28 03 50.0	0.16758	14772	4655	13.2	3761.0	236.0	31.4
RX_J1217.2+2749	12 17 15.3	+27 49 51.0	0.39566	14772	4621	9.2	1035.0	528.0	58.3
RX_J1217.2+2749	12 17 15.3	+27 49 51.0	0.39566	14772	4621	9.2	1186.0	565.0	64.2
RX_J1217.2+2749	12 17 15.3	+27 49 51.0	0.39566	14772	4621	9.2	1326.0	128.0	30.6
RX_J1217.2+2749	12 17 15.3	+27 49 51.0	0.39566	14772	4621	9.2	1472.0	89.0	38.2
RX_J1217.2+2749	12 17 15.3	+27 49 51.0	0.39566	14772	4621	9.2	2574.0	89.0	25.7
RX_J1217.2+2749	12 17 15.3	+27 49 51.0	0.39566	14772	4621	9.2	2963.0	114.0	48.5
RX_J1217.2+2749	12 17 15.3	+27 49 51.0	0.39566	14772	4621	9.2	4059.0	135.0	30.8
RX_J1217.2+2749	12 17 15.3	+27 49 51.0	0.39566	14772	4621	9.2	6718.0	295.0	65.4
RX_J1236.0+2641	12 36 04.1	+26 41 36.0	0.20915	12248	4235	13.3	794.0	317.0	48.9
RX_J1236.0+2641	12 36 04.1	+26 41 36.0	0.20915	12248	4235	13.3	1009.0	365.0	54.0
RX_J1236.0+2641	12 36 04.1	+26 41 36.0	0.20915	12248	4235	13.3	1166.0	305.0	38.8
RX_J1236.0+2641	12 36 04.1	+26 41 36.0	0.20915	12248	4235	13.3	1254.0	122.0	24.8
RX_J1236.0+2641	12 36 04.1	+26 41 36.0	0.20915	12248	4235	13.3	6404.0	42.0	29.3
RX_J1236.0+2641	12 36 04.1	+26 41 36.0	0.20915	12248	4235	13.3	7111.0	429.0	57.9
RX_J1236.0+2641	12 36 04.1	+26 41 36.0	0.20915	12248	4235	13.3	7223.0	51.0	20.8
RX_J1303.7+2633	13 03 46.0	+26 33 13.0	0.43700	13382	7015	7.4	7853.0	139.0	42.6
RX_J1303.7+2633	13 03 46.0	+26 33 13.0	0.43700	13382	7015	7.4	8955.0	93.0	34.2
RX_J1330.8+3119	13 30 53.2	+31 19 32.0	0.24232	12248	4262	13.8	1727.0	166.0	57.5
RX_J1330.8+3119	13 30 53.2	+31 19 32.0	0.24232	12248	4262	13.8	2655.0	451.0	54.9
RX_J1330.8+3119	13 30 53.2	+31 19 32.0	0.24232	12248	4262	13.8	2822.0	73.0	38.2
RX_J1330.8+3119	13 30 53.2	+31 19 32.0	0.24232	12248	4262	13.8	4840.0	410.0	51.2
RX_J1330.8+3119	13 30 53.2	+31 19 32.0	0.24232	12248	4262	13.8	5051.0	119.0	53.7
RX_J1330.8+3119	13 30 53.2	+31 19 32.0	0.24232	12248	4262	13.8	7400.0	334.0	46.2
RX_J1342.1+0505	13 42 06.5	+05 05 24.0	0.26608	12248	2931	11.4	1190.0	269.0	38.6
RX_J1342.1+0505	13 42 06.5	+05 05 24.0	0.26608	12248	2931	11.4	2065.0	42.0	21.8
RX_J1342.1+0505	13 42 06.5	+05 05 24.0	0.26608	12248	2931	11.4	3429.0	110.0	30.2
RX_J1342.1+0505	13 42 06.5	+05 05 24.0	0.26608	12248	2931	11.4	7038.0	563.0	67.0
RX_J1342.1+0505	13 42 06.5	+05 05 24.0	0.26608	12248	2931	11.4	7114.0	351.0	40.6
RX_J1342.1+0505	13 42 06.5	+05 05 24.0	0.26608	12248	2931	11.4	9994.0	44.0	32.0
RX_J1342.7+1844	13 42 46.9	+18 44 43.0	0.38320	12248	2938	10.6	2789.0	91.0	36.0
RX_J1342.7+1844	13 42 46.9	+18 44 43.0	0.38320	12248	2938	10.6	6085.0	62.0	16.4
RX_J1342.7+1844	13 42 46.9	+18 44 43.0	0.38320	12248	2938	10.6	8182.0	524.0	60.7
RX_J1356.4+2515	13 56 25.6	+25 15 23.0	0.16404	12248	2282	11.2	4762.0	128.0	66.9
RX_J1356.4+2515	13 56 25.6	+25 15 23.0	0.16404	12248	2282	11.2	5291.0	99.0	42.8
RX_J1356.4+2515	13 56 25.6	+25 15 23.0	0.16404	12248	2282	11.2	7080.0	84.0	43.3
RX_J1356.4+2515	13 56 25.6	+25 15 23.0	0.16404	12248	2282	11.2	8475.0	131.0	47.4
RX_J1356.4+2515	13 56 25.6	+25 15 23.0	0.16404	12248	2282	11.2	9186.0	271.0	36.1
RX_J1356.4+2515	13 56 25.6	+25 15 23.0	0.16404	12248	2282	11.2	9285.0	116.0	31.5
RX_J1426.2+1955	14 26 13.4	+19 55 24.0	0.21000	13314	5124	21.2	1994.0	121.0	31.7
RX_J1426.2+1955	14 26 13.4	+19 55 24.0	0.21000	13314	5124	21.2	8904.0	42.0	34.9
RX_J1426.2+1955	14 26 13.4	+19 55 24.0	0.21000	13314	5124	21.2	9276.0	39.0	35.3
RX_J1429.6+0321	14 29 40.7	+03 21 26.0	0.25344	12603	3876	9.1	1539.0	414.0	52.0
RX_J1429.6+0321	14 29 40.7	+03 21 26.0	0.25344	12603	3876	9.1	1800.0	151.0	26.9
RX_J1429.6+0321	14 29 40.7	+03 21 26.0	0.25344	12603	3876	9.1	1902.0	39.0	10.7

Table 2 continued

Table 2 *(continued)*

Target	R.A.	Dec.	z	Program	$T_{\rm exp}$	S/N	$v_{\rm Ly\alpha}$	$EW_{\rm Ly\alpha}$	b
					(ks)	(1238 Å)	$(\rm km\,s^{-1})$	(mÅ)	$(\rm km\,s^{-1})$
(1)	(2)	(3)	(4)	(5)	(6)	(7)	(8)	(9)	(10)
RX_J1429.6+0321	14 29 40.7	+03 21 26.0	0.25344	12603	3876	9.1	2466.0	391.0	64.5
RX_J1429.6+0321	14 29 40.7	+03 21 26.0	0.25344	12603	3876	9.1	7873.0	232.0	37.6
RX_J1429.6+0321	14 29 40.7	+03 21 26.0	0.25344	12603	3876	9.1	8253.0	179.0	32.2
RX_J1429.6+0321	14 29 40.7	+03 21 26.0	0.25344	12603	3876	9.1	9947.0	668.0	73.3
RX_J1429.6+0321	14 29 40.7	+03 21 26.0	0.25344	12603	3876	9.1	10059.0	123.0	26.6
RX_J1429.6+0321	14 29 40.7	+03 21 26.0	0.25344	12603	3876	9.1	10142.0	135.0	42.5
RX_J1500.5+5517	15 00 30.8	+55 17 09.0	0.40481	12276	8422	17.2	3598.0	136.0	32.0
RX_J1503.2+6810	15 03 16.5	+68 10 06.0	0.11400	12276	1932	12	7204.0	176.0	43.5
RX_J1503.2+6810	15 03 16.5	+68 10 06.0	0.11400	12276	1932	12	8838.0	264.0	42.3
RX_J1503.2+6810	15 03 16.5	+68 10 06.0	0.11400	12276	1932	12	8935.0	94.0	31.0
RX_J1503.2+6810	15 03 16.5	+68 10 06.0	0.11400	12276	1932	12	9714.0	61.0	22.4
RX_J1544.5+2827	15 44 30.5	+28 27 56.0	0.23137	13423	2096	12.7	2111.0	70.0	26.3
RX_J1544.5+2827	15 44 30.5	+28 27 56.0	0.23137	13423	2096	12.7	6632.0	100.0	30.4
RX_J1544.5+2827	15 44 30.5	+28 27 56.0	0.23137	13423	2096	12.7	9642.0	188.0	35.3
RX_J1544.5+2827	15 44 30.5	+28 27 56.0	0.23137	13423	2096	12.7	9759.0	184.0	35.2
RX_J1608.3+6018	16 08 20.5	+60 18 28.0	0.17800	12276	5158	16.1	854.0	34.0	24.1
RX_J1608.3+6018	16 08 20.5	+60 18 28.0	0.17800	12276	5158	16.1	2906.0	120.0	36.0
RX_J1608.3+6018	16 08 20.5	+60 18 28.0	0.17800	12276	5158	16.1	2964.0	373.0	42.6
RX_J1830.3+7312	18 30 23.3	+73 13 10.0	0.12300	G020	24900	28.3	1553.0	73.0	34.0
RX_J1830.3+7312	18 30 23.3	+73 13 10.0	0.12300	G020	24900	28.3	1971.0	70.0	107.5
RX_J1830.3+7312	18 30 23.3	+73 13 10.0	0.12300	G020	24900	28.3	2390.0	81.0	67.4
RX_J1830.3+7312	18 30 23.3	+73 13 10.0	0.12300	G020	24900	28.3	4261.0	45.0	45.3
RX_J1830.3+7312	18 30 23.3	+73 13 10.0	0.12300	G020	24900	28.3	4767.0	53.0	49.5
RX_J2043.1+0324	20 43 06.2	+03 24 50.0	0.27100	13840	7834	15	1402.0	32.0	20.3
RX_J2043.1+0324	20 43 06.2	+03 24 50.0	0.27100	13840	7834	15	3287.0	91.0	50.8
RX_J2043.1+0324	20 43 06.2	+03 24 50.0	0.27100	13840	7834	15	4080.0	82.0	33.2
RX_J2043.1+0324	20 43 06.2	+03 24 50.0	0.27100	13840	7834	15	5060.0	60.0	30.0
RX_J2043.1+0324	20 43 06.2	+03 24 50.0	0.27100	13840	7834	15	6440.0	37.0	16.9
RX_J2043.1+0324	20 43 06.2	+03 24 50.0	0.27100	13840	7834	15	7448.0	99.0	28.0
RX_J2043.1+0324	20 43 06.2	+03 24 50.0	0.27100	13840	7834	15	8061.0	167.0	46.8
RX_J2139.7+0246	21 39 44.2	+02 46 05.0	0.26000	13840	7854	15.6	4083.0	490.0	50.7
RX_J2139.7+0246	21 39 44.2	+02 46 05.0	0.26000	13840	7854	15.6	4181.0	530.0	54.9
RX_J2139.7+0246	21 39 44.2	+02 46 05.0	0.26000	13840	7854	15.6	9219.0	106.0	34.0
SBS0957+599	10 01 02.6	+59 44 15.0	0.74749	12248	3300	11.2	2198.0	143.0	38.1
SBS0957+599	10 01 02.6	+59 44 15.0	0.74749	12248	3300	11.2	2870.0	226.0	36.2
SBS0957+599	10 01 02.6	+59 44 15.0	0.74749	12248	3300	11.2	3066.0	211.0	49.0
SBS0957+599	10 01 02.6	+59 44 15.0	0.74749	12248	3300	11.2	3273.0	293.0	43.7
SBS0957+599	10 01 02.6	+59 44 15.0	0.74749	12248	3300	11.2	7232.0	49.0	25.7
SBS0957+599	10 01 02.6	+59 44 15.0	0.74749	12248	3300	11.2	9469.0	72.0	29.4
SBS1108+560	11 11 32.1	+55 47 25.0	0.76827	12025	8387	4	661.0	448.0	57.8
SBS1108+560	11 11 32.1	+55 47 25.0	0.76827	12025	8387	4	703.0	268.0	31.0
SBS1108+560	11 11 32.1	+55 47 25.0	0.76827	12025	8387	4	782.0	351.0	51.8
SBS1108+560	11 11 32.1	+55 47 25.0	0.76827	12025	8387	4	947.0	198.0	25.5
SBS1116+523	11 19 48.0	+52 05 54.0	0.35568	14240	4949	14	731.0	259.0	41.6
SBS1116+523	11 19 48.0	+52 05 54.0	0.35568	14240	4949	14	2749.0	61.0	29.2
SBS1116+523	11 19 48.0	+52 05 54.0	0.35568	14240	4949	14	5724.0	200.0	46.0
SBS1116+523	11 19 48.0	+52 05 54.0	0.35568	14240	4949	14	8661.0	122.0	24.8
SBS1116+523	11 19 48.0	+52 05 54.0	0.35568	14240	4949	14	9717.0	21.0	13.9
SBS1122+594	11 25 53.7	+59 10 22.0	0.85142	11520	9874	15	1194.0	838.0	84.6
SBS1122+594	11 25 53.7	+59 10 22.0	0.85142	11520	9874	15	1600.0	135.0	25.1
SBS1122+594	11 25 53.7	+59 10 22.0	0.85142	11520	9874	15	7325.0	43.0	22.1
SBS1122+594	11 25 53.7	+59 10 22.0	0.85142	11520	9874	15	8640.0	148.0	39.3

Table 2 continued

FRENCH & WAKKER

Table 2 *(continued)*

Target	R.A.	Dec.	z	Program	$T_{\exp}$	S/N	$v_{\rm Ly\alpha}$	$EW_{\rm Ly\alpha}$	b
					(ks)	(1238 Å)	(km s^{-1})	(mÅ)	(km s^{-1})
(1)	(2)	(3)	(4)	(5)	(6)	(7)	(8)	(9)	(10)
SBS1122+594	11 25 53.7	+59 10 22.0	0.85142	11520	9874	15	9064.0	71.0	23.4
SBS1122+594	11 25 53.7	+59 10 22.0	0.85142	11520	9874	15	9779.0	32.0	18.3
SBS1503+570	15 04 55.6	+56 49 20.0	0.35894	12276	5163	13.8	708.0	301.0	42.5
SBS1503+570	15 04 55.6	+56 49 20.0	0.35894	12276	5163	13.8	2312.0	55.0	38.8
SBS1503+570	15 04 55.6	+56 49 20.0	0.35894	12276	5163	13.8	8923.0	583.0	69.2
SBS1537+577	15 38 10.0	+57 36 13.0	0.07342	12276	5193	8.8	739.0	132.0	40.1
SBS1537+577	15 38 10.0	+57 36 13.0	0.07342	12276	5193	8.8	3264.0	349.0	63.2
SBS1537+577	15 38 10.0	+57 36 13.0	0.07342	12276	5193	8.8	3548.0	441.0	51.7
SBS1537+577	15 38 10.0	+57 36 13.0	0.07342	12276	5193	8.8	4077.0	50.0	20.7
SBS1537+577	15 38 10.0	+57 36 13.0	0.07342	12276	5193	8.8	8451.0	48.0	32.3
SBS1537+577	15 38 10.0	+57 36 13.0	0.07342	12276	5193	8.8	9008.0	53.0	18.1
SBS1537+577	15 38 10.0	+57 36 13.0	0.07342	12276	5193	8.8	9175.0	66.0	22.2
SBS1537+577	15 38 10.0	+57 36 13.0	0.07342	12276	5193	8.8	9809.0	46.0	28.9
SDSSJ014143.20+134032.0	01 41 43.2	+13 40 32.0	0.04541	12275	7669	5.2	637.0	482.0	78.2
SDSSJ014143.20+134032.0	01 41 43.2	+13 40 32.0	0.04541	12275	7669	5.2	789.0	846.0	123.2
SDSSJ014143.20+134032.0	01 41 43.2	+13 40 32.0	0.04541	12275	7669	5.2	3240.0	555.0	94.9
SDSSJ015530.02-085704.0	01 55 30.0	−08 57 04.0	0.16443	12248	2931	10.5	1642.0	617.0	64.5
SDSSJ015530.02-085704.0	01 55 30.0	−08 57 04.0	0.16443	12248	2931	10.5	4761.0	230.0	54.4
SDSSJ015530.02-085704.0	01 55 30.0	−08 57 04.0	0.16443	12248	2931	10.5	8046.0	81.0	30.8
SDSSJ015952.95+134554.3	01 59 53.0	+13 45 54.0	0.50378	12603	7623	12.9	3524.0	47.0	18.5
SDSSJ015952.95+134554.3	01 59 53.0	+13 45 54.0	0.50378	12603	7623	12.9	4706.0	231.0	38.8
SDSSJ015952.95+134554.3	01 59 53.0	+13 45 54.0	0.50378	12603	7623	12.9	9741.0	58.0	37.5
SDSSJ021218.32-073719.8	02 12 18.3	−07 37 20.0	0.17392	12248	6525	11.2	4756.0	528.0	57.0
SDSSJ021218.32-073719.8	02 12 18.3	−07 37 20.0	0.17392	12248	6525	11.2	4833.0	500.0	58.8
SDSSJ021218.32-073719.8	02 12 18.3	−07 37 20.0	0.17392	12248	6525	11.2	5272.0	123.0	34.5
SDSSJ080838.80+051440.0	08 08 38.8	+05 14 40.0	0.36061	12603	4674	10	2469.0	124.0	40.9
SDSSJ080838.80+051440.0	08 08 38.8	+05 14 40.0	0.36061	12603	4674	10	2594.0	253.0	35.7
SDSSJ080838.80+051440.0	08 08 38.8	+05 14 40.0	0.36061	12603	4674	10	4138.0	106.0	34.2
SDSSJ080838.80+051440.0	08 08 38.8	+05 14 40.0	0.36061	12603	4674	10	4351.0	179.0	40.8
SDSSJ080838.80+051440.0	08 08 38.8	+05 14 40.0	0.36061	12603	4674	10	4854.0	150.0	40.6
SDSSJ080838.80+051440.0	08 08 38.8	+05 14 40.0	0.36061	12603	4674	10	8738.0	783.0	80.9
SDSSJ080838.80+051440.0	08 08 38.8	+05 14 40.0	0.36061	12603	4674	10	8926.0	128.0	24.5
SDSSJ080838.80+051440.0	08 08 38.8	+05 14 40.0	0.36061	12603	4674	10	9476.0	61.0	18.7
SDSSJ080838.80+051440.0	08 08 38.8	+05 14 40.0	0.36061	12603	4674	10	9750.0	52.0	22.6
SDSSJ080908.13+461925.6	08 09 08.1	+46 19 26.0	0.65873	12248	3146	14.3	2272.0	77.0	31.6
SDSSJ080908.13+461925.6	08 09 08.1	+46 19 26.0	0.65873	12248	3146	14.3	3117.0	198.0	33.9
SDSSJ080908.13+461925.6	08 09 08.1	+46 19 26.0	0.65873	12248	3146	14.3	6779.0	544.0	56.3
SDSSJ080908.13+461925.6	08 09 08.1	+46 19 26.0	0.65873	12248	3146	14.3	6880.0	156.0	40.7
SDSSJ080908.13+461925.6	08 09 08.1	+46 19 26.0	0.65873	12248	3146	14.3	7105.0	181.0	52.9
SDSSJ082024.20+233450.0	08 20 24.2	+23 34 50.0	0.47056	11598	5035	11.4	3928.0	110.0	24.4
SDSSJ082024.20+233450.0	08 20 24.2	+23 34 50.0	0.47056	11598	5035	11.4	4081.0	95.0	26.8
SDSSJ082024.20+233450.0	08 20 24.2	+23 34 50.0	0.47056	11598	5035	11.4	4210.0	258.0	35.2
SDSSJ084159.20+140642.0	08 41 59.2	+14 06 42.0	1.25567	13314	11204	13.1	2054.0	300.0	41.1
SDSSJ084159.20+140642.0	08 41 59.2	+14 06 42.0	1.25567	13314	11204	13.1	5445.0	360.0	42.1
SDSSJ084159.20+140642.0	08 41 59.2	+14 06 42.0	1.25567	13314	11204	13.1	8358.0	122.0	25.6
SDSSJ084159.20+140642.0	08 41 59.2	+14 06 42.0	1.25567	13314	11204	13.1	8428.0	178.0	40.4
SDSSJ091052.80+333008.0	09 10 52.8	+33 30 08.0	0.11631	14240	7442	9.2	589.0	211.0	48.2
SDSSJ091052.80+333008.0	09 10 52.8	+33 30 08.0	0.11631	14240	7442	9.2	1824.0	266.0	39.2
SDSSJ091052.80+333008.0	09 10 52.8	+33 30 08.0	0.11631	14240	7442	9.2	1975.0	68.0	24.4
SDSSJ091052.80+333008.0	09 10 52.8	+33 30 08.0	0.11631	14240	7442	9.2	3386.0	122.0	29.6
SDSSJ091052.80+333008.0	09 10 52.8	+33 30 08.0	0.11631	14240	7442	9.2	5800.0	58.0	23.7
SDSSJ091127.30+325337.0	09 11 27.3	+32 53 37.0	0.29038	14240	10028	8.5	2063.0	271.0	39.1

Table 2 continued

Table 2 *(continued)*

Target	R.A.	Dec.	z	Program	$T_{\exp}$	S/N	$v_{\mathrm{Ly\alpha}}$	$EW_{\mathrm{Ly\alpha}}$	b
					(ks)	(1238 Å)	(km s^{-1})	(mÅ)	(km s^{-1})
(1)	(2)	(3)	(4)	(5)	(6)	(7)	(8)	(9)	(10)
SDSSJ091127.30+325337.0	09 11 27.3	+32 53 37.0	0.29038	14240	10028	8.5	3855.0	148.0	34.4
SDSSJ091127.30+325337.0	09 11 27.3	+32 53 37.0	0.29038	14240	10028	8.5	4320.0	608.0	72.0
SDSSJ091127.30+325337.0	09 11 27.3	+32 53 37.0	0.29038	14240	10028	8.5	5487.0	68.0	34.3
SDSSJ091127.30+325337.0	09 11 27.3	+32 53 37.0	0.29038	14240	10028	8.5	8003.0	71.0	32.1
SDSSJ091728.60+271951.0	09 17 28.6	+27 19 51.0	0.07564	14071	15471	11.4	1727.0	68.0	38.9
SDSSJ091728.60+271951.0	09 17 28.6	+27 19 51.0	0.07564	14071	15471	11.4	2028.0	99.0	29.2
SDSSJ091728.60+271951.0	09 17 28.6	+27 19 51.0	0.07564	14071	15471	11.4	5920.0	102.0	38.6
SDSSJ091728.60+271951.0	09 17 28.6	+27 19 51.0	0.07564	14071	15471	11.4	7141.0	384.0	83.0
SDSSJ091728.60+271951.0	09 17 28.6	+27 19 51.0	0.07564	14071	15471	11.4	7282.0	284.0	37.6
SDSSJ091728.60+271951.0	09 17 28.6	+27 19 51.0	0.07564	14071	15471	11.4	8102.0	41.0	21.5
SDSSJ091728.60+271951.0	09 17 28.6	+27 19 51.0	0.07564	14071	15471	11.4	9814.0	103.0	43.4
SDSSJ093706.90+170021.0	09 37 06.9	+17 00 21.0	0.50567	12603	7635	9.2	4332.0	67.0	19.7
SDSSJ093706.90+170021.0	09 37 06.9	+17 00 21.0	0.50567	12603	7635	9.2	4388.0	175.0	40.5
SDSSJ093706.90+170021.0	09 37 06.9	+17 00 21.0	0.50567	12603	7635	9.2	8120.0	155.0	39.4
SDSSJ094840.10+580038.0	09 48 40.1	+58 00 38.0	0.49179	13774	8835	10	1196.0	172.0	47.5
SDSSJ094840.10+580038.0	09 48 40.1	+58 00 38.0	0.49179	13774	8835	10	7262.0	198.0	30.4
SDSSJ094840.10+580038.0	09 48 40.1	+58 00 38.0	0.49179	13774	8835	10	8385.0	904.0	94.7
SDSSJ094840.10+580038.0	09 48 40.1	+58 00 38.0	0.49179	13774	8835	10	8516.0	371.0	39.9
SDSSJ095914.80+320357.0	09 59 14.8	+32 03 57.0	0.56462	12603	2273	11.4	1493.0	623.0	68.0
SDSSJ095914.80+320357.0	09 59 14.8	+32 03 57.0	0.56462	12603	2273	11.4	4493.0	154.0	28.1
SDSSJ095914.80+320357.0	09 59 14.8	+32 03 57.0	0.56462	12603	2273	11.4	4781.0	76.0	30.7
SDSSJ095914.80+320357.0	09 59 14.8	+32 03 57.0	0.56462	12603	2273	11.4	7852.0	315.0	38.3
SDSSJ095914.80+320357.0	09 59 14.8	+32 03 57.0	0.56462	12603	2273	11.4	7940.0	97.0	28.4
SDSSJ095915.60+050355.0	09 59 15.6	+05 03 55.0	0.16263	12248	2931	13.6	1579.0	627.0	64.1
SDSSJ095915.60+050355.0	09 59 15.6	+05 03 55.0	0.16263	12248	2931	13.6	1858.0	37.0	16.8
SDSSJ095915.60+050355.0	09 59 15.6	+05 03 55.0	0.16263	12248	2931	13.6	2167.0	83.0	40.2
SDSSJ095915.60+050355.0	09 59 15.6	+05 03 55.0	0.16263	12248	2931	13.6	3762.0	108.0	40.9
SDSSJ095915.60+050355.0	09 59 15.6	+05 03 55.0	0.16263	12248	2931	13.6	3806.0	129.0	32.6
SDSSJ095915.60+050355.0	09 59 15.6	+05 03 55.0	0.16263	12248	2931	13.6	9951.0	108.0	27.6
SDSSJ104241.30+250123.0	10 42 41.3	+25 01 23.0	0.34157	14071	10068	6.2	6261.0	279.0	40.0
SDSSJ104335.90+115129.0	10 43 35.9	+11 51 29.0	0.79400	14071	4736	13.5	717.0	823.0	92.1
SDSSJ104335.90+115129.0	10 43 35.9	+11 51 29.0	0.79400	14071	4736	13.5	882.0	621.0	67.0
SDSSJ104335.90+115129.0	10 43 35.9	+11 51 29.0	0.79400	14071	4736	13.5	1030.0	391.0	48.1
SDSSJ104335.90+115129.0	10 43 35.9	+11 51 29.0	0.79400	14071	4736	13.5	1974.0	202.0	50.9
SDSSJ104335.90+115129.0	10 43 35.9	+11 51 29.0	0.79400	14071	4736	13.5	2801.0	72.0	32.0
SDSSJ104335.90+115129.0	10 43 35.9	+11 51 29.0	0.79400	14071	4736	13.5	3717.0	43.0	19.3
SDSSJ104335.90+115129.0	10 43 35.9	+11 51 29.0	0.79400	14071	4736	13.5	9920.0	40.0	18.3
SDSSJ105945.30+144142.0	10 59 45.3	+14 41 42.0	0.63171	12248	4217	11.8	652.0	297.0	43.8
SDSSJ105945.30+144142.0	10 59 45.3	+14 41 42.0	0.63171	12248	4217	11.8	713.0	283.0	33.9
SDSSJ105945.30+144142.0	10 59 45.3	+14 41 42.0	0.63171	12248	4217	11.8	1443.0	540.0	57.6
SDSSJ105945.30+144142.0	10 59 45.3	+14 41 42.0	0.63171	12248	4217	11.8	3128.0	424.0	48.5
SDSSJ105945.30+144142.0	10 59 45.3	+14 41 42.0	0.63171	12248	4217	11.8	5278.0	107.0	32.8
SDSSJ105945.30+144142.0	10 59 45.3	+14 41 42.0	0.63171	12248	4217	11.8	5411.0	517.0	89.8
SDSSJ105945.30+144142.0	10 59 45.3	+14 41 42.0	0.63171	12248	4217	11.8	5757.0	146.0	40.9
SDSSJ105945.30+144142.0	10 59 45.3	+14 41 42.0	0.63171	12248	4217	11.8	5853.0	262.0	63.5
SDSSJ105945.30+144142.0	10 59 45.3	+14 41 42.0	0.63171	12248	4217	11.8	7107.0	243.0	47.9
SDSSJ105945.30+144142.0	10 59 45.3	+14 41 42.0	0.63171	12248	4217	11.8	7243.0	410.0	43.1
SDSSJ105945.30+144142.0	10 59 45.3	+14 41 42.0	0.63171	12248	4217	11.8	8076.0	220.0	41.5
SDSSJ105945.30+144142.0	10 59 45.3	+14 41 42.0	0.63171	12248	4217	11.8	9322.0	137.0	34.3
SDSSJ105945.30+144142.0	10 59 45.3	+14 41 42.0	0.63171	12248	4217	11.8	9385.0	144.0	20.5
SDSSJ111443.70+525834.0	11 14 43.7	+52 58 34.0	0.07921	14240	13440	6.9	1163.0	232.0	64.1
SDSSJ111443.70+525834.0	11 14 43.7	+52 58 34.0	0.07921	14240	13440	6.9	2839.0	334.0	59.1

Table 2 continued

FRENCH & WAKKER

Table 2 *(continued)*

Target	R.A.	Dec.	z	Program	$T_{\exp}$	S/N	$v_{\mathrm{Ly}\alpha}$	$EW_{\mathrm{Ly}\alpha}$	b
					(ks)	(1238 Å)	(km s^{-1})	(mÅ)	(km s^{-1})
(1)	(2)	(3)	(4)	(5)	(6)	(7)	(8)	(9)	(10)
SDSSJ111443.70+525834.0	11 14 43.7	+52 58 34.0	0.07921	14240	13440	6.9	5497.0	270.0	39.0
SDSSJ111443.70+525834.0	11 14 43.7	+52 58 34.0	0.07921	14240	13440	6.9	5911.0	155.0	41.4
SDSSJ111443.70+525834.0	11 14 43.7	+52 58 34.0	0.07921	14240	13440	6.9	7316.0	62.0	25.1
SDSSJ111908.70+254505.0	11 19 08.7	+25 45 05.0	0.57967	14772	4701	11.5	6393.0	441.0	51.1
SDSSJ112005.00+041323.0	11 20 05.0	+04 13 23.0	0.54689	12603	4708	8.5	2285.0	27.0	8.4
SDSSJ112005.00+041323.0	11 20 05.0	+04 13 23.0	0.54689	12603	4708	8.5	2578.0	116.0	30.8
SDSSJ112005.00+041323.0	11 20 05.0	+04 13 23.0	0.54689	12603	4708	8.5	6096.0	171.0	29.9
SDSSJ112005.00+041323.0	11 20 05.0	+04 13 23.0	0.54689	12603	4708	8.5	8810.0	157.0	38.6
SDSSJ112005.00+041323.0	11 20 05.0	+04 13 23.0	0.54689	12603	4708	8.5	9533.0	255.0	48.2
SDSSJ112224.10+031802.0	11 22 24.1	+03 18 02.0	0.47528	12603	7588	12.9	1049.0	295.0	41.4
SDSSJ112224.10+031802.0	11 22 24.1	+03 18 02.0	0.47528	12603	7588	12.9	1264.0	423.0	54.7
SDSSJ112224.10+031802.0	11 22 24.1	+03 18 02.0	0.47528	12603	7588	12.9	6606.0	70.0	32.9
SDSSJ112224.10+031802.0	11 22 24.1	+03 18 02.0	0.47528	12603	7588	12.9	8872.0	432.0	56.3
SDSSJ112224.10+031802.0	11 22 24.1	+03 18 02.0	0.47528	12603	7588	12.9	9890.0	51.0	48.7
SDSSJ112439.50+113117.0	11 24 39.5	+11 31 17.0	0.14285	14071	10427	9.4	1047.0	345.0	40.4
SDSSJ112439.50+113117.0	11 24 39.5	+11 31 17.0	0.14285	14071	10427	9.4	1099.0	272.0	34.8
SDSSJ112439.50+113117.0	11 24 39.5	+11 31 17.0	0.14285	14071	10427	9.4	2042.0	80.0	40.6
SDSSJ112439.50+113117.0	11 24 39.5	+11 31 17.0	0.14285	14071	10427	9.4	2176.0	51.0	37.8
SDSSJ112439.50+113117.0	11 24 39.5	+11 31 17.0	0.14285	14071	10427	9.4	3255.0	188.0	41.4
SDSSJ112439.50+113117.0	11 24 39.5	+11 31 17.0	0.14285	14071	10427	9.4	8255.0	108.0	50.1
SDSSJ112448.30+531818.0	11 24 48.3	+53 18 18.0	0.53151	14240	7920	10	664.0	339.0	52.1
SDSSJ112448.30+531818.0	11 24 48.3	+53 18 18.0	0.53151	14240	7920	10	1019.0	71.0	27.5
SDSSJ112448.30+531818.0	11 24 48.3	+53 18 18.0	0.53151	14240	7920	10	1141.0	165.0	38.2
SDSSJ112448.30+531818.0	11 24 48.3	+53 18 18.0	0.53151	14240	7920	10	5752.0	121.0	31.6
SDSSJ112448.30+531818.0	11 24 48.3	+53 18 18.0	0.53151	14240	7920	10	8867.0	66.0	29.4
SDSSJ112448.30+531818.0	11 24 48.3	+53 18 18.0	0.53151	14240	7920	10	9883.0	229.0	45.7
SDSSJ114046.10+113649.0	11 40 46.1	+11 36 49.0	0.68736	14071	10129	9.1	928.0	252.0	40.6
SDSSJ114046.10+113649.0	11 40 46.1	+11 36 49.0	0.68736	14071	10129	9.1	967.0	275.0	33.3
SDSSJ114046.10+113649.0	11 40 46.1	+11 36 49.0	0.68736	14071	10129	9.1	1016.0	209.0	28.1
SDSSJ114646.00+371511.0	11 46 46.0	+37 15 11.0	0.29586	14772	2162	12.5	873.0	267.0	32.1
SDSSJ114646.00+371511.0	11 46 46.0	+37 15 11.0	0.29586	14772	2162	12.5	980.0	226.0	26.8
SDSSJ114646.00+371511.0	11 46 46.0	+37 15 11.0	0.29586	14772	2162	12.5	3085.0	185.0	39.5
SDSSJ114646.00+371511.0	11 46 46.0	+37 15 11.0	0.29586	14772	2162	12.5	6698.0	41.0	25.3
SDSSJ115722.40+114040.0	11 57 22.4	+11 40 40.0	0.29091	14071	10034	10.3	2755.0	294.0	47.9
SDSSJ115722.40+114040.0	11 57 22.4	+11 40 40.0	0.29091	14071	10034	10.3	6200.0	366.0	56.2
SDSSJ115722.40+114040.0	11 57 22.4	+11 40 40.0	0.29091	14071	10034	10.3	6428.0	689.0	73.0
SDSSJ115722.40+114040.0	11 57 22.4	+11 40 40.0	0.29091	14071	10034	10.3	9736.0	90.0	39.6
SDSSJ121640.60+071224.0	12 16 40.6	+07 12 24.0	0.58756	11698	2048	10.2	3845.0	106.0	31.4
SDSSJ121640.60+071224.0	12 16 40.6	+07 12 24.0	0.58756	11698	2048	10.2	7021.0	324.0	43.1
SDSSJ121640.60+071224.0	12 16 40.6	+07 12 24.0	0.58756	11698	2048	10.2	3845.0	106.0	31.4
SDSSJ121640.60+071224.0	12 16 40.6	+07 12 24.0	0.58756	11698	2048	10.2	7021.0	324.0	43.1
SDSSJ121640.60+071224.0	12 16 40.6	+07 12 24.0	0.58756	11698	2048	10.2	7021.0	324.0	43.1
SDSSJ124210.30+321427.0	12 42 10.3	+32 14 27.0	1.49257	14085	13008	12.2	640.0	586.0	65.3
SDSSJ124210.30+321427.0	12 42 10.3	+32 14 27.0	1.49257	14085	13008	12.2	715.0	585.0	71.5
SDSSJ124210.30+321427.0	12 42 10.3	+32 14 27.0	1.49257	14085	13008	12.2	3284.0	180.0	48.8
SDSSJ124210.30+321427.0	12 42 10.3	+32 14 27.0	1.49257	14085	13008	12.2	3711.0	61.0	29.0
SDSSJ124210.30+321427.0	12 42 10.3	+32 14 27.0	1.49257	14085	13008	12.2	3969.0	54.0	12.6
SDSSJ124210.30+321427.0	12 42 10.3	+32 14 27.0	1.49257	14085	13008	12.2	4490.0	131.0	25.3
SDSSJ124210.30+321427.0	12 42 10.3	+32 14 27.0	1.49257	14085	13008	12.2	5370.0	62.0	22.4
SDSSJ124210.30+321427.0	12 42 10.3	+32 14 27.0	1.49257	14085	13008	12.2	5509.0	125.0	25.8
SDSSJ124210.30+321427.0	12 42 10.3	+32 14 27.0	1.49257	14085	13008	12.2	6933.0	483.0	58.4
SDSSJ125846.70+242739.0	12 58 46.7	+24 27 39.0	0.37110	13382	7546	8.3	3177.0	63.0	28.6

Table 2 continued

Table 2 *(continued)*

Target	R.A.	Dec.	z	Program	T_{exp}	S/N	$v_{\mathrm{Ly}\alpha}$	$EW_{\mathrm{Ly}\alpha}$	b
					(ks)	(1238 Å)	$(\mathrm{km\,s^{-1}})$	(mÅ)	$(\mathrm{km\,s^{-1}})$
(1)	(2)	(3)	(4)	(5)	(6)	(7)	(8)	(9)	(10)
SDSSJ130524.30+035731.0	13 05 24.3	+03 57 31.0	0.54566	12603	7588	13.3	374.0	210.0	33.7
SDSSJ130524.30+035731.0	13 05 24.3	+03 57 31.0	0.54566	12603	7588	13.3	425.0	531.0	67.0
SDSSJ130524.30+035731.0	13 05 24.3	+03 57 31.0	0.54566	12603	7588	13.3	7043.0	462.0	51.3
SDSSJ131545.20+152556.0	13 15 45.2	+15 25 56.0	0.44811	12603	4688	10.5	6528.0	192.0	32.5
SDSSJ131545.20+152556.0	13 15 45.2	+15 25 56.0	0.44811	12603	4688	10.5	6702.0	266.0	37.1
SDSSJ131545.20+152556.0	13 15 45.2	+15 25 56.0	0.44811	12603	4688	10.5	8025.0	440.0	50.6
SDSSJ135341.03+361948.0	13 53 41.0	+36 19 48.0	0.14659	13444	10199	19.5	6169.0	266.0	49.6
SDSSJ135341.03+361948.0	13 53 41.0	+36 19 48.0	0.14659	13444	10199	19.5	6528.0	493.0	54.9
SDSSJ135341.03+361948.0	13 53 41.0	+36 19 48.0	0.14659	13444	10199	19.5	6639.0	223.0	30.0
SDSSJ135424.90+243006.3	13 54 24.9	+24 30 06.0	1.89283	12603	6829	10	5826.0	302.0	36.2
SDSSJ135424.90+243006.3	13 54 24.9	+24 30 06.0	1.89283	12603	6829	10	6025.0	136.0	36.5
SDSSJ135424.90+243006.3	13 54 24.9	+24 30 06.0	1.89283	12603	6829	10	8500.0	377.0	41.9
SDSSJ135424.90+243006.3	13 54 24.9	+24 30 06.0	1.89283	12603	6829	10	9616.0	93.0	42.7
SDSSJ135712.60+170444.0	13 57 12.6	+17 04 44.0	0.15050	12248	4223	13.9	3180.0	53.0	24.3
SDSSJ135712.60+170444.0	13 57 12.6	+17 04 44.0	0.15050	12248	4223	13.9	3287.0	64.0	27.1
SDSSJ135712.60+170444.0	13 57 12.6	+17 04 44.0	0.15050	12248	4223	13.9	6640.0	34.0	26.9
SDSSJ135712.60+170444.0	13 57 12.6	+17 04 44.0	0.15050	12248	4223	13.9	7155.0	26.0	18.7
SDSSJ135726.27+043541.4	13 57 26.2	+04 35 41.0	1.23453	12264	14148	21	967.0	348.0	37.3
SDSSJ135726.27+043541.4	13 57 26.2	+04 35 41.0	1.23453	12264	14148	21	1124.0	83.0	24.2
SDSSJ135726.27+043541.4	13 57 26.2	+04 35 41.0	1.23453	12264	14148	21	2586.0	59.0	26.0
SDSSJ135726.27+043541.4	13 57 26.2	+04 35 41.0	1.23453	12264	14148	21	4540.0	32.0	15.7
SDSSJ135726.27+043541.4	13 57 26.2	+04 35 41.0	1.23453	12264	14148	21	5092.0	129.0	26.0
SDSSJ135726.27+043541.4	13 57 26.2	+04 35 41.0	1.23453	12264	14148	21	5825.0	38.0	15.3
SDSSJ135726.27+043541.4	13 57 26.2	+04 35 41.0	1.23453	12264	14148	21	8804.0	89.0	28.6
SDSSJ140428.30+335342.0	14 04 28.3	+33 53 42.0	0.54996	12603	7705	8.9	1515.0	178.0	34.6
SDSSJ140428.30+335342.0	14 04 28.3	+33 53 42.0	0.54996	12603	7705	8.9	2157.0	111.0	29.1
SDSSJ140428.30+335342.0	14 04 28.3	+33 53 42.0	0.54996	12603	7705	8.9	5765.0	314.0	37.5
SDSSJ140428.30+335342.0	14 04 28.3	+33 53 42.0	0.54996	12603	7705	8.9	7913.0	888.0	92.7
SDSSJ141038.40+230447.0	14 10 38.4	+23 04 47.0	0.79580	12958	11275	11.3	2229.0	37.0	18.2
SDSSJ141038.40+230447.0	14 10 38.4	+23 04 47.0	0.79580	12958	11275	11.3	2313.0	31.0	15.4
SDSSJ141038.40+230447.0	14 10 38.4	+23 04 47.0	0.79580	12958	11275	11.3	8671.0	142.0	31.9
SDSSJ141542.90+163414.0	14 15 42.9	+16 34 14.0	0.74350	12486	18479	19	2318.0	3632.0	377.3
SDSSJ141542.90+163414.0	14 15 42.9	+16 34 14.0	0.74350	12486	18479	19	5355.0	67.0	24.4
SDSSJ141542.90+163414.0	14 15 42.9	+16 34 14.0	0.74350	12486	18479	19	9242.0	140.0	45.3
SDSSJ141949.40+060654.0	14 19 49.4	+06 06 54.0	1.64892	13473	11028	11.9	921.0	82.0	15.8
SDSSJ141949.40+060654.0	14 19 49.4	+06 06 54.0	1.64892	13473	11028	11.9	1155.0	85.0	16.9
SDSSJ141949.40+060654.0	14 19 49.4	+06 06 54.0	1.64892	13473	11028	11.9	1411.0	662.0	78.1
SDSSJ141949.40+060654.0	14 19 49.4	+06 06 54.0	1.64892	13473	11028	11.9	1691.0	3001.0	39.3
SDSSJ141949.40+060654.0	14 19 49.4	+06 06 54.0	1.64892	13473	11028	11.9	1825.0	60.0	15.6
SDSSJ141949.40+060654.0	14 19 49.4	+06 06 54.0	1.64892	13473	11028	11.9	5015.0	160.0	52.6
SDSSJ141949.40+060654.0	14 19 49.4	+06 06 54.0	1.64892	13473	11028	11.9	8531.0	167.0	35.3
SDSSJ142859.10+322507.0	14 28 59.1	+32 25 07.0	0.62717	13314	11314	20.7	1994.0	78.0	40.9
SDSSJ142859.10+322507.0	14 28 59.1	+32 25 07.0	0.62717	13314	11314	20.7	3423.0	363.0	42.7
SDSSJ142859.10+322507.0	14 28 59.1	+32 25 07.0	0.62717	13314	11314	20.7	4126.0	260.0	43.3
SDSSJ142859.10+322507.0	14 28 59.1	+32 25 07.0	0.62717	13314	11314	20.7	4220.0	302.0	40.1
SDSSJ142859.10+322507.0	14 28 59.1	+32 25 07.0	0.62717	13314	11314	20.7	6242.0	67.0	23.9
SDSSJ150928.30+070235.0	15 09 28.3	+07 02 35.0	0.41878	12603	7612	11.3	1214.0	93.0	50.8
SDSSJ150928.30+070235.0	15 09 28.3	+07 02 35.0	0.41878	12603	7612	11.3	3911.0	90.0	35.1
SDSSJ150928.30+070235.0	15 09 28.3	+07 02 35.0	0.41878	12603	7612	11.3	7854.0	56.0	19.8
SDSSJ150928.30+070235.0	15 09 28.3	+07 02 35.0	0.41878	12603	7612	11.3	9386.0	822.0	84.3
SDSSJ150952.20+111047.0	15 09 52.2	+11 10 47.0	0.28494	12614	57130	12	1241.0	131.0	64.4
SDSSJ150952.20+111047.0	15 09 52.2	+11 10 47.0	0.28494	12614	57130	12	8256.0	416.0	49.9

Table 2 continued

FRENCH & WAKKER

Table 2 *(continued)*

Target	R.A.	Dec.	z	Program	$T_{\exp}$	S/N	$v_{\mathrm{Ly}\alpha}$	$EW_{\mathrm{Ly}\alpha}$	b
					(ks)	(1238 Å)	$(\mathrm{km\,s^{-1}})$	(mÅ)	$(\mathrm{km\,s^{-1}})$
(1)	(2)	(3)	(4)	(5)	(6)	(7)	(8)	(9)	(10)
SDSSJ151237.15+012846.0	15 12 37.2	+01 28 46.0	0.26625	12603	7590	6.8	2029.0	599.0	74.2
SDSSJ151237.15+012846.0	15 12 37.2	+01 28 46.0	0.26625	12603	7590	6.8	8575.0	2695.0	345.6
SDSSJ151237.15+012846.0	15 12 37.2	+01 28 46.0	0.26625	12603	7590	6.8	8661.0	918.0	94.9
SDSSJ151237.15+012846.0	15 12 37.2	+01 28 46.0	0.26625	12603	7590	6.8	8753.0	755.0	78.6
SDSSJ151237.15+012846.0	15 12 37.2	+01 28 46.0	0.26625	12603	7590	6.8	8831.0	3947.0	480.4
SDSSJ160519.70+144852.2	16 05 19.7	+14 48 52.0	0.37210	12614	8374	15.3	9934.0	249.0	52.3
SDSSJ225738.20+134045.0	22 57 38.2	+13 40 45.0	0.59455	11598	3428	8.8	2582.0	180.0	35.1
SDSSJ225738.20+134045.0	22 57 38.2	+13 40 45.0	0.59455	11598	3428	8.8	8695.0	97.0	39.9
SDSSJ225738.20+134045.0	22 57 38.2	+13 40 45.0	0.59455	11598	3428	8.8	8870.0	500.0	54.6
TON1009	09 09 06.1	+32 36 31.0	0.81028	12603	4740	12.4	1908.0	111.0	33.3
TON1009	09 09 06.1	+32 36 31.0	0.81028	12603	4740	12.4	1980.0	243.0	31.0
TON1009	09 09 06.1	+32 36 31.0	0.81028	12603	4740	12.4	4295.0	333.0	40.4
TON1009	09 09 06.1	+32 36 31.0	0.81028	12603	4740	12.4	7917.0	72.0	32.1
TON1009	09 09 06.1	+32 36 31.0	0.81028	12603	4740	12.4	7971.0	69.0	27.1
TON1015	09 10 37.0	+33 29 24.0	0.35400	14240	4774	14.8	611.0	225.0	37.6
TON1015	09 10 37.0	+33 29 24.0	0.35400	14240	4774	14.8	1833.0	244.0	36.9
TON1015	09 10 37.0	+33 29 24.0	0.35400	14240	4774	14.8	1985.0	80.0	28.9
TON1015	09 10 37.0	+33 29 24.0	0.35400	14240	4774	14.8	3369.0	97.0	27.2
TON1187	10 13 03.1	+35 51 22.0	0.07910	12275	1958	20	4491.0	117.0	41.9
TON1187	10 13 03.1	+35 51 22.0	0.07910	12275	1958	20	4567.0	169.0	29.5
TON1187	10 13 03.1	+35 51 22.0	0.07910	12275	1958	20	5666.0	37.0	29.5
TON1187	10 13 03.1	+35 51 22.0	0.07910	12275	1958	20	8008.0	118.0	50.2
TON1364	11 13 59.7	+35 03 06.0	0.34681	14772	4725	10.8	1790.0	128.0	40.7
TON1364	11 13 59.7	+35 03 06.0	0.34681	14772	4725	10.8	7394.0	205.0	42.4
TON1364	11 13 59.7	+35 03 06.0	0.34681	14772	4725	10.8	8791.0	154.0	43.9
TON1364	11 13 59.7	+35 03 06.0	0.34681	14772	4725	10.8	9072.0	115.0	32.4
TON1364	11 13 59.7	+35 03 06.0	0.34681	14772	4725	10.8	9148.0	71.0	22.4
TON1364	11 13 59.7	+35 03 06.0	0.34681	14772	4725	10.8	9274.0	146.0	34.2
TON236	15 28 40.6	+28 25 29.0	0.45000	12038	6554	20	2032.0	89.0	51.0
TON236	15 28 40.6	+28 25 29.0	0.45000	12038	6554	20	5325.0	48.0	33.8
TON236	15 28 40.6	+28 25 29.0	0.45000	12038	6554	20	6072.0	25.0	22.2
TON488	10 10 00.7	+30 03 21.0	0.25643	12025	10796	18.9	1371.0	454.0	51.0
TON488	10 10 00.7	+30 03 21.0	0.25643	12025	10796	18.9	4076.0	39.0	29.2
TON488	10 10 00.7	+30 03 21.0	0.25643	12025	10796	18.9	4788.0	39.0	30.4
TON488	10 10 00.7	+30 03 21.0	0.25643	12025	10796	18.9	5013.0	128.0	25.6
TON488	10 10 00.7	+30 03 21.0	0.25643	12025	10796	18.9	5640.0	39.0	37.0
TON488	10 10 00.7	+30 03 21.0	0.25643	12025	10796	18.9	5729.0	34.0	16.0
TON52	11 04 07.0	+31 41 11.0	0.43572	12248	2982	10.7	1772.0	117.0	30.8
TON52	11 04 07.0	+31 41 11.0	0.43572	12248	2982	10.7	6458.0	54.0	19.1
TON52	11 04 07.0	+31 41 11.0	0.43572	12248	2982	10.7	8359.0	250.0	80.8
TON52	11 04 07.0	+31 41 11.0	0.43572	12248	2982	10.7	8674.0	60.0	25.5
TON52	11 04 07.0	+31 41 11.0	0.43572	12248	2982	10.7	9642.0	191.0	43.3
TON580	11 31 09.5	+31 14 05.0	0.28900	11519	4903	20.2	2509.0	129.0	44.1
TON580	11 31 09.5	+31 14 05.0	0.28900	11519	4903	20.2	8288.0	78.0	48.1
TON605	12 17 52.1	+30 07 01.0	0.13000	13651	7369	27.8	853.0	456.0	48.7
TON605	12 17 52.1	+30 07 01.0	0.13000	13651	7369	27.8	1048.0	305.0	36.1
TON605	12 17 52.1	+30 07 01.0	0.13000	13651	7369	27.8	3781.0	268.0	37.0
TON605	12 17 52.1	+30 07 01.0	0.13000	13651	7369	27.8	9136.0	124.0	36.1
TON605	12 17 52.1	+30 07 01.0	0.13000	13651	7369	27.8	9255.0	74.0	33.9
TON_S180	00 57 20.0	−22 22 56.0	0.06198	D028	24400	31.8	1932.0	70.0	42.9
TON_S180	00 57 20.0	−22 22 56.0	0.06198	D028	24400	31.8	2795.0	61.0	47.0
TON_S180	00 57 20.0	−22 22 56.0	0.06198	D028	24400	31.8	3003.0	45.0	29.6

Table 2 continued

Table 2 *(continued)*

Target	R.A.	Dec.	z	Program	$T_{\rm exp}$	S/N	$v_{\rm Ly\alpha}$	$EW_{\rm Ly\alpha}$	b
					(ks)	(1238 Å)	(km s^{-1})	(mÅ)	(km s^{-1})
(1)	(2)	(3)	(4)	(5)	(6)	(7)	(8)	(9)	(10)
TON_S180	00 57 20.0	−22 22 56.0	0.06198	D028	24400	31.8	5519.0	274.0	52.1
TON_S180	00 57 20.0	−22 22 56.0	0.06198	D028	24400	31.8	6306.0	59.0	38.3
TON_S180	00 57 20.0	−22 22 56.0	0.06198	D028	24400	31.8	7039.0	260.0	79.2
TON_S210	01 21 51.6	−28 20 57.0	0.11600	12204	5047	36.5	5924.0	35.0	22.9
UM228	00 21 01.0	+00 52 47.0	0.09830	13017	1060	7.1	1738.0	126.0	57.6
UM228	00 21 01.0	+00 52 47.0	0.09830	13017	1060	7.1	2941.0	77.0	27.2
UM228	00 21 01.0	+00 52 47.0	0.09830	13017	1060	7.1	5491.0	277.0	56.2
UM228	00 21 01.0	+00 52 47.0	0.09830	13017	1060	7.1	5816.0	540.0	128.5
UM228	00 21 01.0	+00 52 47.0	0.09830	13017	1060	7.1	9975.0	121.0	56.4
US136	13 01 00.8	+28 19 44.0	1.36000	13314	13429	14.6	1753.0	93.0	32.4
US136	13 01 00.8	+28 19 44.0	1.36000	13314	13429	14.6	2320.0	93.0	40.0
US136	13 01 00.8	+28 19 44.0	1.36000	13314	13429	14.6	2502.0	80.0	26.3
US136	13 01 00.8	+28 19 44.0	1.36000	13314	13429	14.6	4747.0	57.0	30.2
US136	13 01 00.8	+28 19 44.0	1.36000	13314	13429	14.6	6381.0	50.0	18.9
US136	13 01 00.8	+28 19 44.0	1.36000	13314	13429	14.6	9182.0	179.0	23.7
US136	13 01 00.8	+28 19 44.0	1.36000	13314	13429	14.6	9304.0	192.0	42.0
US136	13 01 00.8	+28 19 44.0	1.36000	13314	13429	14.6	9691.0	40.0	19.7
US2816	11 42 12.3	+30 16 13.0	0.48190	12603	4790	10.5	1800.0	100.0	37.2
US2816	11 42 12.3	+30 16 13.0	0.48190	12603	4790	10.5	2854.0	269.0	49.7
US2816	11 42 12.3	+30 16 13.0	0.48190	12603	4790	10.5	3015.0	72.0	21.9
US2816	11 42 12.3	+30 16 13.0	0.48190	12603	4790	10.5	9607.0	414.0	43.5
US2816	11 42 12.3	+30 16 13.0	0.48190	12603	4790	10.5	9666.0	274.0	27.9
US2816	11 42 12.3	+30 16 13.0	0.48190	12603	4790	10.5	9744.0	273.0	32.2
US645	09 29 09.9	+46 44 24.0	0.23998	12248	2415	19.4	1190.0	11.0	6.8
US645	09 29 09.9	+46 44 24.0	0.23998	12248	2415	19.4	4983.0	295.0	32.2
US645	09 29 09.9	+46 44 24.0	0.23998	12248	2415	19.4	5028.0	254.0	27.4
US645	09 29 09.9	+46 44 24.0	0.23998	12248	2415	19.4	7704.0	61.0	36.3
US645	09 29 09.9	+46 44 24.0	0.23998	12248	2415	19.4	8335.0	339.0	52.9
US645	09 29 09.9	+46 44 24.0	0.23998	12248	2415	19.4	8480.0	204.0	35.0
US645	09 29 09.9	+46 44 24.0	0.23998	12248	2415	19.4	8547.0	137.0	22.6
US645	09 29 09.9	+46 44 24.0	0.23998	12248	2415	19.4	8955.0	287.0	59.3
US645	09 29 09.9	+46 44 24.0	0.23998	12248	2415	19.4	9788.0	155.0	35.6
UVQSJ101629.20-315023.6	10 16 29.2	−31 50 24.0	0.24141	14687	10961	22.4	2012.0	116.0	33.6
UVQSJ101629.20-315023.6	10 16 29.2	−31 50 24.0	0.24141	14687	10961	22.4	2110.0	37.0	23.5
UVQSJ101629.20-315023.6	10 16 29.2	−31 50 24.0	0.24141	14687	10961	22.4	2828.0	168.0	27.4
UVQSJ101629.20-315023.6	10 16 29.2	−31 50 24.0	0.24141	14687	10961	22.4	2901.0	37.0	21.7
UVQSJ101629.20-315023.6	10 16 29.2	−31 50 24.0	0.24141	14687	10961	22.4	5278.0	31.0	18.1
UVQSJ101629.20-315023.6	10 16 29.2	−31 50 24.0	0.24141	14687	10961	22.4	8965.0	305.0	42.8
VIIZw348	10 51 00.7	+65 59 40.0	0.03251	13654	4241	8.8	574.0	146.0	44.4
VIIZw348	10 51 00.7	+65 59 40.0	0.03251	13654	4241	8.8	1148.0	345.0	40.4
VIIZw348	10 51 00.7	+65 59 40.0	0.03251	13654	4241	8.8	1795.0	230.0	42.1
VIIZw348	10 51 00.7	+65 59 40.0	0.03251	13654	4241	8.8	3416.0	671.0	69.3
VIIZw348	10 51 00.7	+65 59 40.0	0.03251	13654	4241	8.8	3556.0	293.0	47.1
WCom	12 21 31.7	+28 13 58.0	0.10200	14772	2141	9.1	1619.0	58.0	24.5
WCom	12 21 31.7	+28 13 58.0	0.10200	14772	2141	9.1	2316.0	235.0	36.2
WCom	12 21 31.7	+28 13 58.0	0.10200	14772	2141	9.1	2540.0	269.0	45.8
WCom	12 21 31.7	+28 13 58.0	0.10200	14772	2141	9.1	4167.0	61.0	16.3
WCom	12 21 31.7	+28 13 58.0	0.10200	14772	2141	9.1	4383.0	123.0	33.3
Zw535.012	00 36 21.0	+45 39 54.0	0.04764	14268	5234	18.9	5071.0	50.0	29.7
Zw535.012	00 36 21.0	+45 39 54.0	0.04764	14268	5234	18.9	5153.0	178.0	40.9

NOTE—Summary of COS targets and each measured Lyα absorption line in this study.